Occurrence And Fate Of Microplastics In Urban Freshwater Systems

Mola Zadeh, Marziye

DOI (link to publication from Publisher):
10.54337/aau645718960

Publication date:
2023

Document Version
Publisher's PDF, also known as Version of record

OCCURRENCE AND FATE OF MICROPLASTICS IN URBAN FRESHWATER SYSTEMS

BY
MARZIYE (SHABNAM) MOLAZADEH

DISSERTATION SUBMITTED 2023

AALBORG UNIVERSITY
DENMARK

OCCURRENCE AND FATE OF MICROPLASTICS IN URBAN FRESHWATER SYSTEMS

by

Marziye (Shabnam) Molazadeh

AALBORG UNIVERSITY
DENMARK

Dissertation submitted in September 2023

Dissertation submitted: November 2023

PhD supervisor: Professor Jes Vollertsen
Aalborg University

Assistant PhD supervisor: Assistant Professor Fan Liu,
Aalborg University

PhD committee: Associate Professor Søren Liedtke Thorndahl (chair)
Aalborg University, Denmark

Professor Lian Lundy
NIVA, Middelsex University, UK

Associate Professor Andrej Kržan
National Institute of Chemistry, Slovenia

PhD Series: Faculty of Engineering and Science, Aalborg University

Department: Department of the Built Environment

ISSN (online): 2446-1636
ISBN (online): 978-87-7573-593-8

Published by:
Aalborg University Press
Kroghstræde 3
DK – 9220 Aalborg Ø
Phone: +45 99407140
aauf@forlag.aau.dk
forlag.aau.dk

Printed in Denmark by Stibo Complete, 2023

EDUCATION

2020-2023 PhD of Civil and Environmental Engineering
Aalborg University, Denmark

2013-2017 Master of Civil and Environmental Engineering
Ferdowsi University of Mashhad, Iran

2008-2012 Bachelor of Civil Engineering
Shahid Chamran University of Ahvaz, Iran

KNOWLEDGE DISSEMINATION AT CONFERENCES

May 2022 .
SETAC 2022, Copenhagen, Denmark.
Mapping of occurrence of MPs in the sediments of a stormwater pond (Spotlight presentation)

November 2022
SETAC North America 2022, Pittsburgh, United States of America.
Stormwater ponds, sinks, or sources of microplastics? (Poster presentation)

March 2023
UNESCO – EU H2020 LimnoPlast Conference 2023, Paris, France.
My PhD journey with Limnoplast (Oral presentation)

LIST OF SCIENTIFIC PAPERS

I. **Molazadeh, M.,** Liu, F., Simon-Sanchez, L., Vollertsen, J., 2022. Buoyant microplastics in freshwater sediments – how do they get there? Science of The Total Environment. https://doi.org/10.1016/j.scitotenv.2022.160489

I.I. **Molazadeh, M.,** Liu, F., Lykkemark, J., Iordachescu, L., Nielsen, A.H., Vollertsen, J., 2023. What is hiding below the surface – MPs including TWP in an urban lake. International Environment (Under review).

I.I.I. **Molazadeh, M.,** Calabro, g., Liu, F., Tassin, B., Rovelli, L., Lorke, A., Dris, R., Vollertsen, J., 2023. Buoyant microplastics in turbulent waters – their way to the sediments. Science of The Total Environment (Under review).

ENGLISH SUMMARY

Plastics are one of the most versatile man-made materials. However, their high consumption and disposal cause major environmental issues. As the production and usage of plastic is concentrated in urban areas, these play a significant role in spreading plastic as a pollutant into the environment. Microplastics (MPs) are small pieces of plastic (< 5 mm) which can be released into water bodies in cities by multiple emission sources, and through diverse routes. To manage the environmental problems of MPs and to identify appropriate mitigation efforts, it is important to understand and gain insight into their occurrence and fate in urban areas.

The PhD study investigated the abundance and fate of MPs in urban freshwater systems. Focus was on sediments of stormwater facilities and lakes, which both are considered shallow water systems. The goal was to find trends within MP distribution in the systems and to see if there is patchiness in the MP occurrence pattern or not. Furthermore, studying the governing factors of the observed spatial patterns was part of the aim.

A stormwater pond in Aarhus, Denmark, was studied by sampling sediments across the pond. The spatial distribution of MP in its sediments was uneven, and varied up to two orders of magnitude between sampling locations. The deposition of MPs in the pond's sediments did not follow any pattern related to their size and type. Where MPs ended up in the pond did hence not depend on size and

polymer type (density). Furthermore, the findings revealed that buoyant particles on average made up 96% and 86% of the MP concentration measured as mass and counts, respectively. Small-sized polypropylene (PP) particles were the dominating polymers in most of the sampled sites. The computational fluid dynamics software STAR-CCM+ was employed to study the dominant transport mechanisms that govern the fate of MPs from water to sediments. The result showed that mixing was an explanatory factor for the transport of MPs to the bottom of the pond.

The pollution by MP, including tire wear particles (TWP) across an urban lake receiving the effluent of the aforementioned stormwater pond, as well as other contributions, was addressed next. The sediments of this lake (Brabrand Lake) held large amounts of MP and TWP. PP was the most abundant polymer, like what was seen for the stormwater pond. Then came TWP, emphasizing the importance of considering TWP when taking mitigation decisions. Similar to the pond, the spatial variability of MP including TWP was high in the lake. This emphasized the importance of taking a representative number of samples to accurately capture and reflect the MP pollution level of such system.

The observation that most of the MPs found in the sediments had densities less than water, i.e., they were buoyant, moved the study towards the mechanisms influencing their way from the water to the sediments of shallow water systems. The approach was to assess the effect of turbulence on the transport of PE particles from the flowing water to the sediments in a slow flowing experimental flume. That study

showed that the velocity of PE particles differed several orders of magnitude from the one predicted for still water (laminar flow conditions). This difference was caused by the turbulence of the flow. Moreover, turbulence mixing caused the distribution of particles throughout the water column, and a considerable number of these buoyant particles experienced downward vertical transport.

The findings of the PhD study contributed to the knowledge of the occurrence and spatial variability of MPs in urban water systems. For the first time, it gave insights into the MP pollution level of Danish lakes. These data can be further used to help to select appropriate mitigation measures to prevent aquatic pollution by microplastics. Moreover, it has shed light on the mechanism driving the transport and migration of buoyant plastic particles in shallow water systems using modelling tools and flume experiments. This further contributes to proof of the concept that transport of MPs in many cases is driven by turbulent mixing, and that this phenomenon must be included in assessment of the fate of MPs in water systems.

DANSK RESUME

Plastmaterialer er blandt de mest alsidige menneskeskabte materialer. Dog har deres høje forbrug og bortskaffelse medført alvorlige miljøproblemer. Da koncentreret produktion og brug af plast forekommer i byområder, spiller disse regioner en betydelig rolle i spredningen af denne forurenende faktor i miljøet. Mikroplast kan frigives i vandforekomster i byer fra flere mulige kilder til udledning gennem forskellige ruter. For at håndtere miljøproblemerne med mikroplastikpartikler er det vigtigt at forstå og opnå indsigt i forekomsten og skæbnen for mikroplast i byområder, for at hjælpe med at vælge passende indsatsområder for at mindske problemet.

Ph.d.-studiet undersøgte forekomsten og skæbnen for mikroplastikpartikler (MP) i urbane ferskvandssystemer. Fokus lå på sedimentet i regnvandsanlæg og søer, som begge betragtes som lavvandede vandsystemer. Målet var at finde gradienterne af MP-distribution inden for systemerne og se, om der er uensartethed i spredningsmønsteret for MP eller ej. Derudover var det en del af målet at studere de styrende faktorer for de observerede rumlige mønstre.

Fordelingen af MP-koncentrationen over sedimentet i en regnvandssø var ujævn og variabel med op til to størrelsesordener. Aflejringen af MP i søens sediment fulgte ikke noget mønster, der svarede til deres størrelse og type. Med andre ord var MP-fordelingen i sedimentet ikke størrelses- og polymer type (densitet) selektiv, og den var homogen inden for prøvestationerne. Yderligere viste resultaterne, at

opdriftspartikler udgjorde 96% og 86% af massen og antallet af de samlede registrerede partikler pr. kg sediment, og små Polypropylen (PP)-partikler var de dominerende polymerer på de fleste af de prøvede steder. STAR-CCM+ softwaren blev anvendt til at undersøge de dominerende transportmekanismer, der styrer MP'ers skæbne fra vand til sediment. Resultatet viste, at blanding var en forklarende faktor for transporten af MP til bunden af søen.

Forureningsniveauet og fordelingen af MP og dækslitagepartikler i en sø, der modtager afløbet fra den førnævnte regnvandssø og en opstrøms vådområde og til sidst udledes til det åbne hav, blev vurderet. Brabrand-søens sedimenter indeholder store mængder MP og dækslitagepartikler. Af mikroplastik bestående af dækslitagepartikler og andre var PP den mest almindelige polymer, ligesom i regnvandssø-studiet, efterfulgt af dækslitagepartikler, hvilket understreger vigtigheden af at overveje dækslitagepartikler ved træffelse af reduktionsbeslutninger. Niveauet af rumlig variation i mikroplastik- og dækslitagepartikel-mængden varierede betydeligt mellem prøvestederne. Denne undersøgelse understreger vigtigheden af at tage et repræsentativt antal prøver for at kunne fange og afspejle MP-forureningsniveauet i det undersøgte system på en præcis måde.

Detektering af høj koncentration af opdriftige og små mikroplastik-polymere i sedimentet i de undersøgte vandlegemer ledte os mod at studere mekanismen, der påvirker denne opdagelse i lavvandede vandsystemer. Derfor vurderede ph.d.-studiet også effekten af turbulens på transporten af PE-partikler fra vandoverfladen til

sedimentet i en eksperimentel kanal. Studiet viste, at hastigheden af indsprøjtede PE-partikler adskilte sig med flere størrelsesordener fra deres forventede værdier i stillestående vand (deres naturlige adfærd) på grund af omgivende turbulent strømning. Desuden forårsagede turbulensblanding en fordeling af partikler gennem vandsøjlen, og en betydelig mængde partikler oplevede vertikal transport nedad.

Resultaterne af den nuværende ph.d.-undersøgelse har bidraget til viden om forekomsten og højopløselig rumlig variation af mikroplastikpartikler i danske byvandssystemer. Det har givet indsigt i mikroplastforureningen i danske søer for første gang. Disse data kan yderligere bruges til at hjælpe med at vælge passende reduktionsforanstaltninger. Derudover har det kastet mere lys over mekanismen, der driver transport og migration af opdriftige plastikpartikler i lavvandede vandsystemer ved hjælp af modelleringsværktøjer og eksperimenter i en kanal. Dette bidrager yderligere til at bekræfte konceptet med mikroplastpartiklers transport drevet af blanding.

PREFACE

This thesis has been submitted for assessment in partial fulfilment of the PhD degree. As part of the assessment, co-author statements have been made available to the assessment committee and are also available at the Faculty.

The PhD was carried out in the period from May 2020 to August 2023 at the Department of the Built Environment, Aalborg University. The PhD included a collaboration with the LEESU, Ecole des Ponts, University of Paris Est Creteil, France. The joint study resulted in a manuscript (Paper-III), which is submitted and is under review.

This thesis is based on one published scientific paper (Paper I), and two scientific manuscripts (Paper II and III). Contents of the papers are briefly discussed in the extended summary of the thesis, while additional details are given in the paper and manuscripts.

ACKNOWLEDGEMENTS

Foremost, I wish to express my profound gratitude to Professor Jes Vollertsen, the best-ever supervisor on the whole planet! He has embodied the true essence of being a bridge, not a wall, in the real world for me, and I believe he is the bridge for everyone who knows him. He finds and sees good in everything and everyone, and he has the extraordinary ability to turn even the worst things into good. I consider myself lucky to have the chance to learn from him, he is not only teaching you science but more importantly how to see the world and people. I am so grateful to him for teaching me the meaning of full freedom under responsibility, teaching me it is fine to make mistakes, and it is fine that we might not know some stuff, but we can learn them, he showed me we should believe and trust people and their abilities. This list can go endless… I want him to know that I am forever thankful to him for making the dream of doing my PhD abroad come true, and always keeping the candle of hope lighting in our hearts.

Fan you have been way more than a co-supervisor for me during my PhD journey, I am so thankful for all the support you gave me. You showed me how to be tough and put aside barriers and stay focused on the goals though they are lots of distractors on the path. You taught me we do not need to be perfect in everything, but still, we can enjoy learning new things. You taught me I should not be scared of starting new things on the contrary I should dive into unknowns and embrace changes. Thank you for teaching me how to be confident and ignore

everything and everyone who wants to challenge me and just stay concentrated on my own growth. I am so glad that I got the chance to have you by myside as my co-supervisor to learn from you.

My resilient, ever-smiling, kindest-ever Rupa (mama Rupa), thank you for teaching me how to smile and look for the light in dark moments. You started teaching me from the first day of my journey, and it still continues… You are inspiring me every single moment of being with you. I believe everyone needs a Rupa in his/her life. Someone you can go to, and be yourself with. Thank you for your support without any boundaries and for all the unplanned dinner invitations to your warm home. Your stories that come from your heart and wisdom have always motivated me to keep going regardless of how difficult the situation can get, I am calling them Rupa therapy.

I would like to thank everyone in the group, they should know that they have not been just colleagues for me but my second family, I will definitely miss a lot Lucian while he is laughing loudly in the coffee breaks, Ramus funny stories, Claudias unlimited kindness and huges, Alvise while his going around and working hard, having cookie breaks (it is in the afternoon don't confuse it with coffee breaks) with Laura, Lili laughing loudly in the office and corridors (you can hear it even if you are in the lab), Jeanettes Danish cakes with lots of sugar, Nana's soothing smiles and Lucas philosophical attitudes towards life.

I would also like to give a special thanks to Jytte Denker and Henrik Koch, our super lab technicians. Nothing could work out in our lab without them.

I owe my deepest gratitude to my parents who my success was not possible without their support. They have always been pushing me to go beyond my boundaries and encouraging me to leave my comfort zone and giving me the wings to fly and confidence to pursue my dreams. Their belief in my abilities, and constant encouragement in each and every step of my life have been invaluable sources of strength. Their belief in my potential and their unwavering love have been my pillars of strength. I would also like to thank Ghaem for all the sacrifices he made for me to start the journey and for his endless support and help….

TABLE OF CONTENTS

TABLE OF FIGURES

CHAPTER 1. INTRODUCTION

Our modern life is highly dependent on plastic for different purposes, from industrial to medical usage. However, extensive production and usage of synthetic polymers, along with their properties like durability, have caused them to become significant environmental pollutants. Tiny particles (< 5mm) manufactured intentionally or originating from fragmentation of large plastic items due to for example, exposure to solar ultraviolet radiation, weathering, and mechanical stresses, are commonly defined as microplastics (MPs) (Andrady, 2011). Being widely used and generated in contemporary societies, MPs in cities can be emitted to water systems from different sources. In urban areas, stormwater, wastewater, and combined sewer overflows have been commonly recognized as substantial contributors of MP to the environment (Schernewski et al., 2020).

Wastewater is known to receive MPs from a variety of sources like households, shops, offices, industries and, to some extent, stormwater. Studies like Simon et al. (2018) and Chand et al. (2021) and (2022) have shown that municipal wastewater is highly polluted with MPs and holds a quite high concentration of them, but advanced WWTPs, on the other hand are quite efficient in retaining these particles. As shown by Bollmann et al. (2019), this indicates that other wastewater-related discharges, such as combined sewer overflows and misconnected wastewater, play a significant role in the release of MPs into the environment.

Being generated from rain and storm events in urban areas, surface water runoff can come into contact with numerous particulate and soluble pollutants, including MPs. The runoff can cause the mobilization and transport of contaminants from terrestrial environments to downstream aquatic systems. All outdoor activities that produce plastic debris have the potential to introduce MPs into stormwater.

Stormwater is either drained into the sewage system and treated at WWTPs (‘combined system’) or transported separately to the recipient with or without treatment. In cities with combined sewer systems, the fate of MPs differs with precipitation intensities and volume. On rainy days without sewer overflow, a mix of wastewater and stormwater runoff, both containing MPs, reach the WWTP. After receiving treatment, the wastewater, which is now treated but still contains a small fraction of the original MPs, is discharged to a receiving water body. However, during heavy rainfall, when sewer overflow happens because the sewer exceeds its hydraulic capacity, the system discharges a portion of the water directly to the receiving water without treatment.

MPs released into separate stormwater collection pipes end up either in stormwater management facilities such as retention ponds or are discharged into nearby streams, rivers, and lakes, or in coastal cities also directly to the sea. Modern cities, which have separate facilities for stormwater management, treat part of their stormwater in manmade or natural ponds, in which stormwater is held from days to

weeks before discharge. In this way, depending on retention time and characteristics of the particulate materials, a fraction will be retained in the pond while the remaining particles will be emitted into the environment.

The purpose of stormwater systems is to collect and treat wet weather runoff to a level where damages to the recipient water systems are avoided. This covers hydraulic impacts by mitigating the peak flow and managing contaminants in the runoff. In retention ponds, the latter occurs largely by trapping and immobilizing incoming pollutants into their sediments. The main process here is the sedimentation of particulates.

Originally, the main focus of stormwater management has been to treat 'traditional' pollutants such as heavy metals and nutrients. Over the past decade or two, there has also been an increased awareness that stormwater is a pathway for conveying emergent pollutants like MPs to the aquatic environment if the systems are not efficient enough in capturing them. MPs in stormwater ponds might have travelled significant distances before reaching the pond, as for example, the findings of MPs not related to traffic in a rural highway pond (Liu et al., 2019a, 2019b).

Urban lakes are an important part of inland ecosystems because they support the life of many species. They furthermore act as water reservoirs, protect the surrounding area from floods, provide recreational services, etc. (Eriksen et al., 2013, Islam et al., 2022). MPs

in such lakes can be a potential threat to the biota and species living there. MPs can physically damage fish, birds, zooplanktons, etc. They can be ingested by the lake's biota either directly or indirectly through the food chain. The direct intake of MPs by the organisms can cause internal injuries. MPs can furthermore leach toxic chemicals, which can affect the organisms in the lake. MPs of different shapes and sizes are discharged into the lakes. For example, MPs from the breakdown of larger plastic pieces are usually on the form of fragments (Meng et al., 2020), foams come from food packings (Meng et al., 2020), and fibers are sourced from textiles (Meng et al., 2020) and fishing nets (Timmers et al., 2005). Intentionally added MPs from personal care products, water treatment systems, or sandblasting are usually pellets (Veerasingam et al., 2016; Meng et al., 2020).

MPs can be transported to urban lakes via different pathways. Some lakes receive surface runoff from urban and highway catchments. The MP input to lakes by surface runoff is influenced by the season (Horton et al., 2017; Liu et al., 2019 (C)). Storm events can increase MP inflow to the lakes. Moreover, in some place's wastewater treatment plant effluent, which still contains MPs, and combined sewer overflow is discharged to such lakes. Given that lakes have lower flow velocities than rivers and thus can retain water for a longer time, these water bodies can be potential sinks of MPs. MP pollution level of lakes has been shown to be comparable to that of marine waters. Moreover, inland lakes, especially in densely populated urban

areas, are much smaller than the ocean (Ding et al., 2019; Yonkos et al., 2014), which leads to a higher accumulation of MPs in sediments.

The dominant MP polymer types detected in lake systems are PET, PVC, PP and PE (Yang et al., 2021). Worldwide, MPs in Asian lakes are according to Yang et al. dominated by PP (25.0%), followed by PET (22.6%), PE (19.0 %), PA (9.7%), PS (8.1%), and PVC (1.3%). In Europe, PP is the main polymer in lakes and makes up 50.0 % of the polymers. This is followed by PS (27.3%), PE (15.5%), PVC (0.2%), PET (1.3%) and others (5.8%). In America, PP is again the dominant polymer, constituting 33.8% of the particles, followed by PE (25.1%), PS (11.9%) and PVC (10%) (Yang et al., 2021). According to the same source, MPs in Asian lake sediments consist to 22.7% of the buoyant polymers PP and PE whereas PET is the dominant polymer (40.4%). In Europe, PA is the major polymer in lake sediments, accounting for 79.9%, followed by PS with 10.0%, PP (0.1%) and others (10%). The data for America shows that PE is the main polymer in sediments of American lakes, constituting 67.7% of the identified MPs. PP stands in the second position with 16%, followed by PET (3.7%), PVC (0.6%), PS (0.7%) and others (11.3%). Which polymers have been reported in freshwaters, and their sediments are hence quite mixed.

According to the data, PP and PE, which have densities lower than that of water, are among the most abundant polymers in both water and sediments. Considering density only, particles that have a density higher than that of water (negatively buoyant) should settle and those

with a density lower than water (positively buoyant) should float at the water surface. Thus, heavy polymers like PVC or PET should predominantly be found in the sediments while light polymers such as PE and PP should predominantly be found in the water. As this is confuted by data from numerous monitoring efforts, there must be other process leading to the deposition of light MPs and to heavy MPs staying in the water.

One such process could be growth and accumulation of microbes, algae, and invertebrates on microplastic particles, which then can change the overall density or facilitate the adhesion of minerals and organic matter (Lobelle and Cunliffe, 2011). These overgrown particles might have densities different from the original MP, leading to different sinking and rising patterns (Ye and Andrady, 1991; Long et al., 2015). Sinking fecal pellets containing ingested MPs, can be another mechanism by which positively buoyant particles can be transported to the sediments (Cole et al., 2016). Buoyant MPs can also flocculate or clump together with non-buoyant particles, forming larger and denser agglomerates which may become heavy enough to sink in water or light enough to float at the surface.

Another mechanism involved in changing the rising and sinking pattern of MPs can be turbulence-induced mixing originating from currents in the water, such as those caused by inflow into shallow water systems, surface wind, temperature gradients, and wave breaking in the surf zone. In marine systems, wind-caused mixing can convey low-density MPs several meters down (Kukulka et al., 2012).

The particle's vertical transport driven by the ambient turbulence is affected by particle characteristics such as density, shape, and size.

The buoyancy of a particle is controlled by its density, while its size and shape influences the drag force the particle experiences, and hence the terminal velocity it can achieve in a liquid. In the aquatic environment, density, size, and shape are furthermore strongly related to biofouling, i.e., biofilm growth and adhesion of material to the surface of the particle (Shamkhani et al., 2021). For particles with low marginal density from the ambient fluid, particle size furthermore affects the relaxation time, which defines as the particle's response time to changes in ambient flow.

Particles of small size and small marginal density are more likely to get entrained with the flow and have a greater tendency to remain suspended in the water column and consequently be carried by water currents over longer distances before eventually settling out into sediments. On the other hand, large MPs, or particles with high marginal density, have higher relaxation time and tend to either settle or float more quickly.

It's important to emphasize that microplastic behavior and its migration in freshwater environments is complex as it is influenced by numerous factors. However, little is known about the complex motion of MPs, which must be better understood to develop successful management strategies. It is this issue, which is the focus of the current thesis: The motion, transport, and spread of MPs in turbulent freshwater systems.

CHAPTER 2. STUDY AIM AND OBJECTIVES

Freshwater systems are among other important in terms of their ecosystem value and as conveyance systems for MPs from inland sources to the oceans. However, lack of knowledge on the abundance and spatial pattern of MPs, and on the mechanisms and processes governing their transport and fate, delays taking effective mitigation measures and tackle the plastic pollution issue. It is the aim of this PhD study, to investigate the abundance of MP in freshwater systems and assess the governing mechanism behind the observed patterns. Focus is on lakes and stormwater facilities.

To address this aim, the study was divided into three research questions, with each being intended to address a specific sub-issue.

Research question 1: What is the fate of MPs in stormwater retention ponds?
To answer this, the abundance and distribution of MPs in the sediments of an urban stormwater pond in terms of MP mass and number concentration, size distributions, and polymer composition was assessed. The driving factors for the observed spatial patterns were investigated. Furthermore, a CFD model was set up to gain insights into the motion of buoyant MPs in shallow, highly dynamic water systems (Molazadeh et al., 2022).

Research question 2: What is the fate of MPs in an urban lake and what are the potential sources?

This objective was addressed by evaluating the MPs pollution level and distribution pattern in sediments from an urban lake.

Research question 3: How is the motion and transport behavior of buoyant MPs in a turbulent flow regime?

This aim was addressed by tracking the motion of marginally buoyant PE particles in a rectangular flume under various turbulent flow conditions, employing a particle tracking velocimetry technique.

CHAPTER 3. METHODOLOGY

The PhD study was carried out focusing on three subtopics, one for each research question:

- Investigate the fate of MPs a in stormwater retention pond
- Investigate the fate of MPs in an urban lake
- Investigate the transport of MPs in a turbulent flow regime

The first and second research focus was addressed by field campaigns where respectively a stormwater retention pond and a lake was sampled at many locations. MPs where then extracted from the samples and analyzed. For the retention pond, a simple and down scaled model of the stormwater pond was built in STAR-CCM+ to simulate the transport of buoyant MPs from the water to the sediments. The third research focus was addressed with a study carried out in an experimental flume where PE particles were injected into the flume and their trajectories tracked using particle tracking velocimetry.

3.1. THE FATE OF MPS IN STORMWATER RETENTION PONDS

The fate of MPs in the stormwater retention ponds was investigated by assessing the MP abundance and spatial distribution in the

sediment of an inland stormwater pond located in the city of Aarhus, Denmark.

Thirteen sediment samples were collected from the pond (Fig 3-1), using a van Veen grab sampler. The pond receives runoff from residential and commercial areas, and occasionally also illicit discharges of wastewater. It has an average stormwater residence time of 2 weeks (Molazadeh et al., 2022). For microplastic extraction and identification, samples underwent physical and chemical treatments including preoxidation, Sodium Dodecyl Sulfate (SDS) treatment, enzymatic treatment, and density separation. Samples were sieved through a 500 µm mesh. MPs below 500 µm were identified and quantified by microscopy coupled to a Fourier Transform Infrared microscope (µFTIR with Focal Plane Array). This approach has been proven to be a rather reliable method for MP quantification. MPs > 500 µm were visually sorted under a stereomicroscope and analyzed for their chemical composition by employing an ATR-FTIR. The commercial software package STAR-CCM++ was employed to model dynamic transport of light weight particles representing MPs. The CFD model was based on the Reynolds-averaged Navier-Stokes (RANS) equations, with a lagrangian phase to track particles, and the k-ε turbulence model. Further details are in Paper-I.

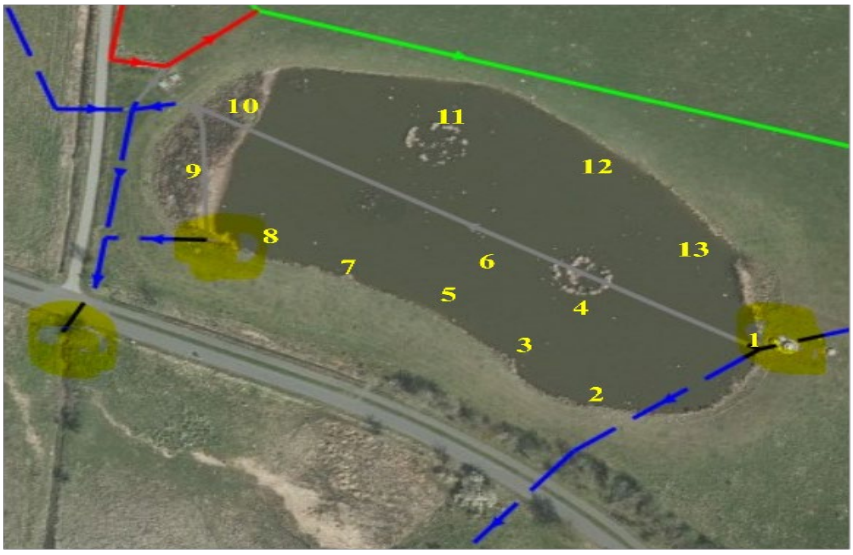

Fig 3-1. Sampling locations

3.2. THE FATE OF MPS IN URBAN LAKES

The fate of MPs including tire wear particles in urban lakes were assessed by studying the MP occurrence and distribution in the sediment phase of an urban lake, named Brabrand Lake, located in Aarhus, Denmark. The lake has a surface area of 153.8 ha and has a 310 km^2 catchment area. Its average depth is 1.1 m. To assess the MP pollution level, occurrence and distribution of MP across the lake was mapped by 13 sediment samples taken with a van Veen grab sampler in August 2021 (Fig 3-2). MPs in the size range of 10-5000 µm were extracted and analyzed following same method as

mentioned in the previous section, i.e., by applying a series of bio-chemical and physical extraction steps. The samples where then analyzed by Py-GC/MS for tire wear particles and μFTIR for other MPs. Further details are given in Paper-II.

Fig 3-2. Brabrand lake sampling points

3.3. BOUYANT MICROPLASTIC TRANSPORT IN AN EXPRIMENTAL FLUME

The transport behavior of marginally buoyant MPs in response to different flow conditions was assessed by injecting 40-47 µm spherical PE particles (ρ= 995 kg m^{-3}, Fig 3-3) in a 2 m long, 0.3 m wide, and 0.3 m deep, rectangular flume and following the particles trajectories by a particle tracking velocimetry technique (PTV). Different sets of experiments with having different bed types (medium gravel, fine gravel, medium sand, cohesive sediment, glass) at the bottom of the flume and different inlet velocities were conducted. For all the experiments the water level in the flume was kept at constant depth (h = 27 cm). Fig 3-4 shows the experimental flume. A high-speed camera and a laser, used to illuminate the area of interest in the flume, were employed to measure the instantaneous velocities in each test and track the trajectory of particles (Fig 3-5). A series of images was captured at a rate of 14.8 Hz for durations of 30 seconds. The rapid acquisition of images allowed for the tracking and monitoring of individual moving MPs while they passed through the field of view. The recorded images were further processed using a MATLAB image processing toolbox (The MathWorks Inc., 2020a) and the particle trajectories were tracked using algorithms developed by Standford University (Particle Tracking, Standford). Further details can be found in Paper-III.

Fig 3-3. PE particles used for injection

Fig 3-4. Rectangular glass flume

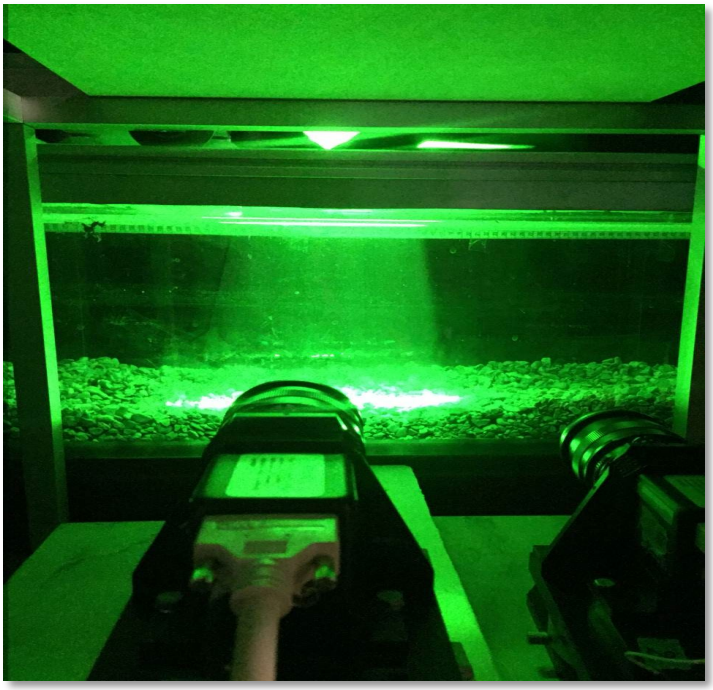

Fig 3-5. High speed camera and laser

CHAPTER 4. RESEARCH OUTCOMES

The research of the PhD study resulted in 3 scientific papers, aimed to address the three main research topics:

- Investigate the fate of MPs in a stormwater retention pond
- Investigate the fate of MPs in an urban lake
- Investigate the transport of MPs in a turbulent flow regime

4.1. OCCURANCE OF MICROPLASTICS IN SEDIMENTS OF STORMWATER RETENTION PONDS

The results of Paper-I showed high abundance of MPs in all 13 samples taken from a stormwater treatment pond in Aarhus, Denmark. The avarage MP concentration was found to be 44,396.86 item kg^{-1} corresponding to 11,839.98 μg kg^{-1}. There was no systematic variation of neither number nor mass concentration in the pond. The findings revealed that buoyant particles made up 96% and 86% of respectively the mass and the number of the total detected particles per kg of sediments. Small-sized PP particles were the dominating polymers at most of the sampled sites. Deposition of MPs in the pond's sediments did not follow any distinguishable pattern corresponding to their size and type. For each sampling location, the vast number of MPs were in the finest fraction (10–100 μm), whereas the coarsest portion (500–1000 μm) gave the least contribution to particle numbers. In contrast to the MP number, the finest particles represented a minor contribution to MP mass. The study further showed that mixing can be an explanatory factor for the transport of small sized and buoyant MPs from the water compartment the sediments of the pond. It was also found that MP abundance was positively correlated with organic matter content and the silt fraction of sediments, resulting in a greater accumulation of MPs in sediments with higher organic matter and silt contents.

4.2. FATE OF MICROPLASTICS INCLUDING TIRE WEAR PARTICLES IN SEDIMENTS OF URBAN LAKES

Paper-II mapped the occurrence and spatial MP pollution variability, including tire wear particles, in Brabrand Lake sediments. It attempted to identify local sources of MP pollution into the lake and investigate the relative abundance of different MPs. The Brabrand lake sediments hosted large amounts of MPs with a global average for MPs identified by µFTIR of 11,312 counts kg^{-1}, corresponding to 259.54 mg kg^{-1}. The global average concentration of tire wear particles over the lake was 19 mg kg^{-1}. No clear trend for MP concentration distribution was observed and the level of spatial variability in MP abundance varied widely, up to 6 orders of magnitude for MPs identified by µFTIR, among sampling sites. The same went for tire wear particles but to a lesser degree. PP and tire wear particles were the most abundant polymers across the lake.

Identifying potential MP input pathways and sources to the lake could help to answer the question of why Brabrand Lake was that polluted. MPs could have entered it via a river passing an upstream wetland and then discharging to the lake, or by another small stream which enters the lake and conveys discharge from a wastewater treatment plant. Besides inflow from the streams, discharge of treated and untreated stormwater represent other potential pathways to carry microplastics from to the lake and thus contribute to its high abundance of MPs.

Additionally, windborne MPs might be a source as might fragmentation of plastic litter in the lake itself.

4.3. TRANSPORT BEHVEIOUR OF PE PARTICLES IN RESPONSE TO DIFFERENT FLOW VELOCITIES AND BED CHARACTERISTICS

In Paper-III, a visualization technique (particle image velocimetry (PIV) and particle tracking velocimetry (PTV) was applied to investigate how ambient water regimes and conditions can bring buoyant PE particles, which are among the most abundant polymers identified in sediments from the natural environment, in contact with the bed. An experimental flume was used to study how turbulence affected their upward and downward movement compared to their intrinsic rising velocity while they were carried within the flow. Different sets of experiments with different flow velocities and bed types were conducted. The results showed that the turbulent flow regime led to the particle motion being rather chaotic, with velocities varying several orders of magnitude from their predicted velocity in still water (laminar flow conditions). Moreover, the results showed that turbulence distributed particles in the water column and a significant amount of the PE particles experienced significant downward vertical transport, which in turn enhanced the likelihood of them coming in contact with the bed and potentially sticking there. Under the studied conditions, the particles could move downward with an average velocity 255 times higher than their intrinsic rising velocity. The findings showed that mixing can be an explanatory

reason for detecting buoyant polymers in the sediment compartments of water bodies.

CHAPTER 5. CONCLUSIONS

The PhD study was divided into three main research questions, and for each question the following conclusion was drawn.

Research question 1: What is the fate of MPs in stormwater retention ponds?

Paper-I reported that buoyant particles made up the majority of identified particles in the sediments of the studied stormwater pond. Moreover, deposition of MPs in the pond's sediments did not follow any discernible pattern corresponding to their size and type. In other words, MP distribution in the sediments of the pond was not size and type (density) selective but distributed randomly between the sampling stations. The results of the computable fluid dynamics modelling showed that mixing was an explanatory factor for transport of MPs to the bottom of the water body, and that it spread them throughout the pond regardless of their characteristics. In the shallow yet highly dynamic water system studied, the dominant transport mechanism of MP from water to sediments was advection combined with turbulent dispersion (mixing). Hence, whether an MP reached the bottom of the pond was not significantly affected by its intrinsic rising or sinking velocity in quiescent water. Consequently, the intergraded effect of local hydrodynamic conditions can affect when an MP hits the pond bottom. Whether it gets immobilized at the sediment bed will then depend on the physicochemical properties of the bed and the MP in question. These findings contribute to understand why intrinsically

buoyant MPs are found in shallow water sediments, and can help improving solutions to avoid their spreading into natural water bodies.

Research question 2: What is the fate of MPs in an urban lake and what are the potential sources?

The results of Paper-II demonstrated that Brabrand Lake was highly polluted with MPs. The average MP pollution of the lake was even above that of sewage sludge, suggesting that lake sediment can serve as a long-term sink of plastic. The high MP concentration variability between sampling sites showed that spatial variability and patchiness must be considered when designing monitoring campaigns. The results furthermore emphasized the importance of considering TWP when taking mitigation decision as it was found to be the second most abundant polymer in the lake sediments. The comparison of equivalent sizes of buoyant and non-buoyant particles revealed that both buoyant and non-buoyant particles had similar distribution patterns. This implies that the predominant factor influencing their movement from water to sediment is likely related to turbulent transport and their small size, rather than to their density.

Research question 3: How is the motion and transport behavior of buoyant MPs in a turbulent flow regime?

The transport behavior of buoyant PE particles was investigated in an experimental flume by monitoring particles close to the bed (~6 cm from the bed). The motion of the observed particles was rather chaotic, and their trajectories tended to be random. The PE particles were moving both upward and downward at several orders of magnitude above their predicted Stocks velocity. This motion was mainly governed by the turbulent ambient flow. Even though in some experiments the net transport of MPs was upwards, many single particles moved towards the bed, some of which reached the bed zone where they might get trapped. This demonstrated that induced eddies had the capability to overcome the upward motion tendency of particles and transport them to the bottom part of the flume. Hence, transport of particles by turbulent induced mixing had a significant effect on MP transport.

5.1. MAIN CONTRIBUTIONS TO THE SCIENCE

Understanding the transport of MPs is critical in order to take effective mitigation measures and control the spread of this contaminant. However, scientific knowledge on physical transport mechanisms driving the motion of MPs within fluvial environments is very limited. The objective of this PhD was to provide insight into the fate of MPs in urban water systems as well as studying the processes responsible for transport of buoyant MPs from the water to the sediments.

Buoyant microplastics have been found to make up a major portion of MPs in sediments of various water bodies. However, there is lack of research that provide fundamental insights into the dominant processes and mechanisms driving the transport and migration of MPs from the water to the sediments. **Paper I** was among the very first studies combined field sampling data with computational fluid dynamic modeling results, to help to close the knowledge gap on migration processes of buoyant MP particles. Moreover, the high resolution field sampling in this study underlined the importance of taking a large number of samples to account for the patchiness of MPs in aquatic sediments.

Paper II contributed to improve the knowledge on MPs including TWPs in sediments of an urban lake. The lake is important for its neighboring region due to its proximity to the city's water supply wells, its significance as a habitat for various bird species, and its popularity as a local recreational site. Additionally, the outflow from the lake discharges into Aarhus Bay, making it a potential upstream source of plastic pollution in the bay. Given these factors, it becomes crucial to assess the load of MP, including TWP which are potentially more toxic than most MPs but often overlooked, and to implement effective mitigation strategies. This study provides useful information about the spatial pollution distribution and the level of contamination in the lake, information which can be used for future monitoring surveys and assessing environmental impacts.

The study carried out on microplastic motion under turbulent conditions, and tracking their trajectories in an experimental flume employing particle tracking velocimetry (**Paper III**), is the most innovative in this PhD thesis. It opens new paths to the investigation of microplastic transport, especially showing how this emerging contaminant interacts with the ambient flow and is affected by local hydrodynamics. It is of high importance to increase the knowledge on MP transport in fluvial environment and focus the effort to assess the transport behavior of different type, shape, and size of MPs exposed to various flow conditions.

LITERATURE

Andrady, A.L., 2011. Microplastics in the marine environment. Mar. Pollut. Bull. 62,1596–1605. https://doi.org/10.1016/j.marpolbul.2011.05.030.

Schernewski, G., Radtke, H., Hauk, R., Baresel, C., Olshammar, M., Osinski, R., Oberbeckmann, S., 2020. Transport and behavior of microplastics emissions from urban sources in the Baltic Sea. Front. Environ. Sci. 8, 579361. https://doi.org/10. 3389/fenvs.2020.579361

Chand, R., Kohansal, K., Toor, S., Pedersen, T.H., Vollertsen, J., 2022. Microplastics degradation through hydrothermal liquefaction of wastewater treatment sludge. J. Clean. Prod. 335, 130383. https://doi.org/10.1016/j.jclepro.2022.130383.

Chand,R., Rasmussen, L.A., Tumlin, S., Vollertsen, J., 2021. The occurrence and fate of microplastics in a mesophilic anaerobic digester receiving sewage sludge, grease, and fatty slurries. J. Science of The Total Environment. 798. 0048-9697,https://doi.org/10.1016/j.scitotenv.2021.149287.

Bollmann UE, Simon M, Vollertsen J, Bester K (2019). Assessment of input of organic micropollutants and microplastics into the Baltic Sea by urban waters. Marine Pollution Bulletin, 148: 149–155;

Liu F, Olesen KB, Borregaard AR, Vollertsen J (2019a). Microplastics in urban and highway stormwater retention ponds. Science of the Total Environment, 671, 992-1000

Liu F, Vianello A, Vollertsen J (2019b). Retention of microplastics in sediments of urban and highway stormwater retention ponds. Environmental Pollution, 255: 113335;

T. Islam, Y. Li, M.M. Rob, H. Cheng, Microplastic pollution in Bangladesh: research and management needs, Environ. Pollut. 308 (2022), 119697, https://doi. org/10.1016/j.envpol.2022.119697.

M. Eriksen, S. Mason, S. Wilson, C. Box, A. Zellers, W. Edwards, H. Farley, S. Amato, Microplastic pollution in the surface waters of the laurentian great lakes, Mar. Pollut. Bull. 77 (2013) 177–182, https://doi.org/10.1016/j.marpolbul.2013.10.007.

Meng, Y., Kelly, F.J., Wright, S.L., 2020. Advances and challenges of microplastic pollution in freshwater ecosystems: a UK perspective. Environ. Pollut. 256, 113445.

Hendrickson, E., Minor, E.C., Schreiner, K., 2018. Microplastic abundance and composition in western lake superior as determined via microscopy, pyr-GC/MS, and FTIR. Environ. sci. & tech. 52, 1787–1796.

Timmers, M.A., Kistner, C.A., Donohue, M.J., 2005. Marine Debris of the Northwestern. Hawaiian Islands: Ghost Net Identification. US Department of Commerce, National Oceanic and Atmospheric Administration, National Sea Grant College Program.

Timmers, M.A., Kistner, C.A., Donohue, M.J., 2005. Marine Debris of the Northwestern Hawaiian Islands: Ghost Net Identification. US Department of Commerce, National Oceanic and Atmospheric Administration, National Sea Grant College Program.

Liu, C., Zhang, W., Song, S., Li, H., 2019 (C). A novel method to improve carboxymethyl cellulose performance in the flotation of talc. Miner. Eng. 131, 23–27.

Chapter 3. Shamkhany, A., Li, Z., Patel, P., Karimpour, Sh., 2021. Evidence of Microplastic Size Impact on Mobility and Transport in the Marine Environment: A Review and Synthesis of Recent Research. Frontiers in Marine Science. 10.3389/fmars.2021.760649

Siyuan Yang, Ming Zhou, Xin Chen, Liping Hu, Yifeng Xu, Weng Fu, Chao Li, 2021. A comparative review of microplastics in lake systems from different countries and regions, Chemosphere, 286. Part.

Ye, S., and Andrady, A. L. (1991). Fouling of floating plastic debris under Biscayne
Bay exposure conditions. Mar. Pollut. Bull. 22, 608–613

Long, M., Moriceau, B., Gallinari, M., Lambert, C., Huvet, A., Raffray, J., et al. (2015). Interactions between microplastics and phytoplankton aggregates: impact on their respective fates. Mar. Chem. 175, 39–46.

Lobelle, D., Cunliffe, M., 2011. Early microbial biofilm formation on marine plastic debris. Mar. Pollut. Bull. 62, 197–200.

Cole, M., Lindeque, K.P., Fileman, E., Clark, J., Lewis, C., Halsband, C., Galloway, S.T., 2016.

Microplastics alter the properties and sinking rates of zooplankton faecal pellets. Environ. Sci.Technol. 50, 3239–3246. https://doi.org/10.1021/acs.est.5b05905

Kukulka, T., Proskurowski, G., Morét-Ferguson, S.,Meyer, D.W., Law, K.L., 2012. The effect of wind mixing on the vertical distribution of buoyant plastic debris. Geophys. Res. Lett. 39. https://doi.org/10.1029/2012GL051116.

https://web.stanford.edu/~nto/software_tracking.shtml/ (accessed 25 July 2023)

Paper-I

Buoyant microplastics in freshwater sediments – How do they get there?

Science of the Total Environment 860 (2023) 160489

Contents lists available at ScienceDirect

Science of the Total Environment

journal homepage: www.elsevier.com/locate/scitotenv

Buoyant microplastics in freshwater sediments – How do they get there?

Marziye Molazadeh [a,*], Fan Liu [a], Laura Simon-Sánchez [b], Jes Vollersten [a]

[a] Aalborg University, Section of Civil and Environmental Engineering, Department of the Built Environment, Thomas Manns Vej 23, 9220 Aalborg Øst, Denmark
[b] Institute of Environmental Science and Technology (ICTA-UAB), Universitat Autònoma de Barcelona, 08193 Cerdanyola del Vallès, Barcelona, Spain

HIGHLIGHTS

- MP content in the pond sediments varied up to two orders of magnitude.
- Buoyant MPs made up 95.4 % of the MP-mass and 83.5 % of the MP-number.
- No trend in the spatial distribution of MPs – neither concentration, size, nor polymer
- Mixing is an important factor for transporting buoyant MPs to the pond sediments.
- Sediment contents of silt and organic matter correlate with the MP-distribution.

GRAPHICAL ABSTRACT

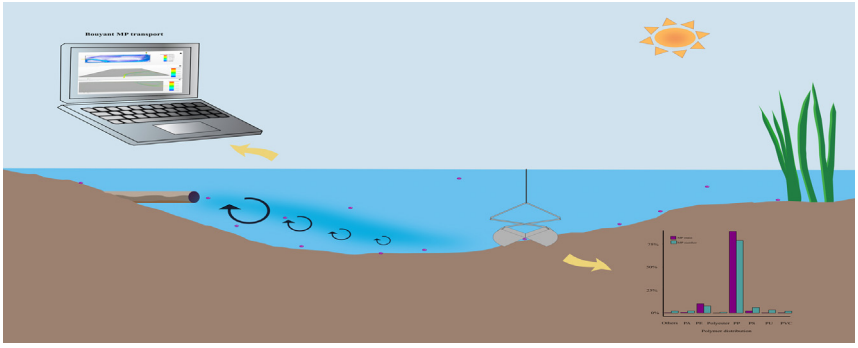

ARTICLE INFO

Editor: Dimitra A Lambropoulou

Keywords:
Buoyant MPs
Stormwater ponds
Sediments
CFD

ABSTRACT

The accumulation of microplastics (MPs) in the sediments of a stormwater treatment pond was studied to gain knowledge on how these facilities protect the natural environment against this emerging pollutant. Thirteen sediment samples were analyzed for MPs down to 10 μm, mapping the pattern of accumulation in the pond. The average abundance in terms of MP-number and mass was 11.8 μg kg^{-1} and 44,383 item kg^{-1}, respectively. They were rather unevenly distributed, with concentrations varying up to two orders of magnitude within the pond, showing that a trustworthy quantification of MPs retained by such units must rely on many and well-distributed subsamples. Buoyant MPs made up 95.4 % of the MP-mass and 83.5 % of the MP-number and in most of the sampled locations, polypropylene dominated the polymer fingerprint, followed by polyethylene. No spatial pattern in the distribution of MPs in the pond was identified. Instead, the MP content correlated to the organic matter and silt content, indicating that the processes leading to deposition could be similar. A computational fluid dynamics model was set up and used to simulate the transport mechanisms governing the conveyance of MPs in the pond from water to sediments. The results showed that the combination of advection and dispersion were likely the driving mechanism for buoyant (and non-buoyant) MPs to get in contact with the sediment bed and spread over the pond. Once in contact with the sediments, the MPs would have some probability of being permanently incorporated and hereby preventing them from entering the downstream aquatic environment.

1. Introduction

Plastics are an inevitable part of the modern world, and today's humans depend extensively on plastics for commercial, industrial, medical, and municipal applications. However, the ever-increasing production and use of plastic products has also paved the way for them to become serious environmental pollutants. The bulk of the plastic produced each year is used to make single-use products like disposable packaging or other short-lived items that are discarded within a year of manufacture (Hopewell et al., 2009). It is estimated that worldwide only 9 % of the plastic ever made is recycled and 12 % incinerated (Geyer et al., 2017). The rest is disposed of

* Corresponding author.
E-mail address: marziyem@build.aau.dk (M. Molazadeh).

http://dx.doi.org/10.1016/j.scitotenv.2022.160489
Received 8 August 2022; Received in revised form 17 November 2022; Accepted 21 November 2022
Available online 28 November 2022

at landfills or mismanaged, ending up in natural habitats. Despite the high persistence of synthetic polymers, large plastic items eventually fragmentate, mainly because of weathering caused by exposure to solar ultraviolet radiation and gradual loss of weight due to physical damage (Andrady, 2011). This degradation produces microplastics (MPs), commonly defined as plastic particles smaller than 5 mm in size (Arthur et al., 2009). Plastic particles which are derived from fragmentation of larger plastic items are commonly termed secondary MPs. Some MP particles are intentionally manufactured, for example, for direct usage in cosmetics and abrasives, or as raw materials to produce larger plastic items. These are commonly defined as primary MPs (Cole et al., 2011).

MPs, whether they be primary or secondary ones, are detrimental to the environment since they can be associated with a wide range of pollutants and toxic substances either from their production process, due to their adsorption characteristics, or by ingestion throughout the food web (Besseling et al., 2019; Cole et al., 2011). Since most plastic is produced and used inland (Boucher et al., 2019), urban areas are identified as important contributors of MPs into the environment. MPs can be introduced into urban freshwater and marine systems from various sources and through diverse routes. Stormwater, wastewater, and combined sewer overflows are commonly considered significant potential sources, discharging MPs to water bodies in urban areas (Schernewski et al., 2020). Freshwater MPs can ultimately end up in oceans if effective mitigation measures are not taken.

Stormwater runoff can be quite polluted as it 'cleans' the city's surfaces of all sorts of dirt and debris. It collects soluble and particulate pollutants, including MPs, and conveys them to downstream environments. It is hence common to install stormwater treatment facilities to protect the aquatic ecosystems. Their purpose is to detain and treat wet weather runoff flows to prevent damaging recipient water systems by mitigating the peak flow (F. Li et al., 2019; Duan et al., 2016) and trapping incoming particles into their bottom sediments (Gu et al., 2016). Retainment of particles is considered the most important process in stormwater runoff pollution removal. However, when it comes to MPs, there is a lack of knowledge on the degree to which they are retained, and which mechanisms are involved, leading to an inability to quantify their efficiency towards MPs and an inability to optimize their design towards this pollutant. MPs cannot per se be expected to behave like the bulk of stormwater particles as these mainly consist of sand, silt, and clay mixed with some organic debris. MPs, comprising both buoyant and non-buoyant polymers, may follow different floating and settling patterns. They may also have different physical properties such as Zeta potential, which would affect flocculation and attachment to surfaces.

The variability of MP type and load on stormwater facilities mainly depends on the pluviometric regime and the urbanization characteristic of the catchment. To date, MPs in the sediments of stormwater ponds have only been documented in a few studies (Liu et al., 2019b; Olesen et al., 2019; Ziajahromi et al., 2020; Moruzzi et al., 2020; Lutz et al., 2021). The majority of these were of polymers lighter than water (Liu et al., 2019b; Olesen et al., 2019; Lutz et al., 2021) and cannot be expected to have sunken to the bottom. Other transport mechanisms must hence have been in play for these floating MPs to reach the sediments. Possible candidates for such mechanisms are the ballasting of particles by biofilm formation, aggregation with other stormwater non-buoyant particles, ingestion and excretion by aquatic biota, as well as turbulent transport. These mechanisms have been reported to affect sedimentation and accumulation of buoyant MPs in some systems under some conditions (Kooi et al., 2017; Olesen et al., 2019).

However, research providing fundamental knowledge on prevailing processes and mechanisms that govern the movement and transport of MPs from water to sediments of shallow water systems is surprisingly scarce, and the MP migration processes remain poorly understood. It is necessary to address these and understand how shallow water bodies act as sinks for microplastics to actively design technical solutions for MP pollution management such as stormwater ponds, and to assess the efficiency of existing systems. The knowledge is furthermore important when understanding how natural shallow water bodies act as sinks for microplastics.

It is the objective to contribute to fill the knowledge gap on how MPs are retained by ponds designed to treat stormwater runoff, hereby mitigating impacts on the natural environment. The approach is to investigate the distribution of MPs in the sediments of one such pond in terms of MP-mass and number concentration, size distributions, and polymer composition. The results are intended to inform future studies on how to consider spatial variability of MPs in stormwater pond sediments, for example when sampling to quantify pond retention efficiencies. The driving factors for the observed spatial patterns are evaluated, as is the relation to sediment characteristics. For this evaluation, a 3D computable fluid dynamics (CFD) model was set up to gain a fundamental understanding of buoyant MP particle transport from the water to the sediments. These findings are intended to shed light on some key aspects of (buoyant) MP motion and fate in shallow, highly dynamic water systems.

2. Material and methods

2.1. Sample collection

Thirteen sediment samples were collected in August 2020 from a stormwater pond in Aarhus, Denmark (Fig. 1), using a Van Veen grab sampler. The pond receives runoff from residential and commercial areas, and occasionally illicit discharges of wastewater. The pond has an average stormwater residence time of two weeks and was constructed in 2008. The samples were taken during one dry weather day with no rain occurring for more than two days prior to the sampling. From each grab of sediments, the top 5–8 cm were collected and stored in glass jars, resulting in 2–3 kg bulk sediments for each location. All jars were transported to the laboratory and stored at 4 °C until further analysis.

2.2. Physicochemical characteristics of sediments

The organic matter content of the sediments was measured as loss-on-ignition by heating the dried sediments to 550 °C for 4 h in a muffle furnace (ASTM, 2000). To determine the grain size distributions, sediments were first treated with hydrogen peroxide (H_2O_2) to remove organic matter and consequently avoid hindering the size classification process. The oxidation was done as described in Section 2.3. Sediments were then dried at 105 °C for 24 h and homogenized. Collected sediment samples were characterized and separated into five different size fractions: <2 μm (clay), 2–63 μm (silt), 63–200 μm (fine sand), 200–630 μm (medium sand) and 630–3500 μm (coarse sand). The grain size distribution of each sample was determined using sieves with different mesh sizes for sediments larger than 63 μm and a hydrometer test for sediments smaller than 63 μm (Asadi et al., 2019).

2.3. Microplastic extraction

The bulk sediment (2–3 kg) samples were homogenized and subsamples representing 1.5 kg wet weight were treated. The subsamples were divided into several smaller batches and pre-oxidized in 5 L beakers by gradually adding 50 % hydrogen peroxide (H_2O_2) and Milli-Q water to the sample. H_2O_2 was added to a maximum of 10 % final concentration. The samples were stirred while oxidizing. The oxidation was continued until no foaming occurred when adding hydrogen peroxide. This procedure was repeated in all the batches until all 1.5 kg of sediments had been oxidized. The resulting oxidized sediments were combined and wet sieved on a 2 mm stainless steel sieve (Retsch GmbH, Germany). The sieved samples (<2 mm) were transferred to covered crystallizing dishes and placed in an oven at 50 °C for 5 days. For every sample, a dried sediment subsample of 200 g was taken for MP extraction and underwent density separation. The MP abundance was normalized to a concentration based on this dry weight. The process was performed in a 2-L pear-shaped separation funnel containing a sodium polytungstate (SPT) solution of density 1.89 g cm^{-3}.

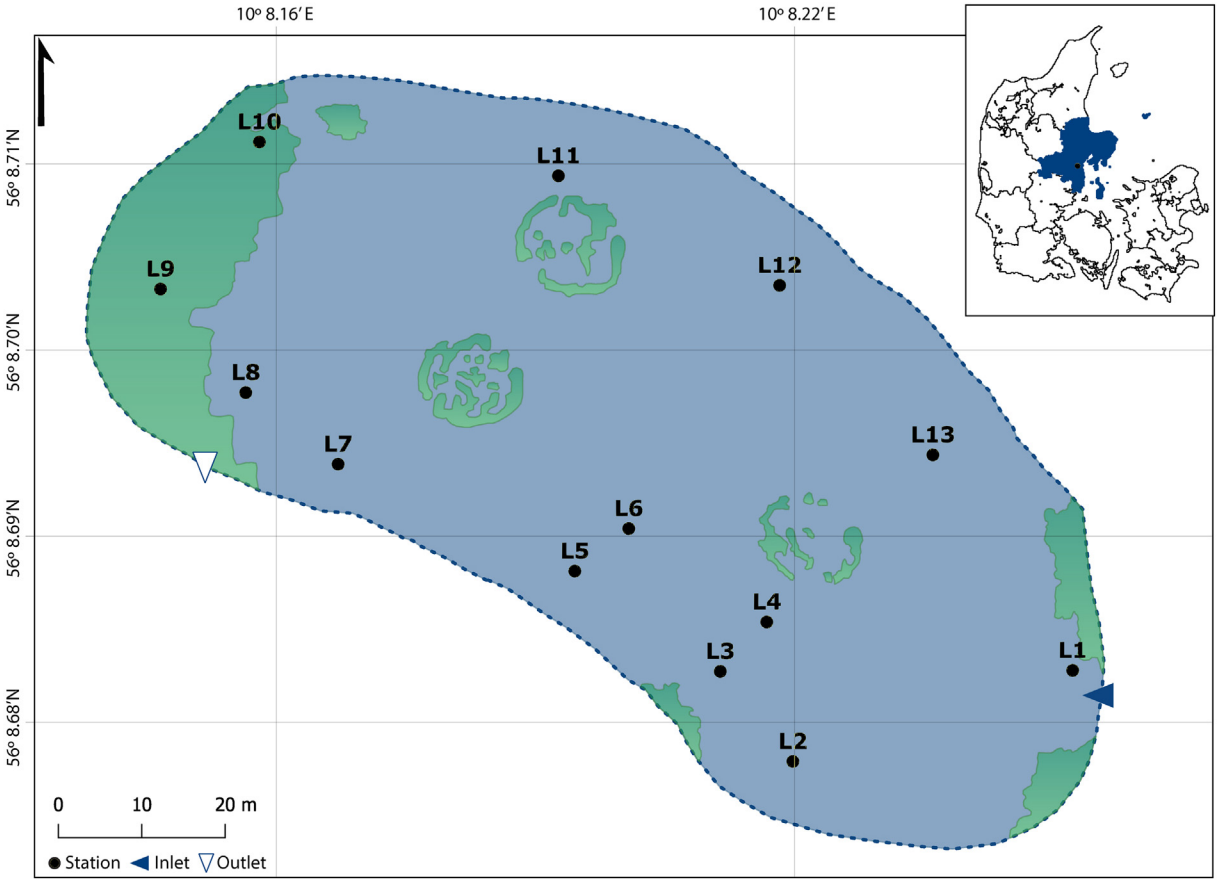

Fig. 1. Map of the pond showing the location of all the sampling stations. L stands for location. The green area in the left, where samples 9 and 10 were taken, is a shallow part of the pond with water depths about 0.2 m. The green areas in the centre (the circles) are areas with lower water depth (about 0.5 m) while the ones on the sides are some vegetation that has grown into the pond.

The mixture of sediments and SPT was aerated by compressed air from the bottom of the funnel for 30 min and left to settle for 24 h. Three-quarter of the bottom part was drained off and the floating particles collected and kept in a glass beaker. The process was repeated twice, meaning that the discarded part, which included the sediments, was collected and transferred back to the separation funnel and the whole process repeated to minimize the loss of particles in this step. The collected floating particles from both repetitions were filtered on a 10 μm steel filter. Subsequently, the filter was ultrasonicated to detach the particles and transfer them into a 300 mL sodium dodecyl sulfate solution (SDS, 5 % w/vol). The samples were incubated for 48 h at 50 °C and continuously mixed. The filtered particles went through enzyme purification steps with a blend of cellulase (Cellulase enzyme blend®, Sigma-Aldrich) and cellulolytic enzymes (Viscozyme®L, Sigma-Aldrich), again for 48 h at 50 °C, followed by protease, also at 50 °C for 48 h (Protease from Bacillus sp.®, Sigma-Aldrich) (Chand et al., 2022). A Fenton oxidation was performed by transferring the filtered particles into 200 mL of Milli-Q water and adding 145 mL of 50 % H_2O_2, 65 mL of 0.1 M NaOH, and 62 mL of 0.1 M $FeSO_4$ while maintaining the temperature at 15–30 °C. In order to separate larger particles (MP > 500 μm) from smaller ones (10 < MP < 500 μm), a 500 μm mesh sieve and a 10 μm stainless steel filter were used. The large particles retained on the sieve were collected and dried in an oven at 50–60 °C for later analysis. The smaller particles were transferred to a 250 mL separation funnel containing SPT (density of 1.89 g cm^{-3}) and the same separation procedure as previously described was performed. The particles were then filtered and collected into ultra-pure HPLC grade 50 % ethanol using an ultra-sonicating bath. The ethanol solution containing the particles was transferred to 10 mL vials and the ethanol evaporated in an evaporation bath (TurboVap® LV, Biotage) at 50 °C. Finally, the ethanol level in the vials was adjusted to 5 mL and particles were suspended in ultra-pure HPLC quality 50 % ethanol.

2.4. MP identification and quantification

Particles >500 μm suspected to be of plastic were manually sorted and imaged under a stereomicroscope (ZEISS, SteREO Discovery.V8, Oberkochen Germany). Particle dimensions were measured using ZenCore (Zen2Core SP1 from ZEISS) software. The particles were then analyzed by ATR-FTIR spectrometry (Cary 630, Agilent Technologies, with a single reflection diamond ATR). Interpretation of the particles' IR spectra was done using OMNIC software and its library (Thermo Fisher Scientific Inc., 8.2.0.387 version 1). However, particles above 1 mm in longest dimension were only occasionally detected in the samples and hence deemed outliers and not included in the study. Hence 1 mm was chosen as the upper size limit when reporting the data. For analyzing particles between 10 and 500 μm, FPA-μFTIR imaging was applied (Agilent Cary 620 FTIR microscope equipped with a 128 × 128 pixel FPA (Mercury Cadmium Telluride detector) and coupled to an Agilent 670 IR spectroscope). Sample deposition steps and instrument settings were similar to that of Chand et al. (2022) and Rasmussen et al. (2021). Briefly, a small sub-sample was taken of the particle suspension (the 5 mL of 50 % ethanol) using a glass pipette and deposited on a zinc selenide window (Ø13 × 2 mm, Crystran, UK) held in a compression cell with a Ø10 mm free area (Pike Technologies, USA). The window with its deposited particles was dried on a heating plate at 50 °C and the process repeated until the window was homogeneously covered by particles. Three windows from each sample were scanned. The resulting 3 × 3.2 million spectra from the scanning of the 10 × 10 mm area were processed applying the software siMPle, a software for

the automated detection of MP from μFTIR chemical imaging datasets (Primpke et al., 2020). siMPle analyses each individual spectrum by comparing it to a reference library and uses this to build images of MP particles (Liu et al., 2019a). The database used contained 124 reference spectra of plastics belonging to 35 polymer groups as well as natural organic materials, namely 7 groups which can be misinterpreted as plastics. The software provides particle dimensions, area, volume, and mass estimates of MPs (Primpke et al., 2020).

2.5. Contamination assessment

To avoid potential contamination during sample processing, all glassware and other equipment were rinsed three times with particle-free water and stainless-steel filters were muffled at 500 °C before use. Samples were covered with aluminium foils or glass watches during each treatment step. All liquid reagents were filtered through 0.7 μm glass fibre filters prior to use. Additionally, cotton lab coats were worn during all experimental steps. To minimize contamination from the ambient air, samples were processed inside a clean fume hood and the air in the FTIR and microscope lab room was continuously filtered with a Dustbox® (Hochleistungsluftreininger, Germany) holding a HEPA filter (H14, 7.5 m^2). Although many precautions were taken, contamination cannot be completely avoided. Considering this potential background contamination, three laboratory procedural blanks were analyzed in parallel with the samples. 200 g of muffled (500 °C) sediment surrogate, consisting of 75–1000 μm sand, was used for each blank. This amount is similar to the mass processed per sample. The blank control samples went through the same processes as the sediment samples. In the first iteration of using siMPle to identify MPs, an extraordinary amount of PP and PE particles were detected in some samples. The spectra of these suspicious particles were checked one by one, and many were found to be false positive identifications of some unknown natural material. To avoid these false positives, their spectra were included in the siMPle library as natural materials and assigned to a new group named 'fake particles'. Subsequently, all samples were analyzed again with the siMPle software using the new library. An example of these spectra is given in supplementary materials Fig. S1.

2.6. Statistical analysis

Statistical analyses were performed using R (version 3.5.3) and at a significance level of 0.05. The normality of the data was assessed by Shapiro-Wilks test. Kruskal-Wallis test was applied to investigate if there were differences in MP sizes and masses between different samples. Wilcoxon rank-sum test for pairwise comparisons was performed to compare the size and mass distribution of MP particles and identify those samples that differed significantly.

2.7. CFD simulations

The STARCCM + + commercial software was used to simulate flow fields. The particle tracking facility of the software was used to calculate MPs trajectories. For the continuous phase, a segregated flow model was used with the density of the fluid assumed constant. The fluid flow equations solved by the CFD model are based on the conservation of mass and momentum (Versteeg and Malalasekera, 1995). The flow was simulated as steady-state. All numerical simulations performed in this study solved the Reynolds-Averaged Navier-Stokes (RANS) equations with the k-ε (production and dissipation of turbulent kinetic energy) turbulence model. Details of the theoretical formulation can be found in the user guide of STARCCM + +. The inlet boundary condition was defined as velocity inlet corresponding to a storm condition with a relatively high inlet flow velocity. For the sloped walls and bottom of the pond, a non-slip wall condition was defined and the boundary condition for the outlet was assumed as a pressure outlet. The boundary condition for the water surface was set as a symmetry plane (Adamsson et al., 2005; Tamayol et al., 2010; Khan et al., 2013). The mesh sensitivity analysis of the results was performed by comparing velocities from the simulations with different numbers of meshes to ensure the solution was independent of mesh size and number. Four mesh densities were assessed: 14,586,364, 3,730,862, 1,892,719 and 1,101,167 cells. The number of 3,730,862 cells was found adequately fine and used in the subsequent analysis.

The Lagrangian Multiphase approach named 'particle tracking', was chosen to model the dispersed phase (i.e., MPs). A one-way coupling (uncoupled) approach between the flow field and MP load was chosen.

Several scenarios with varying inlet velocity, particle sizes and material densities were simulated, leading to similar conclusion thus one example is illustrated. In the example model the particles were modelled as spherical solids of 100 μm diameter and 900 g cm^{-3} density. To model particle dispersion, the effect of the fluid turbulence on the particle motion, the turbulent dispersion model was activated. Drag, gravitation, and buoyancy are the dominant forces exerted on the particles by the surroundings, including the continuous phase. These forces were included in the model. The drag coefficient was modelled using the Schiller-Naumann correlation. The boundary condition for the Lagrangian phase was assigned to 'escape' for all walls, meaning that once a MP hit the pond bottom or a wall, it was removed from the simulation.

3. Result and discussion

3.1. MP abundance

MPs were abundant in the pond with a global average for the 13 samples of 44,383 item kg^{-1} and 11.8 mg kg^{-1} of dry sediments (Table S1). The blank contamination was low compared to the measured concentrations with the highest contamination accounting for 0.1 % of the averaged measured value in terms of MP number concentration and 0.003 % in terms of MP mass concentration. Due to the low contamination compared to the MP abundance, the results were not corrected for contamination. A detailed description of MP contamination in blanks is given in supplementary materials in the section "MPs in blanks in supplementary file".

Comparing to other studies, our findings were lower than those of Olesen et al. (2019), who found 401.5 mg kg^{-1} and 9.5 × 10^5 item kg^{-1} in the sediments of a stormwater pond in Denmark. That pond was constructed in 1993 and dredged 10–15 years before sampling. It is in same region of Denmark as our pond and experiences similar climate conditions including rainfall patterns. The same goes for the seven stormwater retention ponds investigated by Liu et al. (2019b), which were constructed between 2005 and 2009. One of those ponds was the same as in the current study (termed C1 in their study). For that pond, they found approx. 2 times lower MP number and mass concentrations, even though they applied a quite similar sample purification and analysis approach. However, their sediment sample 'only' comprised three grab samples which were combined before analysis, whereas our study collected and analyzed thirteen separate samples from various positions in that pond. A likely explanation is hence sampling uncertainty caused by the high spatial variation in the pond (Table S1 in the supplementary materials, details in Section 3.2).

The MP concentrations extracted from sediments of a Gold Coast (Australia) stormwater wetland (Ziajahromi et al., 2020) and five open stormwater drainage systems in Australia (Lutz et al., 2021) were also lower than the average MP concentration detected in the present work. Ziajahromi et al. (2020) reported an average of 595 ± 120 item kg^{-1} dry sediment at the pond inlet and 320 ± 42 item kg^{-1} at its outlet. The mean concentration quantified by Lutz et al. (2021) for the five drainage systems was 664 item kg^{-1}. Other factors than inhomogeneity in the spatial distribution of MP can have led to the differences among the studies. One is that loadings from the catchment might differ due to land use, climate conditions such as rainfall patterns and amounts, and hydraulic loading (catchment impervious area per pond surface area, m^2/m^2). Age and hereby time for accumulation of MP might also have differed. Another possibility is that sample preparation can differ, where differences in filter mesh sizes, specific density of liquids used for density separation, and protocols for removal of organic material can lead to differences in extracted

MP. Once extracted, the instrument used for chemical quantification of extracted samples makes a difference on which MP polymer types can be identified and to what size they can be quantified (Primpke et al., 2020a,b). How much of a difference can be attributed to the analytical method is unclear, but several orders of magnitude have been reported (Lv et al., 2019), and it seems likely that this is one of the major reasons for the observed differences between studies.

MPs were assigned to six commonly used size fractions (Fig. 2) (Peng et al., 2017; Zheng et al., 2020; Liu et al., 2021). Most of the identified MPs, 4130 particles or 72.3 %, were in the size range of 10–100 μm. However, they contributed only 3.4 % to the total mass. Conversely, few large-sized particles (93 MPs of 500–1000 μm) constituted 50.4 % of the mass. MP abundance decreased as size increased (Fig. 2A), an observation which has also been made in other MP studies (Liu et al., 2019b).

The μFTIR analysis identified MPs belonging to 18 of the 35 addressed polymer types. Among these, 11 types were identified only in low amounts, accounting for 0.5 % and 2.2 % of MPs mass and number concentrations, respectively. These were assigned to a group termed 'Others'. Details regarding these polymers can be found in the supplementary materials (Table S2). Overall, the sum of the buoyant polymers (Polyethylene (PE): 0.9 g m^{-3}, Polypropylene (PP): 0.9 g m^{-3}) comprised 95.4 % and 83.5 % of mass and number of the identified MPs in the sediments. The water phase of same pond was studied by Liu et al. (2019a) who found that PP and PE together constituted >95 % of both the MP mass and number in the pond water.

PP was the dominant polymer, making up 85.6 % and 76.0 % of MP mass and number concentrations, respectively. The second most abundant polymer was PE, followed by Polystyrene (PS) and Polyamide (PA) in terms of mass and number (Fig. 2B). Although the number of Polyurethane (PU) particles was higher than that of Polyvinyl chloride (PVC), PVC contributed more to the total mass of particles, which can be due to the lower density of PU particles compared to PVC ones. These results are in accordance with several recently reported studies, where PP and PE were predominant polymers in the sediments (Lutz et al., 2021; Liu et al., 2019b; He et al., 2020; Olesen et al., 2019; Fan et al., 2019; all covering freshwater systems). Finding high concentrations of PP and PE in the sediments can be associated with their widespread use, from food packaging to the automotive industry. However, these materials are buoyant and must hence have been conveyed to the pond sediments by other mechanisms than simple density settling. A discussion of such mechanisms is given in Section 3.3.

3.2. Spatial MP distribution

Spatial distribution of MPs in the pond showed no systematic trends in terms of neither number nor mass concentrations (Table S1 and Fig. 3A). L2 and L6 were respectively the least and the most polluted locations in terms of number even though they were not far apart. Considering mass concentration, the least and most polluted locations were L2 and L11, which were on each their side of the pond.

Ziajahromi et al. (2020) sampled sediments close to the inlet and outlet of an Australian wetland, reporting the lowest MP concentration (number) at the outlet. They ascribed this to faster settling of high-density polymers and biofouling-assist settling of low-density polymers, albeit with no experimental verification hereof. It should be noted that the authors restricted their sampling to two locations (inlet and outlet), limiting the statistical strength of their statement.

The polymer composition at sampling sites did not follow a clear trend across the pond. Buoyant MPs, and especially those of PP, dominated at nearly all locations, both in terms of mass and number (Fig. 4A). PE was also common at all locations, albeit to a lesser degree. With respect to the non-buoyant polymers, polystyrene, polyamide (PA), polyurethane (PU), and PVC occurred at significant concentrations. The fact that both negatively and positively buoyant MPs were found reflect that the transport mechanism to the sediments was not simple sedimentation in calm water, but that the deposition was governed by some other mechanism.

For all sampling locations, the largest number of MPs were in the finest fraction (10–100 μm) and the lowest number in the coarsest fraction (500–1000 μm), which agrees with many previous studies, for example Kooi et al. (2021) who used a similar analytical technique as in the present study to characterize >60,000 MPs from different aquatic compartments and how they distributed in terms and size and other parameters. While the highest particle counts were found in the finest fraction, it only represented a minor contribution to the total mass (Fig. 4B), which is in line with what for example Huber et al. (2022) addressed for degradation of polypropylene from packaging materials and what Rasmussen et al. (2021) reported for raw wastewater.

The size and mass distribution of particles in each sample are illustrated in Fig. S2A, B and Table S3. No clear trend of size distribution versus location in the pond could be identified. This conclusion was confirmed by comparing the size distribution at all sites applying a non-parametric Kruskal-Wallis test (as data were not normally distributed as tested by a Shapiro-Wilk normality test). While the size distribution at some sites differed significantly ($p < 0.05$) from some others, the location of these sites showed no clear trend. Moreover, some sites, regardless of their locations, revealed a similar distribution of individual particles size ($p > 0.05$) (Table S4). Likewise, the mass of particles followed similar behavior to size (Table S5). In other words, the chance of finding a MP of a certain mass or size at a certain location in the pond did not show a systematic trend. The seeming randomness of the distribution of MPs in the sediments implies that the phenomena leading to their entrapment are complex. Gu et al. (2016) pointed out that a wide range of factors such as wind, vegetation, inflow patterns, construction of the outlet, turbulence levels, and

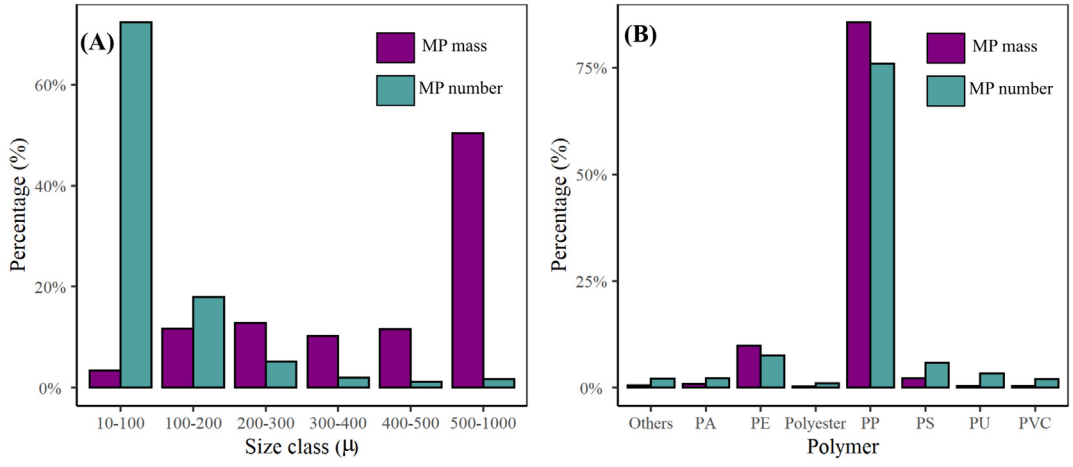

Fig. 2. MP percentage in each size class (A) and polymeric composition (B) of identified particles in terms of MP mass and number concentration.

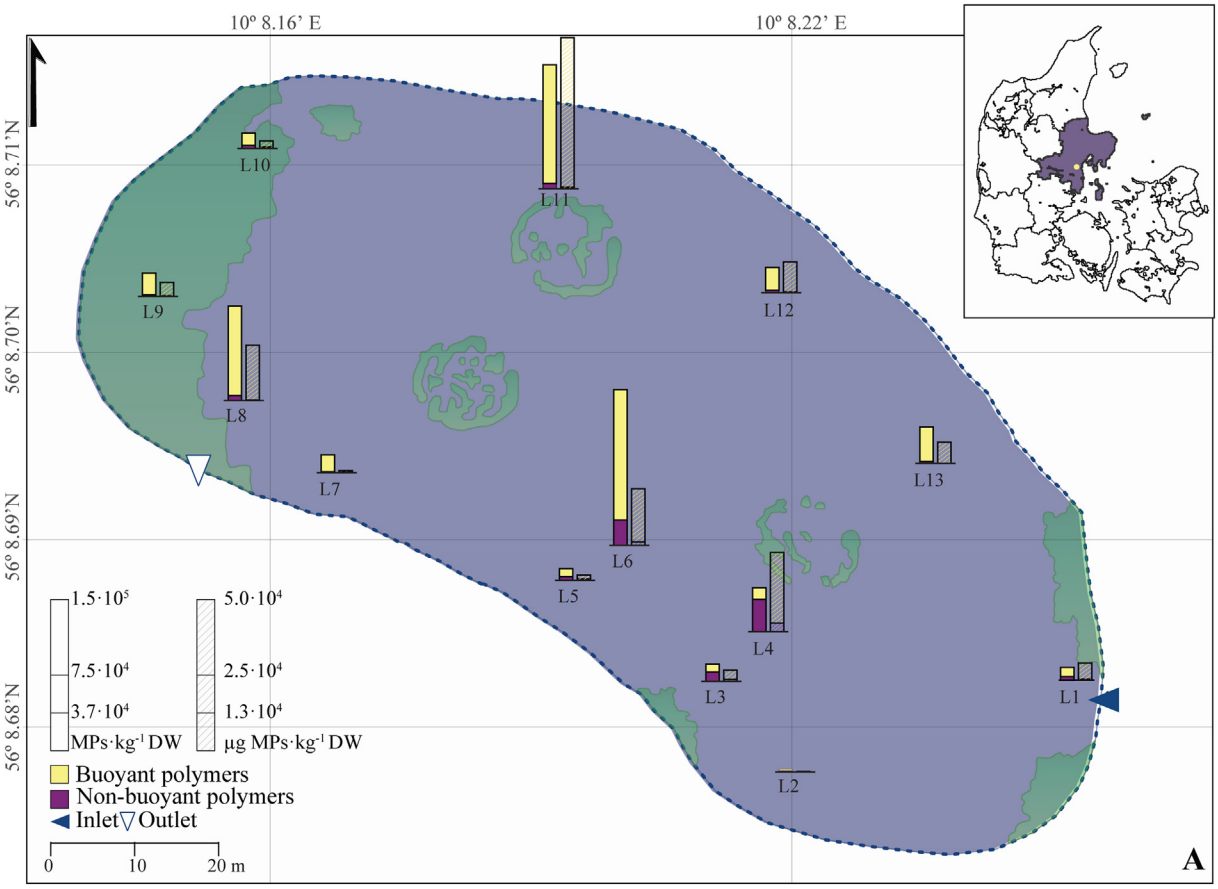

Fig. 3. Map showing the spatial distribution of MPs in terms of mass and number over the pond.

more, cannot be neglected when trying to conceptualize how particles are retained in a stormwater pond. It seems likely that the reason for the seemingly random distribution of MPs in the sediments of the studied pond is linked to such phenomena.

Contrary to our findings, Besseling et al. (2017), and using a hydraulic modelling approach to estimate the fate of non-buoyant micro- and nanoplastics, found that MP accumulation sites were dependent of particle size and argued that large-sized MP particle must be more abundant upstream than downstream, since they settle faster. This difference in findings can be due to gravimetric settling not being the main driving process for conveying MPs, especially the buoyant ones, from the water column to the sediments.

While there was no clear trend of where the MPs ended up in the pond, there was a clear positive correlation between organic matter and MP content in terms of both number ($r = 0.77$, $p < 0.05$) and mass ($r = 0.65$, $p < 0.05$) concentrations (Figs. S3 and S4). A similar trend was observed for silt and MP number ($r = 0.64$, $p < 0.05$) as well as mass ($r = 0.56$, $p < 0.05$) concentrations. No correlation was seen between clay and MP nor sand and MP. These findings agree with several other studies, where Liu et al. (2021), Corcoran et al. (2020), and Liu et al. (2019b) all found that MP abundance in sediments correlated positively with organic matter content, and Falahudin et al. (2020) and Liu et al. (2021) found that MP correlated positively with the silt content of marine and river sediments, respectively. One reason might be that hydrophobic organic matter agglomerates with hydrophobic MPs (Mato et al., 2001; Hong et al., 2017). Moreover, while correlation does not necessarily imply causality, the fact that sediment MP contents correlated with silt and organic matter implies that the transport mechanisms causing differences in these parameters may also be related or even similar.

He et al. (2020), on the other hand, reported a positive correlation with the clay content of river sediments. However, F. Li et al. (2019) and Y. Li et al. (2019) showed that settling of low-density polymer particles was not affected by adding clay particles to the suspension. These contradictory findings across varied aquatic systems and conditions suggest that the occurrence of MPs in sediments cannot be simply predicted by only the composition of the sediments, but is influenced by other site-specific confounding factors, among them site-specific hydrodynamics.

3.3. Transport mechanisms

The finding that there was no systematic relationship between sampling location and MP characteristics in terms of mass, size, and polymer composition shows that simple gravimetric settling cannot explain how MPs end up in the sediments of the pond. The question hence arises what can explain the observed MP-distribution, especially the fact that most MPs in the sediments were buoyant. One mechanism can be ballasted sedimentation where non-buoyant biofilm forms on a buoyant MP, allowing the ballasted particle to settle. Flocculation with non-buoyant particles will have a similar effect. These processes are known to occur in the deeper waters of the marine environment (Semcesen and Wells, 2021). Biological uptake and excretion as part of a non-buoyant fecal pellet would lead to a similar phenomenon (Cole et al., 2016).

Another mechanism is that buoyant MPs can be trapped by downwards moving flow currents, for example induced by inflow or wind. When the buoyancy-induced rising velocity of a MP is small compared to the downwards velocity of the current, the MP is conveyed to deeper waters. In the marine environment, wind induced mixing can lead to buoyant MPs reaching tens of meters into the water column (Kukulka et al., 2012). In shallow waters, MP conveyed by such downwards flow currents would have some probability of encountering the sediment bed and adhere to it.

In stormwater ponds the water flow is intrinsically unsteady and turbulent because of mixing induced by factors such as wind, intermittent inflow,

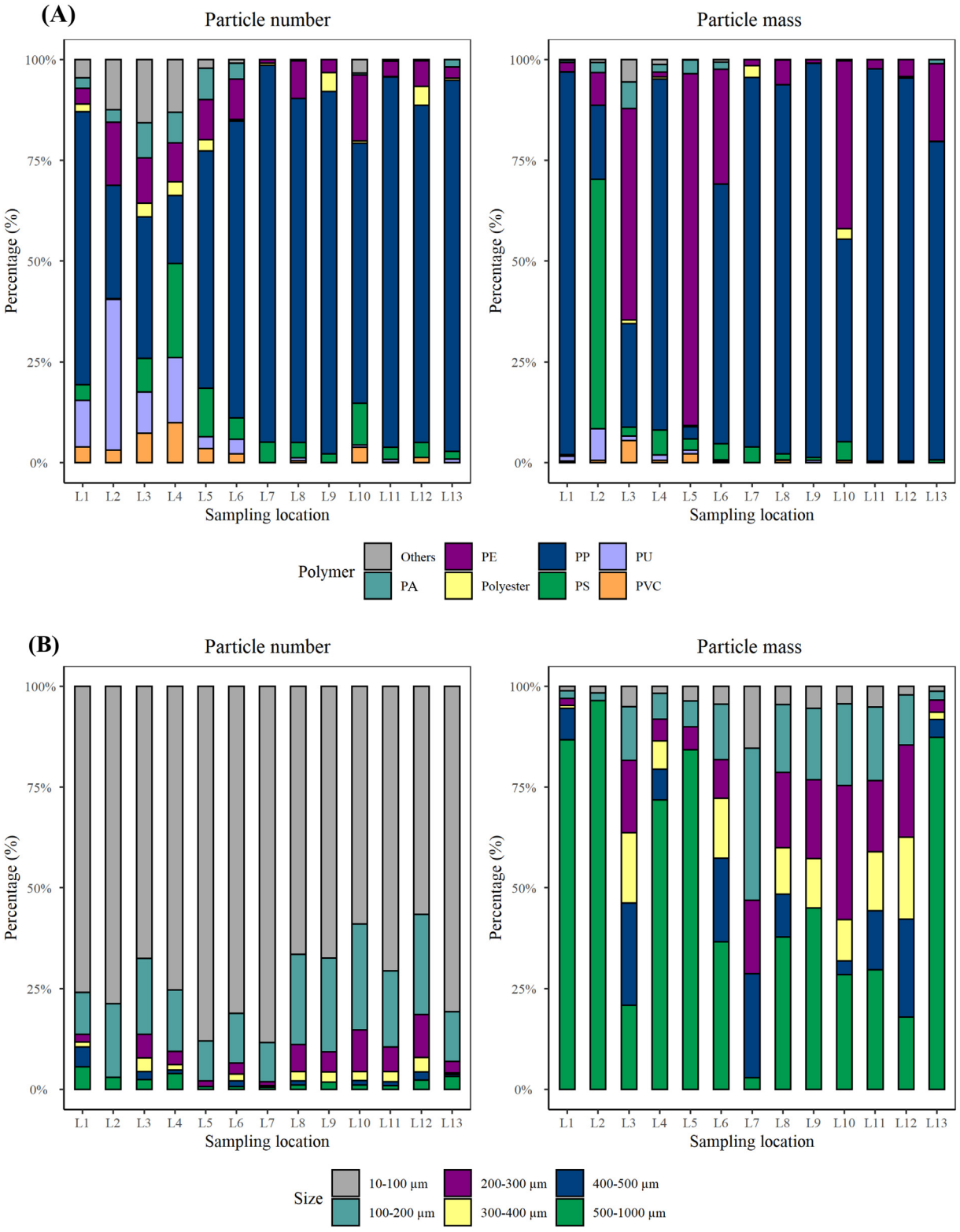

Fig. 4. Type distribution (A) and size distribution (B) of MPs identified at each sampling location based on particles number and mass.

diurnal temperature gradients, as well as their shallow depth (Hvitved-Jacobsen et al., 2010). The studied pond had a maximum depth of 1.2 m and wind induced mixing may lead to transport of MPs to its bottom, as wind over such water body can significantly affects its 3D flow pattern (Bentzen et al., 2008). Stormwater inflow can also introduce substantial mixing (Wium-Andersen et al., 2012), which might lead to similar transport processes. It hence seems reasonable to assume that downwards flow currents can convey MPs to the bottom of the pond where they may become trapped by the sediment bed.

To understand how downwards convective flow can lead to buoyant MPs reaching the sediment bed, particle trajectories were simulated with STAR-CCM+. The pond shape was simplified (Fig. 5) and downscaled 50

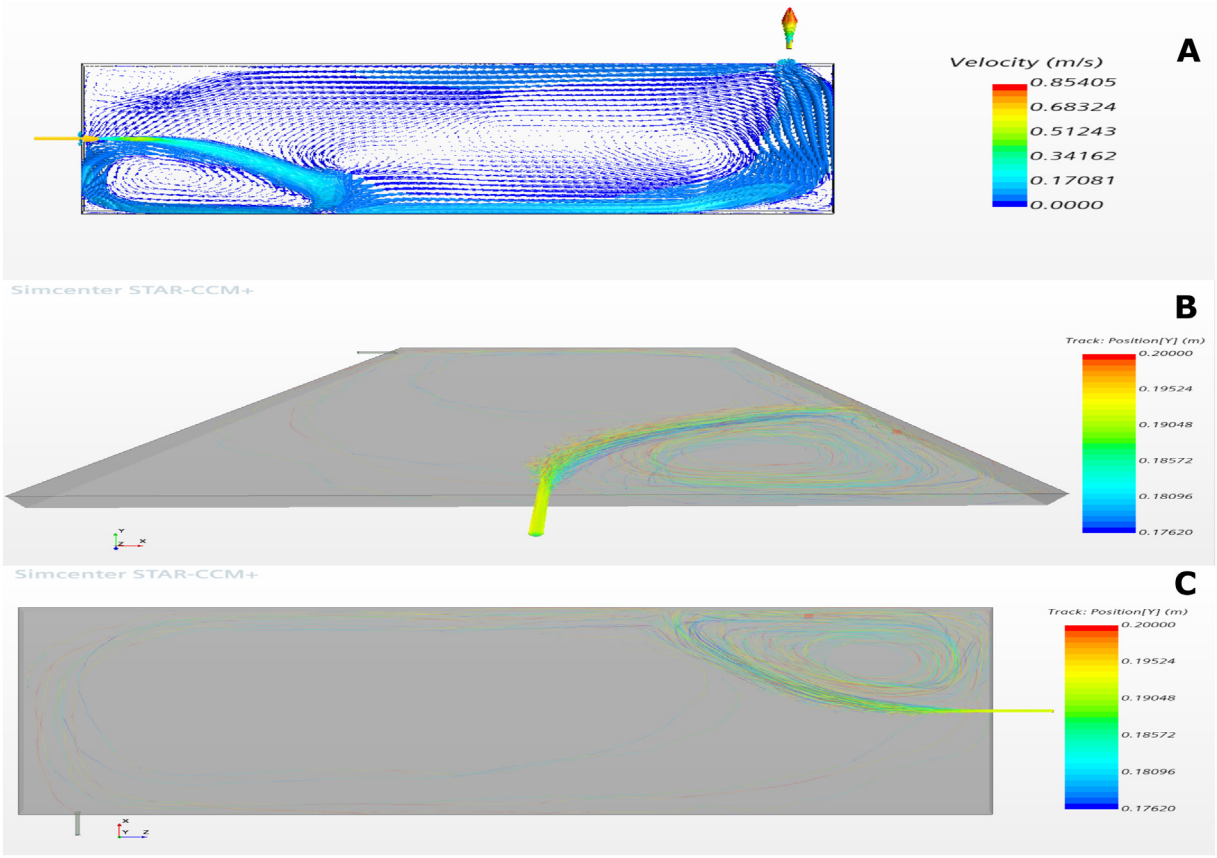

Fig. 5. Top view of velocity vectors indicating direction and magnitude of the flow velocity field for the modelled pond (A). Trajectories of the particles in the pond in 3D view (B), and top view (C). The trajectories are color-coded to show their z-position (dept below the water surface) in the flow field with respect to the corresponding particle position. Model particles were spheres of 100 μm diameter and 0.9 g cm^{-3} density.

times compared to the real one. Several scenarios were simulated, leading to similar conclusions: mixing-induced particle transport (dispersion) can explain why MPs – buoyant as well as non-buoyant – reach the sediment bed where they may become immobilized. To illustrate this, Fig. 5 shows a scenario where the inlet velocity was 0.7 m s^{-1} and spherical model particles of 100 μm diameter and 0.9 g cm^{-3} density were used as surrogates for buoyant MPs, corresponding to the particles having a Stokes settling velocity of $-5.4\ 10^{-5}$ m s^{-1}. Once a MP reached the sediment bed, it was simulated as being immobilized.

While biological and physio-chemical processes, e.g., biofilm growth and aggregation, may play a role in conveying buoyant MPs to the sediment bed of stormwater ponds they are hence strictly speaking not required to explain why these MPs accumulate in the pond sediments. Furthermore, biofilm growth is generally a slow process (Fazey and Ryan, 2016) and hence its effect might be small considering the typical water residence times in well-designed stormwater ponds (around 2 weeks, Hvitved-Jacobsen et al., 2010). Moreover, Besseling et al. (2017) in a modelling study found that the settling of MPs was rather unaffected by aggregation. It is hence quite possible that turbulent mixing (dispersion) is the governing processes for transporting small MPs from the water column of a stormwater pond, or a similar shallow water body, to its sediments.

The CFD modelling showed that the hydraulics were quite far from plug flow (Fig. 5A). The surface flow field in the pond mainly consisted of two asymmetry eddies (circulations), with the first clockwise in the lower-left corner and the second counterclockwise around the pond edge, forming a large stagnant zone at its centre. The trajectories of the MPs followed the same pattern as the flow (Fig. 5B). The color of the trajectories indicates the depth below the water surface, with the dark blue being the deepest. Once a particle hit the bottom, it was simulated sticking to it and hence retained by the sediments. The MP's downwards (or upwards) velocity caused by the eddies tended to be significantly above the numerical value of the settling (or rising) velocity. The particles hence followed the flow field. The simulations further showed that most particles sooner or later hit the bottom and hence were retained.

The simulation discussed above and shown in Fig. 5 is only one example of an indefinite number of possible configurations of pond shape, hydraulic conditions, MP size, MP density, MP shape, and so on. Nevertheless, it is a realistic one and as such shows that advective transport and dispersion can be an efficient mechanism to transport buoyant MPs to the pond bottom where they may stick to the sediments.

Other scenarios were simulated where the polymer density was modified to reflect phenomena like ballasting due to biofilm growth and non-buoyant polymers. These showed that capturing efficiency increased for non-buoyant particles as they had slightly different trajectories when the flow underwent acceleration in x, y, or z directions. I.e., when the flow lines bent because they got close to a surface such as the pond bottom. Here the inertia of the particles tended to keep them on a 'straighter' line pointing towards the surface, increasing the rate of hitting that surface compared to the buoyant ones. Examples of such simulations are shown in supplementary material, Fig. S5 and S6. Depending on density and size, particles travelled some distances before being immobilized by the pond bottom. The reason was that both buoyant and non-buoyant particles were conveyed by eddies and if the upward velocity component was larger than the settling velocity, they tended to follow the eddies until escaping them and their trajectory terminated (Figs. S5 and S6).

It must again be stressed that the above simulations are only a few among legion possible scenarios and that the model pond was strongly simplified compared to the real one. It furthermore ignores important aspects

such as resuspension of sediments, plant growth, variations in inflow, wind speed, wind direction, stratification, etcetera. The simulations hence solely yield a proof of concept that mixing due to for example inflow of stormwater can lead to a high fraction of buoyant particles in the inlet reaching the sediment bed. Where they in reality will end up and where they ultimately will accumulate cannot be predicted hereby. It can furthermore be argued that mixing may also lead to entrapment of buoyant MPs under other highly turbulent flows regimes, such as rivers, shipping fairways, and the upper layers of open waters, where dispersion (mixing) may govern the MP transport till the MPs reach the bottom of the water body or deeper zones where the flow is less turbulent or even laminar.

4. Conclusion

The MP-content of the 13 collected samples varied up to two orders of magnitude, illustrating that a simple grab sample in such pond is unlikely to be representative. The by far largest part of the MPs was buoyant with small-sized low density PP particles dominating at most locations. There was no trend of how MPs distributed in the pond, neither regarding masses, numbers, sizes, or polymer types. In other words, the spatial distribution of MPs was independent of MP properties. The findings consequently indicated that simple density driven settling in quiescent water, as for example described by Stokes Law, cannot explain how the MPs ended up in the sediments. The study also showed that there was statistically significant correlation between the content of MP, organic matter, and silt, but not between MP and clay, indicating that particles of natural organic matter, silt, and MP particles seemed to behave similar with respect to being immobilized in the pond sediments.

Computable fluid dynamics modelling allowed identifying a likely mechanism for transport of MPs – also the buoyant ones – from the water column to the sediments. In the shallow and highly dynamic water of the pond, the dominating mechanism for conveying MPs from the water column to the sediments and spread across the pond was advection combined with turbulent dispersion (mixing).

Once an MP reaches the sediments, it has some probability of being permanently immobilized by them. That probability will depend on local hydrodynamic condition and sediment physicochemical properties.

CRediT authorship contribution statement

Marziye (Shabnam) Molazadeh carried out the experiments and simulation, interpreted the results, and wrote the initial draft. Laura Simon-Sanchez drew the maps. Fan Liu contributed to the sampling and co-supervised the project. Jes Vollertsen supervised the project. All authors contributed to the final manuscript.

Data availability

Data will be made available on request.

Declaration of competing interest

The authors declare no competing interests.

Acknowledgements

This work was carried out within the Limnoplast project. This project has received funding from the European Union's Horizon 2020 research and innovation programme under the Marie Skłodowska-Curie grant agreement No 860720.

Appendix A. Supplementary data

Supplementary data to this article can be found online at https://doi.org/10.1016/j.scitotenv.2022.160489.

References

Adamsson, A., Bergdahl, L., Lyngfelt, S., 2005. Measurement and three-dimensional simulation of flow in a rectangular detention tank. Urban Water J. 2 (4), 277–287. https://doi.org/10.1080/15730620500386545.

Andrady, A.L., 2011. Microplastics in the marine environment. Mar. Pollut. Bull. 62, 1596–1605. https://doi.org/10.1016/j.marpolbul.2011.05.030.

Arthur, C., Baker, J.E., Bamford, H.A., 2009. Proceedings of the International Research Workshop on the Occurrence, Effects, and Fate of Microplastic Marine Debris, September 9-11, 2008. University of Washington Tacoma, Tacoma, WA, USA.

Asadi, A.M., Maizar, Hertika, S.A., Iranawati, F., Yuwandita, A.Y., 2019. Microplastics in the sediment of intertidal areas of Lamongan, Indonesia. Int. J. Bioflux Soc. 12, 1065–1073. http://www.bioflux.com.ro/aacl.

ASTM, 2000. Standard test methods for moisture, ash, and organic matter of peat and other organic soils. Method D 2974-00. American Society for Testing and Materials, West Conshohocken, PA 2000. American Society for Testing and Materials.

Bentzen, T.R., Larsen, T., Rasmussen, M.R., 2008. Wind effects on retention time in highway ponds. Water Sci.Technol. 57, 1713–1720. https://doi.org/10.2166/wst.2008.267.

Besseling, E., Quik, J.T.K., Sun, M., Koelmans, A.A., 2017. Fate of nano- and microplastic in freshwater systems: a modeling study. Environ. Pollut. 220 (A), 540–548. https://doi.org/10.1016/j.envpol.2016.10.001.

Besseling, E., Hasselerharm, P.R., Foekema, E.M., Koelmans, A.A., 2019. Quantifying ecological risks of aquatic micro- and nanoplastic. Crit. Rev. Environ. Sci. Technol. 49 (1), 32–80. https://doi.org/10.1080/10643389.2018.1531688.

Boucher, J., Faure, F., Pompini, O., Plummer, Z., Wieser, O., de Alencastro, L.F., 2019. (Micro) plastic fluxes and stocks in Lake Geneva basin. TrAC Trends Anal. Chem. 112, 66–74. https://doi.org/10.1016/j.trac.2018.11.037.

Chand, R., Kohansal, K., Toor, S., Pedersen, T.H., Vollertsen, J., 2022. Microplastics degradation through hydrothermal liquefaction of wastewater treatment sludge. J. Clean. Prod. 335, 130383. https://doi.org/10.1016/j.jclepro.2022.130383.

Cole, M., Lindeque, P., Halsband, C., Galloway, T.S., 2011. Microplastics as contaminants in the marine environment: a review. Mar. Pollut. Bull. 62, 2588–2597. https://doi.org/10.1016/j.marpolbul.2011.09.025.

Cole, M., Lindeque, K.P., Fileman, E., Clark, J., Lewis, C., Halsband, C., Galloway, S.T., 2016. Microplastics alter the properties and sinking rates of zooplankton faecal pellets. Environ. Sci.Technol. 50, 3239–3246. https://doi.org/10.1021/acs.est.5b05905.

Corcoran, P.L., Belontz, S.L., Ryan, K., Walzak, M.J., 2020. Factors controlling the distribution of microplastic particles in benthic sediment of the Thames River, Canada. Environ. Sci. Technol. https://doi.org/10.1021/acs.est.9b04896.

Duan, H.F., Li, F., Yan, H., 2016. Multi-objective optimal design of detention tanks in the urban stormwater drainage system: LID implementation and analysis. Water Resour. Manag. 30 (13), 4635–4648. https://doi.org/10.1007/s11269-016-1444-1.

Falahudin, D., Cordova, M.R., Sun, X., Yogaswara, D., Wulandari, I., Hindarti, D., Arifin, Z., 2020. The first occurrence, spatial distribution and characteristics of microplastic particles in sediments from Banten Bay, Indonesia. Sci. Total Environ. 705, 135304. https://doi.org/10.1016/j.scitotenv.2019.135304.

Fan, Y., Zheng, K., Zewen, Z., Guangshi, C., Peng, X., 2019. Distribution, sedimentary record, and persistence of microplastics in the Pearl River catchment, China. Environ. Pollut. 251, 862–870. https://doi.org/10.1016/j.envpol.2019.05.056.

Fazey, F.M.C., Ryan, P.G., 2016. Biofouling on buoyant marine plastics: an experimental study into the effect of size on surface longevity. Environ. Pollut. 210, 354–360. https://doi.org/10.1016/j.envpol.2016.01.026.

Geyer, R., Jambeck, J.R., Law, K.L., 2017. Production, use, and fate of all plastics ever made. Sci. Adv. 3. https://doi.org/10.1126/sciadv.1700782.

Gu, L., Dai, B., Zhu, D.Z., Hua, Z., Liu, X., Duin, B., Mahmood, K., 2016. Sediment modelling and design optimization for stormwater ponds. Can. Water Resour. J. 42 (1), 70–87. https://doi.org/10.1080/07011784.2016.1210542.

He, B., Goonetilleke, A., Ayoko, G.A., Rintoul, L., 2020. Abundance, distribution patterns, and identification of microplastics in Brisbane River sediments,Australia. Sci. Total Environ. 700, 134467. https://doi.org/10.1016/j.scitotenv.2019.134467.

Hong, S.H., Shim, W.J., Hong, L., 2017. Methods of analysing chemicals associated with microplastics: a review. Anal. Methods https://doi.org/10.1039/x0xx00000x.

Hopewell, J., Dvorak, R., Kosior, E., 2009. Plastics recycling: challenges and opportunities. Philos. Trans. R. Soc. B Biol. Sci. 364 (1526), 2115–2126. https://doi.org/10.1098/rstb.2008.0311.

Huber, M., Archodoulaki, V.M., Pomakhina, E., Pukanszky, B., Zinocker, E., Gahleitner, M., 2022. Environmental degradation and formation of secondary microplastics from packaging material: a polypropylene film case study. Polym. Degrad. Stab. 195, 109794. https://doi.org/10.1016/j.polymdegradstab. 2021.109794.

Hvitved-Jacobsen, T., Vollertsen, J., Nielsen, A.H., 2010. Urban and Highway Stormwater Pollution – Concepts and Engineering. CRC Press/Taylor & Francis Group. ISBN: 978-1-4398-2685-0, p. 347 https://doi.org/10.1201/9781439826867 (section 9.3.1.7).

Khan, S., Melville, B.W., ASCE, M., Shamseldin, A.Y., Fischer, C., 2013. Investigation of flow patterns in storm water retention ponds using CFD. J. Environ. Eng. 139, 61–69. https://doi.org/10.1061/(ASCE)EE doi:1943-7870.0000540.

Kooi, M., Besseling, E., Kroeze, C., Wenzel, A.P.V., Koelmans, A.A., 2017. Modeling the Fate and Transport of Plastic Debris in Freshwaters: Review and Guidance. Part of the Handbook of Environmental Chemistry Book Series. 58, pp. 125–152. https://doi.org/10.1007/978-3-319-61615-5_7.

Kooi, M., Primpke, S., Mintenig, S.M., Lorenz, C., Gerdts, G., Koelmans, A.A., 2021. Characterizing the multidimensionality of microplastics across environmental compartments. Water Res. 202, 117429. https://doi.org/10.1016/j.watres.2021.117429.

Kukulka, T., Proskurowski, G., Morét-Ferguson, S., Meyer, D.W., Law, K.L., 2012. The effect of wind mixing on the vertical distribution of buoyant plastic debris. Geophys. Res. Lett. 39. https://doi.org/10.1029/2012GL051116.

Li, F., Yan, X.F., Duan, H.F., 2019. Sustainable design of urban stormwater drainage systems by implementing detention tank and LID measures for flooding risk control and water quality management. Water Resour.Manag. 33 (9), 3271–3288. https://doi.org/10.1007/s11269-019-02300-0.

Li, Y., Wang, X., Fu, W., Xia, X., Liu, C., Min, J., Zhang, W., Crittenden, J.C., 2019. Interactions between nano/micro plastics and suspended sediment in water: implications on aggregation and settling. Water Res. 161, 486–495. https://doi.org/10.1016/j.watres.2019.06.018.

Liu, F., Olesen, K.B., Borregaard, A.R., Vollertsen, J., 2019a. Microplastics in urban and highway stormwater retention ponds. Sci. Total Environ. 671, 992–1000. https://doi.org/10.1016/j.scitotenv.2019.03.416.

Liu, F., Vianello, A., Vollertsen, J., 2019b. Retention of microplastics in sediments of urban and highway stormwater retention ponds *. Environ. Pollut. 255, 113335. https://doi.org/10.1016/j.envpol.2019.113335.

Liu, Y., Zhang, J., Tang, Y., He, Y., Li, Y., You, J., Breider, F., Tao, S., Liu, W., 2021. Effects of anthropogenic discharge and hydraulic deposition on the distribution and accumulation of microplastics in surface sediments of a typical seagoing river: the Haihe River. J. Hazard. Mater. 404 (B), 124180. https://doi.org/10.1016/j.jhazmat.2020.124180.

Lutz, N., Fogarty, J., Rate, A., 2021. Accumulation and potential for transport of microplastics in stormwater drains into marine environments, Perth region,Western Australia. Mar. Pollut. Bull. 68, 112362. https://doi.org/10.1016/j.marpolbul.2021.112362.

Lv, L., Yan, X., Feng, L., Jiang, S., Lu, Z., Xie, H., Sun, S., Chen, J., Li, C., 2019. Challenge for the detection of microplastics in the environment. Water Environ. Res. https://doi.org/10.1002/wer.1281.

Mato, Y., Isobe, T., Takada, H., Kanehiro, H., Ohtake, C., Kaminuma, T., 2001. Plastic resin pellets as a transport medium for toxic chemicals in the marine environment. Environ. Sci. Technol. https://doi.org/10.1021/es0010498.

Moruzzi, R.B., Speranza, L.G., Conceição, F.T.D., Martins, S.T.D.S., Busquets, R., Campos, L.C., 2020. Stormwater detention reservoirs: an opportunity for monitoring and a potential site to prevent the spread of urban microplastics. Water 12 (7), 1994. https://doi.org/10.3390/w12071994.

Olesen, K.B., Stephansen, D.A., van Alst, N., Vollertsen, J., 2019. Microplastics in a stormwater pond. Water (Switzerland) 11 (7), 1466. https://doi.org/10.3390/w11071466.

Peng, G., Zhu, B., Yang, D., Su, L., Shi, H., Li, D., 2017. Microplastics in sediments of the Changjiang Estuary, China☆. Environ. Pollut. 225, 283–290. https://doi.org/10.1016/j.envpol.2016.12.064.

Primpke, S., Cross, R.K., Mintenig, S.M., Simon, M., Vianello, A., Gerdts, G., Vollertsen, J., 2020. EXPRESS: toward the systematic identification of microplastics in the environment: evaluation of a new independent software tool (siMPle) for spectroscopic analysis. Appl. Spectrosc. 74, 1127–1138. https://doi.org/10.1177/0003702820917760.

Primpke, S., Christiansen, S.K., Cowger, W., Frond, H.D., Deshpande, A., Fischer, M., Holland, E.B., Meynes, M., O'Donnell, B.A., Ossmann, B.E., Pittroff, M., Sarau, G., Scholz-Bo¨ttcher, B.M., Wiggin, J.K., 2020. Critical assessment of analytical methods for the harmonized and cost-efficient analysis of microplastics. Appl. Spectrosc. 74, 1012–1047. https://doi.org/10.1177/0003702820921465.

Rasmussen, L.A., Iordachescu, L., Tumlin, S., Vollertsen, J., 2021. A complete mass balance for plastics in a wastewater treatment plant - macroplastics contributes more than microplastics. Water Res. 201, 117307. https://doi.org/10.1016/j.watres.2021.117307.

Schernewski, G., Radtke, H., Hauk, R., Baresel, C., Olshammar, M., Osinski, R., Oberbeckmann, S., 2020. Transport and behavior of microplastics emissions from urban sources in the Baltic Sea. Front. Environ. Sci. 8, 579361. https://doi.org/10.3389/fenvs.2020.579361.

Semcesen, O.P., Wells, G.M., 2021. Biofilm growth on buoyant microplastics leads to changes in settling rates: implications for microplastic retention in the Great Lakes. Mar. Pollut. Bull. 170, 112573. https://doi.org/10.1016/j.marpolbul.2021.112573.

Tamayol, A., Firoozabadi, B., Ashjari, M.A., 2010. Hydrodynamics of secondary settling tanks and increasing their performance using baffles. J. Environ. Eng. 136 (1), 32–39. https://doi.org/10.1061/(ASCE)EE.1943-7870.0000126.

Versteeg, H.K., Malalasekera, W., 1995. An Introduction to Computational Fluid Dynamics: The Finite Volume Method. Longman Scientific and Technical, New York, NY, USA.

Wium-Andersen, T., Nielsen, A.H., Hvitved-Jacobsen, T., Vollertsen, J., 2012. Modeling nutrient and pollutant removal in three wet detention ponds. In: Rauch, S., Morrison, G. (Eds.), Urban Environment. Alliance for Global Sustainability Bookseries 19. https://doi.org/10.1007/978-94-007-2540-9_22.

Zheng, Y., Lia, J., Cao, W., Jiang, F., Zhao, C., Ding, H., Wang, M., Gao, F., Sun, C., 2020. Vertical distribution of microplastics in bay sediment reflecting effects of sedimentation dynamics and anthropogenic activities. Mar. Pollut. Bull. 152, 110885. https://doi.org/10.1016/j.marpolbul.2020.110885.

Ziajahromi, S., Drapper, D., Hornbuckle, A., Rintoul, L., Leusch, F.D.L., 2020. Microplastic pollution in a stormwater floating treatment wetland: detection of tyre particles in sediment. Sci. Total Environ. 713, 136356. https://doi.org/10.1016/j.scitotenv.2019.136356.

Paper-II

What is hiding below the surface – MPs including TWP in an urban lake

Environment International 182 (2023) 108282

Contents lists available at ScienceDirect

Environment International

journal homepage: www.elsevier.com/locate/envint

Full length article

What is hiding below the surface – MPs including TWP in an urban lake

Marziye (Shabnam) Molazadeh *, Fan Liu, Jeanette Lykkemark, Lucian lordachescu, Asbjørn Haaning Nielsen, Jes Vollertsen

Aalborg University, Section of Civil and Environmental Engineering, Department of the Built Environment, Thomas Manns Vej 23, 9220 Aalborg Øst, Denmark

ARTICLE INFO

Handling Editor: Adrian Covaci

Keywords:
Urban Lake
Sediments
Microplastics
Tyre wear particles
μFTIR
Py-GC/MS

ABSTRACT

Inland lakes play an important role as habitats for local species and are often essential drinking water reservoirs. However, there is limited information about the presence of microplastics (MPs) in these water bodies. Thirteen sediment samples were collected across a Danish urban lake to map MPs, including tyre wear particles (TWP). The lower size detection limit was 10 μm. MPs were quantified as counts, size, and polymer type by Fourier-transform infrared microspectroscopy (μFTIR) and mass estimated from the 2D projections of the MPs. As TWP cannot be determined by μFTIR, counts and sizes could not be quantified by this technique. Instead, TWP mass was determined by pyrolysis gas chromatography mass spectrometry (Py-GC/MS). The average MP abundance was 279 mg kg^{-1} (μFTIR), of which 19 mg kg^{-1} (Py-GC/MS) were TWP. For MPs other than tyre wear, the average MP count concentration was 11,312 counts kg^{-1}. Urban runoff from combined sewer overflows and separate stormwater outlets combined with outflow from a wastewater treatment plant were potential point sources. The spatial variation was substantial, with concentrations varying several orders of magnitude. There was no pattern in concentration across the lake, and the distribution of high and low values seemed random. This indicates that large sampling campaigns encompassing the entire lake are key to an accurate quantification. No preferential spatial trend in polymer characteristics was identified. For MPs other than TWP, the size of buoyant and non-buoyant polymers showed no significant difference across the lake, suggesting that the same processes brought them to the sediment, regardless of their density. Moreover, MP abundance was not correlated to sediment properties, further indicating a random occurrence of MPs in the lake sediments. These findings shed light on the occurrence and distribution of MPs, including TWP, in an inland lake, improving the basis for making mitigation decisions.

1. Introduction

Plastic is versatile, resilient, cheap, and lightweight. These properties have led to its ever-growing use, with manufacture currently reaching approximately 300 million tons worldwide in the last 50 years (Bharath et al., 2021). Upon use, most plastic is landfilled or burned, while some is simply dumped in the environment (Yang et al., 2022). Only about 9 % of plastic waste is recycled globally, leading to significant stress on the environment and natural resources (OECD, 2023).

Once MPs are in the environment, they tend to persist. Their breakdown into smaller MPs, chemical degradation, and biological decomposition is slow and strongly dependent on the environment they are in (Corcoran, 2020). Where there is no light and little oxidative potential, they may persist for generations (Simon-Sánchez et al., 2022). MPs are found all over the globe, from the high artic (Gündoğdu et al., 2021) to the world's desserts (Wang et al., 2021). The spreading is facilitated by their small size and low density, leading to them being easily spread and transported by wind and water over long distances (Reimonn et al., 2019). MPs are present in habitats worldwide, from soil to water and atmosphere (Molazadeh et al., 2022; Simon-Sánchez et al., 2022; Vianello et al., 2019), even in habitats of sparsely populated regions, such as Antarctica (Kelly et al., 2020).

Plastics are suspected to cause physical harm to organisms such as fish, mammals, invertebrates, and birds upon intake (Cole et al., 2015; Lusher et al., 2016; Monclús et al., 2022). Small MPs and nanoplastics (NP) might also translocate into the tissue of organisms, causing detrimental impacts (Dong et al., 2023). Finally, some MPs may act as vectors for toxic compounds, either by sorbing pollutants from the environment or by containing toxic additives (Besseling et al., 2019; Cole et al., 2011). An example of the latter is tyre wear particles (TWP), a MP type

* Corresponding author.
E-mail address: marziyem@build.aau.dk (M.(S. Molazadeh).

https://doi.org/10.1016/j.envint.2023.108282
Received 26 July 2023; Received in revised form 14 October 2023; Accepted 20 October 2023
Available online 31 October 2023

which lately has been identified as a potentially rather toxic part of the microplastic litter (Knight et al., 2020).

MPs in freshwaters have in recent years received increasing attention, partly because freshwaters can convey MPs to the marine environment, and partly because MPs may affect their ecosystems. Inland lakes are, in this respect, of considerable importance as they provide habitats for local species and often act as drinking water reservoirs (Eriksen et al., 2013; Islam et al., 2022). Some of these are urban lakes which receive urban and highway runoff, resulting in them receiving more anthropogenic pollutants, e.g., MPs, than many natural lakes (Hengstmann et al., 2021).

The level of MP pollution in lakes has been shown to be comparable to that of marine waters (Ding et al., 2019; Yonkos et al., 2014). Moreover, inland lakes, especially in densely populated urban areas, are typically much smaller than the open sea, which leads to less dilution and hence potentially higher concentration and accumulation in their sediments. While the presence of MPs in lakes has been reported by several studies (Mercy et al., 2023; Scopetani et al., 2019; Srinivasalu et al., 2021; Malla-Pradhan et al., 2022), their occurrence and distribution in urban lakes is less well documented, and data on TWP is scarce. The objective of the present study is to add knowledge on MP including TWP in such lakes by studying their occurrence in the sediments and analysing their spatial variability within a lake. The MPs are quantified by Fourier-transform infrared microspectroscopy (μFTIR imaging) and by pyrolysis gas chromatography mass spectrometry (Py-GC/MS) for TWP.

2. Material and methods

2.1. Site description and sample collection

Brabrand Lake (Brabrand Sø) is in the western part of Aarhus city, Denmark, and is surrounded by a dense littoral zone with reeds and wet meadows (Matamoros et al., 2012). It receives water from Aarhus River (Århus Å) after it has passed the artificial wetland Århus Engsø (56°144706 N, 10°096916 E) established in 1998. It discharges to the lower part of Aarhus River at Andebroen (56°140339 N, 10°144498 E), which ultimately discharges to the Aarhus Bay in the centre of the city. The lake furthermore receives urban runoff from numerous separate stormwater outlets and combined sewer overflows, as well as discharge from a wastewater treatment plant (WWTP) (Viby Renseanlæg) via Døde Å (Dead River) (56°137945, 10°136352). The treatment plant serves pprox.. 120,000 population equivalents and applies mechanical pre-treatment, nitrification, denitrification, phosphorous removal, and a final polishing of the effluent through a sand filter. The lake covers 153.8 ha and has a total catchment of 31,000 ha. The average water depth is 0.85 m, and the maximum is 2.70 m (Fig. 1). Moreover, the water in the lake has an average hydraulic retention time of 12 days. The full extent of the lake was dredged in 1988–1995, where 0.5 million m^3 of sediment was removed to a depth between 0 and 0.9 m. Legacy pollution from before the establishment of the wastewater treatment plant was hereby removed.

To assess the amount of MPs including TWP accumulated in the lake sediments, five transects were laid out at which a total of 13 samples were collected (Fig. 1). A Van Veen grab was used for the sampling, which was conducted in August 2021. The sediment was sampled in a

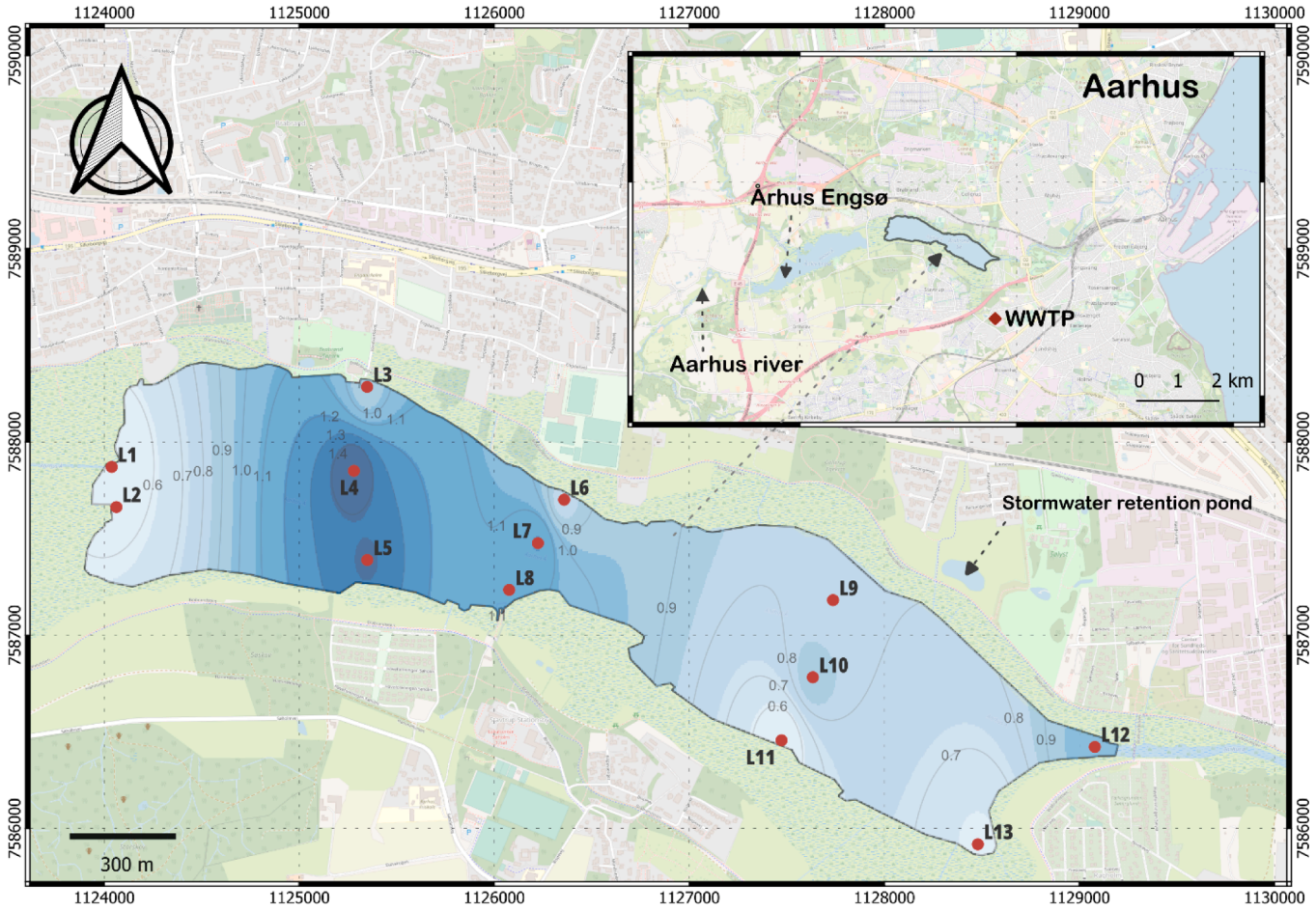

Fig. 1. Map of the lake showing the sampling stations (L1–L13). The inlet is in the western part of the lake, while the outlet is in its eastern part.

dry period, defined as no rain at least 2 days prior to the activity. For each sampling location, 2–3 kg of bulk sediment from the top 5–8 cm of each grab was collected and stored in a glass jar. The lake has an annual sediment accumulation rate of about 1 cm per year (Søndergaard et al., 2008). Thus, the samples are expected to represent recent sediment deposition covering about 5–8 years. The samples were immediately transferred to the laboratory and stored at 5 °C for further analysis.

2.2. Sediment characteristics

Sediments were characterised for organic matter content and grain size distribution. The former was done by muffling dried sediment of known weight at 550 °C for 4 h in a muffle furnace, and the weight loss on ignition was determined (ASTM, 2000). The grain size distribution followed the same procedure as described by Molazdeh et al. (2023). In brief, sieves with different mesh sizes were used for size classification of grains > 63 μm and hydrometer tests were used for grains < 63 μm (Asadi et al., 2019).

2.3. MP extraction

MPs were isolated by following the procedure described by Molazdeh et al. (2023). In brief, approximately 1.5 kg of homogenised subsample was taken from the jar and transferred into a pre-cleaned glass beaker. The subsample was pre-oxidised by gradually adding hydrogen peroxide (50 % H_2O_2) and Milli-Q water while gently stirring the sediment to achieve a maximum of 10 % H_2O_2 as the final concentration. The process was repeated until no foaming occurred when adding H_2O_2. The oxidised samples were wet sieved through 2 mm and 5 mm stainless steel sieves (Retsch GmbH, Germany) before drying in an oven at 50 °C until a constant dry weight was achieved. Of the < 2 mm dried samples, subsamples of 100 g went through density separation using sodium polytungstate (SPT) solution ($\rho = 1.8$ g cm^{-3}) in a 2 L pear-shaped separator funnel.

The mixture of sediment and SPT in the funnel was aerated for 30 min by passing filtered compressed air from the bottom, then left to settle for 24 h, upon which the settled fraction was drained away while the floating fraction was filtered through a 10 μm stainless steel filter. The collected particles were then transferred into a sodium dodecyl sulphate (SDS, 5 % w/vol) solution with a constant stirring and incubated at 50 °C for 48 h. To further degrade the remaining organic material, the particles underwent a two-step enzymatic digestion using a blend of cellulase (Cellulase enzyme blend®, Sigma-Aldrich) and cellulolytic enzymes (Viscozyme®L, Sigma-Aldrich) for 48 h, followed by protease, for another 48 h (Protease from Bacillus sp.®, Sigma-Aldrich) (Chand et al., 2022; Molazadeh et al., 2023). Both steps were performed at 50 °C. Subsequently, the samples underwent a Fenton oxidation by transferring the filtered particles into 200 mL of Milli-Q water, with the addition of 145 mL 50 % H_2O_2 and 62 mL of 0.1 M iron sulphate ($FeSO_4$). The pH of the mixture was adjusted to 3 by adding 65 mL of 0.1 M sodium hydroxide (NaOH) while the temperature was maintained at 15–30 °C. The collected particles were split into two size fractions by filtering over a 10 μm and a 500 μm stainless steel mesh. The large particles retained on the larger mesh were collected and dried at 55 °C, after which they were added to the fraction of 2–5 mm and analysed one by one. Particles < 500 μm were transferred to a 250 mL separation funnel with SPT solution ($\rho = 1.8$ g cm^{-3}), and went through a second density separation following the same procedure as described previously. The floating particles were filtered through a 10 μm stainless filter and transferred into 50 % ethanol (HPLC grade), upon which they were transferred to a 10 mL glass vial and dried in an automated solvent evaporator (TurboVap® LV, Biotage) at 50 °C. Finally, 5 mL 50 % ethanol was added to the vial to mobilise the particles.

2.4. MP and TWP analysis

2.4.1. Particles > 500 μm

Potential MPs > 500 μm were visually sorted and photographed under a stereomicroscope (ZEISS, SteREO Discovery.V8, Oberkochen Germany). The software ZenCore (Zen2Core SP1 from ZEISS) was used to measure their morphology. All suspicious particles were then analysed by Attenuated total reflectance (ATR) FTIR spectrometry (Cary 630 Agilent Technologies, with a single reflection diamond ATR) for chemical composition. The obtained IR spectra were compared with a commercial library in the software OMNIC (Thermo Fisher Scientific Inc., 8.2.0.387 version 1). If particles suspected to contain TWP had been seen, these would have been analysed by Py-GC/MS. The particle mass was estimated from the area of the particle images applying the same approach as for the MP < 500 μm.

2.4.2. Particles < 500 μm

2.4.2.1. MP analysis. After homogenising the 5 mL solution well, an aliquot was deposited on a Ø13 × 2 mm circular zinc selenide window using a glass capillary micropipette. The window was restricted by a compression cell with a Ø10 mm effective area (Pike Technologies). The window with its deposited aliquot was dried on a heating plate at 55 °C. This procedure was repeated until enough particles were deposited on the window. For each sample, the deposition was done for at least three windows to ensure that the deposited volume was representative of the whole sample. After drying, the window was scanned employing focal plane array (FPA) μFTIR imaging (Agilent Cary 620 FTIR microscope equipped with a 128 × 128 pixel FPA Mercury Cadmium Telluride detector, coupled with an Agilent 670 IR spectroscope), resulting in a pixel resolution of 5.5 μm. The acquired IR map was analysed by siMPle, a freeware for automated MP detection (Primpke et al., 2020b). The software allows detection of MP polymer type, size, and shape of particles, and estimates their mass based here on. The library used for this study was based on the library used by Rist et al. (2020), but extended to 380 reference spectra, covering both synthetic and natural materials (Molazade et al., 2023).

2.4.2.2. TWP analysis. Py-GC/MS was used to measure the concentration of TWP in the sediment extracts. An aliquot of 50–750 μL from the 5 mL concentrates was added to a sample cup using a glass capillary micropipette and dried on a heating plate at 30 °C. The Py-GC/MS consisted of a microfurnace pyrolyzer EGA/Py-3030D (FrontierLab, Japan) and an auto-shot sampler AS-1020E (FrontierLab, Japan) unit connected to a Thermo Scientific TRACE 1310 GC and an ISQ™ single quadrupole GC/MS part, using helium as the carrier gas. The gas from the pyrolyzer was injected in split mode (ratio 30:1). Deuterated polystyrene (PS-d8, 0.2 g/L) dissolved in dichloromethane was used as internal standard. The procedure consisted of a pyrolysis step at 600 °C with an interface at 280 °C. The temperature in the GC-oven was first set to 40 °C and the column heated for 2.5 min, then the temperature was increased gradually (10.5 °C min^{-1}) to reach a final temperature of 300 °C for 5 min. The mass spectrometer was run in EI positive mode (70 eV; *m/z* range: 35–500, scan time: 0.204 s), and the transfer line and ion source were maintained at 250 °C and 200 °C, respectively. Blank control was conducted between every sample. Quantification was done using an external calibration curve generated for the selected indicator compound, 4-vinylcyclohexene. Which indicators to use for quantification of tyre tread material is debated (Rødland et al., 2023). Initial studies in our lab had shown that 4-vinylcyclohexene was an appropriate marker for the mix of cryo-milled car and truck tyre tread used to establish an external calibration curve. This marker has also been used by several other studies to quantify car tyre material (More et al., 2023; Mun et al., 2022). The tread material was sourced from Denmark and Sweden (Genan, Denmark), i.e., following the suggestion of Miller et al.

(2022) that regionally representative tyre tread mixes should be used to interpret the pyrograms.

2.5. Equivalent diameter (D_{eq})

The equivalent diameter (D_{eq}) of each particle was calculated according to Wadell (1932), using each particle's three side lengths A, B, and C (Eq. (1)). The particle's major and minor dimensions were obtained from the siMPle software while the third dimension was estimated as 60 % of the minor dimension as described by Simon et al. (2018) and later modified by Liu et al., (2019a). The D_{eq} was then calculated by assuming a sphere of the same volume as the ellipsoid (Eq. (1)).

$$D_{eq} = \sqrt[3]{ABC}$$

2.6. QA/QC

Several measures were taken to reduce the procedural contamination. All labware were flushed thrice with particle-free water while all filters were muffled at 500 °C prior to use. Cotton lab coats were always worn in the lab. Samples were always handled inside a fume hood and covered with aluminium foils or glass watches. All solutions were pre-filtered on 0.7 μm glass fibre filters. In addition, an air filtering device with HEPA filter (H14, 7.5 m^2) was continuously filtering the air in the lab. However, due to the pervasive presence of MPs, some contamination is inevitable. Hence, triplicate laboratory procedural blanks were prepared using washed sand (75–1000 μm, Baskarp Sand No. 15) muffled at 500 °C alongside the lake samples (Molazadeh et al., 2023). The blank control samples went through the same processes as the sediment samples. The lower size detection limit for MPs was considered as 11 μm, given that particles comprising just 1 pixel (5.5 μm) were excluded from the data analysis using siMPle, and the filter mesh size used in sample preparation was 10 μm.

The sample preparation may cause some loss of MP due to incomplete separation during, for instance, density separation. The extraction efficiency of the applied extraction protocol was assessed in a separate method study for the Danish EPA (Liu et al., 2023), which ran parallel to the current study. Here a recovery test was conducted by adding a known number of easily distinguishable plastic beads to muddy marine sediments, which then underwent the previously described sample preparation process. Four types of beads (polypropylene (PP) 45–63 and 75–90 μm; polystyrene (PS) 45–63 and 90–106 μm, Cospheric) were spiked to 24 subsamples, 6 from each of the 4 natural sediments. The MPs used for the spiking represent the most abundant environmental MPs in terms of polymer density and size, as detected by the applied protocol (Molazadeh et al., 2023). The microbeads were manually counted under a stereomicroscope (ZEISS, SteREO Discovery.V8) before being spiked to the sediment (Fig. S1). After extraction, the recovery rate was determined by counting the microbeads in the extracted aliquots, yielding average recovery rates between 50 and 90 %, mainly depending on the sediment type.

Some natural materials have spectra quite close to those of PP and polyethylene (PE). To prevent false positive identifications, these spectra were incorporated into the siMPle library as natural materials, categorised under a group named 'fake particles' (Molazade et al., 2023).

2.6 . Statistical analysis

The Shapiro-Wilk normality test was applied to assess the normality of datasets. To investigate if there were significant differences in MP sizes and mass between samples, a non-parametric Kruskal-Wallis test was performed. If differences existed, a Wilcoxon rank sum test was used for pairwise comparison. Moreover, the test was also performed on particle size comparing buoyant and non-buoyant polymers.

3. Result and discussion

3.1. Overall MP and TWP abundance

3.1.1. MP concentrations excluding TWP

Regarding MPs that could be identified by μFTIR imaging, i.e., excluding TWP, which is discussed in section 3.1.2, Brabrand Lake sediments held quite many MPs, with a global average of 11,312 count kg^{-1}, corresponding to an estimated mass of 260 mg kg^{-1} (dry weight, Table S1). The blank contamination was low compared to the measured concentrations, namely 167 item kg^{-1} and 11.99 μg kg^{-1}, corresponding to 1.48 % and 0.00546 % of the average MP number and mass concentration, respectively (for details see supplementary materials, the section on MPs in blanks). The results were not corrected for recovery as MP is a diverse group of materials, and it is debatable if measured MP concentrations should be corrected based on recovery deducted from 'ideal' particles such as microbeads.

Fig. 2 compares the MP level in Brabrand Lake sediment with other solid matrices. These data all originate from the same lab as the present study and were prepared by quite similar procedures and analysed by the same μFTIR instrument. The main reason for choosing these datasets was that comparing data analysed the same way should be less prone to quantification bias than comparing datasets across laboratories. TWP could not be included in the comparison as those studies did not report this parameter.

The lake sediment held on average 22 times more MP mass than those of sediment from a stormwater pond discharging directly to it (Molazadeh et al., 2022). However, the MP mass concentration in the lake was lower than that of a stormwater pond in another Danish city, studied by Olsen et al. (2019) (402 mg kg^{-1}). The lake sediment was on the other hand much more polluted than sediment from a Danish fjord. It held 55 times more MP than what was found in marine sediment from Odense Fjord, Denmark (Liu et al., 2021a). Comparing to a completely different matrix, namely sewage sludge, the lake sediment was slightly more polluted than sludge from a Swedish WWTP (230 mg kg^{-1}) but less polluted than digested sludge from the same plant (370 mg kg^{-1}) (Chand et al., 2021). Comparing to another type of matrix, namely the dust that accumulates on roads, the lake sediment was on average 2 times more polluted than that of road dust collected in an industrial area (Rasmussen et al., 2023). All data were compared on a dry matter basis (Fig. 2A). Comparing the number of detected MPs in the Brabrand Lake, i.e., the MP counts instead of the mass, to those other matrices, the pollution level was significantly lower than other urban matrices but in the range of the marine sediment (Odense Fjord) (Fig. 2B).

Most MPs have in literature been reported as particle counts and not mass. Compared to other lakes in different continents, our findings showed a significantly higher MP count concentration in sediment (Bharath et al., 2020; Yin et al., 2020; Gopinath et al., 2020a; Li et al., 2019; Qin et al., 2019; Dean et al., 2018; Merga et al., 2020). For instance, 396 count kg^{-1} was reported in sediment of Lake Vesijarvi in Finland (Scopetani et al., 2019). That in sediment of Lake Michigan in North America ranged from 33 to 6229 count kg^{-1} (Lenaker et al., 2019). Some of the most polluted lake sediment reported was from Lake Bizerte in Tunisia with 7960 count kg^{-1}, high but still 1.4 times below the present study (Abidli et al., 2017). However, Tangxun Lake in China (Shi et al., 2022) held on average 1.6 times more MP than Brabrand Lake, with $1.81 \pm 1.75 \times 10^4$ count kg^{-1}.

Several factors are likely to have contributed to the differences between studies: for example, true differences in concentrations at the locations, differences in sampling strategy, and differences in analytical approach. The latter is known to affect the results quite significantly, for example when analytical methods have different lower-size quantification limits and differences in analytical accuracy, making comparison across studies quite challenging (Primpke et al., 2020a,b). Moreover, the size range investigated in different studies can affect the comparison. In the current study, MPs in the range of 10–5000 μm were investigated

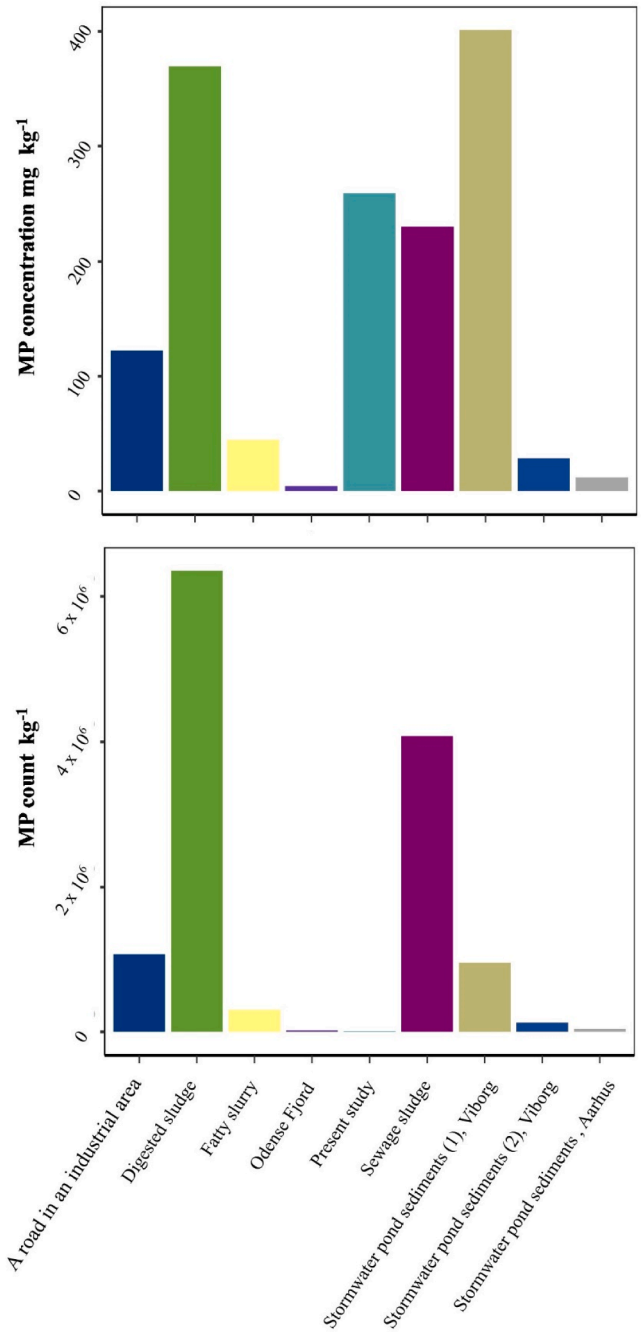

Fig. 2. MP contents reported by authors from the same lab measured in different solid matrices in terms of estimated mass (A) and count (B) per kg of dry matter. The figure only shows those MPs that could be identified by μFTIR imaging and TWP is hence not included in the datasets.

(Fig. 3). Small-sized particles tended to be more abundant, and most MPs (63 %) were smaller than 100 μm. In contrast, MPs > 400 μm accounted for only a small portion of the MPs, namely 3.5 % of all counts. Compared to for example the findings of Bharath et al., 2020 who investigated MPs > 300 μm and reported that the majority (47 %) were in the size range 300–1000 μm, in the current work only 6.6 % were in this size range and 93 % were smaller than the 300 μm which was Bharath et al.'s lower limit. In the study conducted by Lenaker et al. (2019) in Lake Michigan, MPs of their smallest size fraction (125–355 μm) made up 62 % of the MPs, while such MPs in the current study only made up around 20 %. We would have found roughly 70 % less MPs had we only studied particles > 125 μm. Lenaker et al. reported that

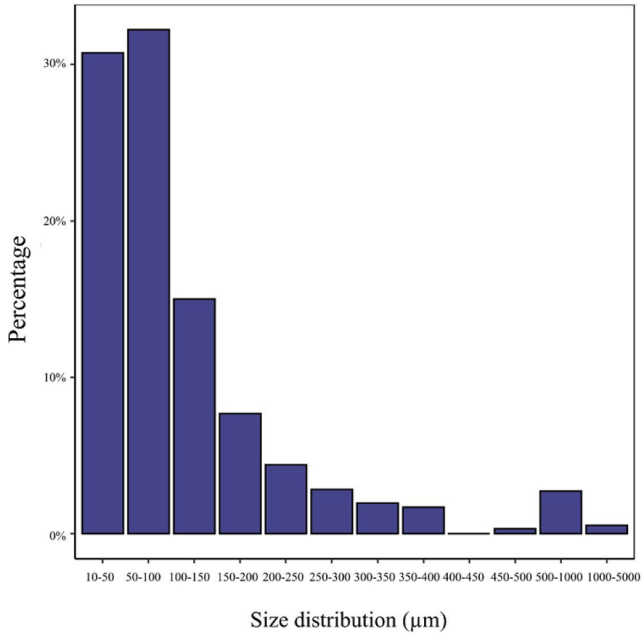

Fig. 3. Percentage of MP by counts after sorting MPs into bins according to their major dimension.

355–999 μm MPs made up 24 % of all MPs, while this size range in our study contributed only about 5 %. Shi et al. (2022) found that particles < 1000 μm were dominant in the sediments of Tangxun Lake in China when studying MPs to sizes below 50 μm (no lower size limit was stated). The same was concluded in the current study where 99.5 % of MPs were < 1000 μm.

There are several potential input pathways and sources to the lake. MPs could come via Aarhus River; however, the river passes an artificial wetland established in 1998, 3 years after the lake was dredged, and it seems reasonable to assume that much pollution would be retained here (Ziajahromi et al., 2020). Urban runoff from combined sewer overflows and separate stormwater outlets combined with outflow from the WWTP seems more likely to be significant sources (Ballent et al., 2016). Furthermore, separate stormwater can hold misconnected wastewater which then is discharged to the lake (Panasiuk et al., 2015). Diffuse sources may also play a role, as wind can carry MPs from the city and into the lake, and natural surface runoff via small streams and channels can convey MPs to the lake (Wang et al., 2022). Last but not least, MPs generated from the fragmentation of larger plastic litter cannot be excluded as a source (Lechner and Ramler, 2015).

3.1.2. *Occurrence of TWP in the lake*

The global average concentration of TWP over the lake was 19 mg kg^{-1} (Table S1). The TWP concentration of the present study can be compared to those from other laboratories, mainly because Py-GC/MS is not affected by the lower size limitation, for which data are reported in section 3.1.2. However, few such data exist for urban lakes. Hence compared to other environments, the lake was on average 264 times more polluted than the most polluted sediment sampled from the southern German Bight, and river Weser, Northwest Germany (0.072 mg kg^{-1}) (Goßmann et al., 2021). The authors measured TWP in 10 sediment samples (3 from the southern German Bight, 7 from river Weser) and reported that only 6 showed tyre wear indicator signals. It is worth noticing that the river sediments containing TWP were taken in close vicinity to a highway or city. The sediments obtained from the German Bight were collected at locations that were further away from the coastline (Goßmann et al., 2021). The TWP concentration in Brabrand Lake was lower than that of dust from a parking lot located in a commercial area and a road in an industrial area, holding respectively

69 and 2868 mg kg^{-1} TWP (Rasmussen et al., 2023). The average concentration of tyre and road wear particles (TRWP) in sediment samples from the river Seine (France), Chesapeake Bay (U.S.), and Yodo-Lake Biwa (Japan) watersheds were respectively 4500, 910 and 770 mg kg^{-1} (Unice et al., 2013). This is higher than in the present study, but to exactly what degree is not clear since Unice et al. analysed styrene butadiene rubber plus natural rubber based on styrene as marker compound and from this estimated the amount of TRWP, while the present study applied 4-vinylcyclohexene as a quantification compound for TWP by means of an external calibration curve made by a mixture of regionally sourced tyre particles. Firstly, TRWP differs from TWP by also including material from the road and its dust. Secondly, 4-vinylcyclohexene is a more specific marker for styrene butadiene rubber and butadiene rubber than styrene (Goßmann et al., 2021) but does not mark natural rubber. Direct comparison between these numbers is hence somewhat problematic.

In a modelling study conducted by Unice et al. (2019) the authors projected that 49 % of total TWP emissions go to runoff, thus runoff is a significant source of TWP to downstream systems if it doesn't receive proper treatment. Runoff from various point discharges to Brabrand Lake could hence be an important source of this pollutant in the lake.

3.2. Spatial distribution of MP

3.2.1. Mps excluding TWP

While MPs were found at all 13 locations across the lake, the spatial variation was substantial (Fig. 4). No clear trend was seen as high and low MP-concentrations seemed randomly spread across the lake. The highest abundance by counts was at L12 (38,460 counts kg^{-1}), the easternmost sampling location close to the lake outlet, while the lowest was at L1 (747 counts kg^{-1}), the westernmost sampling location where Aarhus River discharges to the lake (Table S1 and Fig. 4A). However, just south of L1 there was L2, which held 15 times more MP counts. When measured by estimated particle mass, the variation was even larger. L1 was again the least polluted location with a rather low concentration of 0.042 mg kg^{-1}. For MP mass, the highest concentration was, however found in the lake's middle region L8 (2,701 mg kg^{-1}), which was 6 orders of magnitude above L1. The variability in estimated mass was much higher than the variability in counts, which was caused by a few large MPs. For identical particle shapes, the mass comes in the third power of its dimension, and finding some large MPs hence results in a much larger estimated mass. In a study of one the stormwater ponds discharging to Brabrand Lake, Molazade et al. (2022) found a quite similar variability in the pond. Similarly, Liu et al. (2022) and Gopinath et al., (2020b) found great spatial variability for Chaohu Lake and Red Hills Lake.

When the purpose of a sampling campaign is monitoring a MP contamination level in aquatic sediments, spatial variability must hence be considered. Basing a conclusion on one or just a few grab samples is likely to yield unreliable results, either over- or underestimating the contamination level. To account for the patchiness, a quite large sampling campaign must be designed. Even the rather decent campaign of the current study was on the low side of what is recommendable if the goal is to estimate the total amount of MPs in Brabrand Lake.

The reasons for the patchiness can only be speculated on. There are probably many factors that interact and contribute to the observed variability, among which the closeness to a source can be one. It could for example be argued for L1 that it is dominated by the water from Aarhus River, which was 'pretreated' in the artificial wetland, and hence maybe low on MP. Or maybe the 'water jet' from the river flushes light particles like MPs further into the lake. Local hydraulic conditions may also explain other high or low concentrations. Maybe L2 is in a

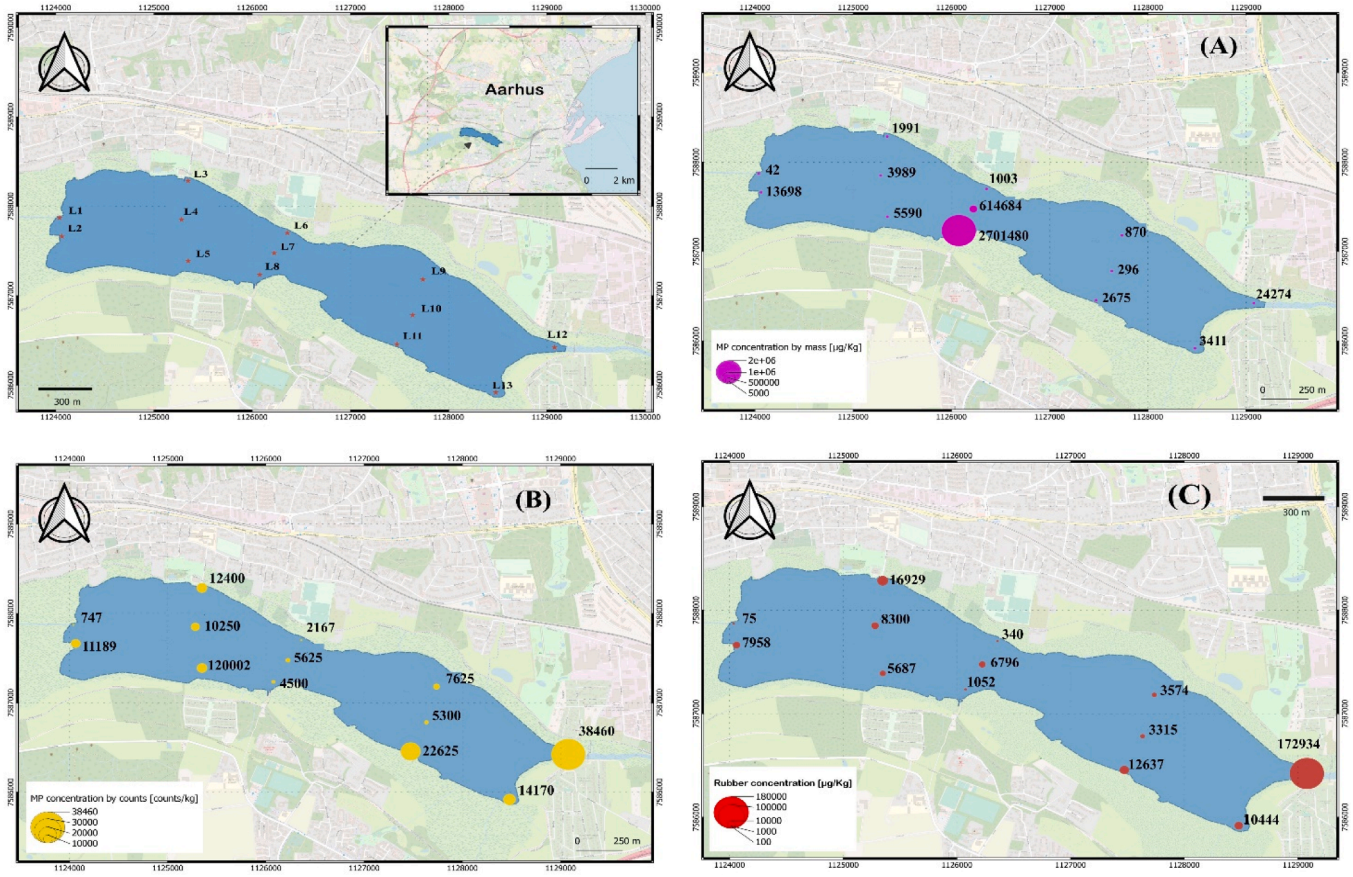

Fig. 4. Spatial distribution of MP mass (A) and counts (B) identified by µFTIR and TWP (C) over the lake.

deposition zone, leading to light particles settling out. Maybe it is protected from the predominant westerly wind. Leads et al. (2023) reported for example, that wind direction on the day of sampling was the greatest contributing factor to the MP abundance they found. However, without very detailed studies – and maybe even then – it seems unachievable to establish causality between observations and influencing factors in a system which is as dynamic as a shallow urban lake. From a pragmatic viewpoint, the patchiness might instead be treated as random.

3.2.2. Tyre wear particles

Like other MPs, the spatial distribution of settled tyre particles seemed random, and no preferential pattern could be identified (Fig. 4C). The concentration of TWP at the outlet of the lake (L12) was one order of magnitude above the highest concentration in the rest of it. L12 also held the highest MP count of other plastic types, while it in terms of mass of those MPs ranked as the third most polluted location. TWP was present in lowest concentrations at L1, which also was the least polluted in terms of other plastic types. In general, there was, however no correlation between the mass of TWP and the mass of other MP types at a location. With the caveat that it may be problematic to compare mass estimated by μFTIR and mass determined by Py-GC/MS, TWP was a minor contributor to the total MP mass at 2 of the locations (Table S1). In other cases, it was present in concentrations roughly corresponding to (3 sampling locations), or above (8 sampling locations), the sum of other plastic types (Table S1), illustrating that when assessing the MP contamination of this lake, contamination caused by tyre particles should not be overlooked.

3.3. Polymer composition, size, and mass

3.3.1. Polymer composition

In addition to tyre wear material identified by Py-GC/MS, a total of 15 polymer types were identified by μFTIR. Of those, 5 were present in rather low concentrations and were lumped into a group called 'Others' (see supplementary information for the polymer types, Table S2). They accounted for 0.15 % of the particle mass estimated by μFTIR, and 4.2 % of the particle counts. The dominant polymers as particle mass and as found by μFTIR were PP (78.7 %), PVC (10.7 %) and polyester (5 %), together constituting 94.5 % of all MPs (Fig. 5). The high composition of PP held true also when measured as particle number (34 %), now followed by polyester (23 %) and PE (15 %). The prevalence of PP in sediments of freshwater systems have been reported by other authors, for example Olesen et al. (2019), Liu et al. (2019b), Bharath et al. (2020), and Molazadeh et al. (2022). The high level of PP is probably linked to its high consumption in daily life (plastic Europe 2020). Including TWP in the analysis, the ranking changed as tyre wear particles stood as the second most abundant polymer across the lake, constituting 6.9 % of the total MPs identified. Such comparison must though be taken with a grain of salt, as comparing concentration data using different analytical approaches is not always reliable. So did Primpke et al. (2020c) find that when estimating mass from μFTIR data, the polymer masses were overestimated in samples containing larger and many particles. Doing a quite similar comparison, Kirstein et al. (2021) on the other hand found that masses correlated well when concentrations were high, but poorly when they were low.

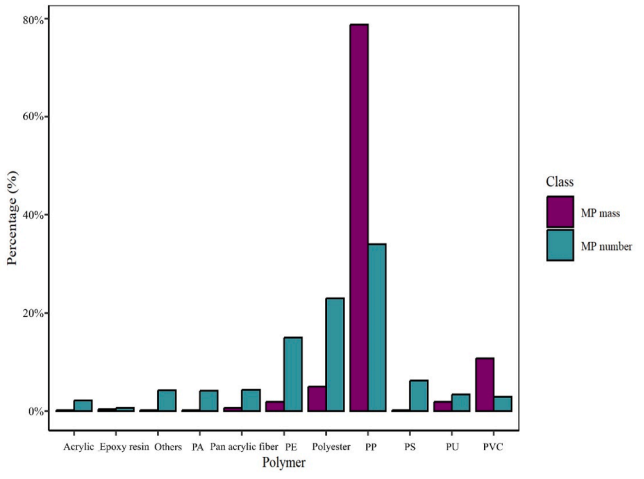

Fig. 5. Polymer composition of the MPs detected in the lake by μFTIR. The concentration is given as particle counts and estimated mass. The tyre wear particles were excluded in this graph since their number cannot be identified by Py-GC/MS.

No preferential spatial distribution of polymer composition was seen in the lake, indicating a rather random distribution. This held true for particle counts and mass (Fig. 6). Of MPs detected by μFTIR, buoyant polymers (PP + PE) were abundant at most sampling locations. Considering that PP and PE are lighter than water, there must be some process or processes causing MPs that intrinsically float to reach the sediments of the lake. This could, for instance, be mixing induced by turbulence, aggregation with microorganisms and naturally occurring particles, biofouling, and mineral formation (Lobelle and Cunliffe, 2011, Semcesen and Wells, 2021, Molazadeh et al., 2022). What is the dominant process remains speculation but considering that the average hydraulic residence time in the lake is only 12 days, and that the lake is only around a meter deep and not stratified, physical turbulence-driven transport seems a likely candidate for being the dominant mechanism (Molazadeh et al., 2022). Considering TWP, it dominated the polymer type of most sampling locations (Table S1 and S2), however, due to the limitation of Py-GC/MS to detect the number of particles, this polymer is not included in Fig. 6.

3.3.2. MP size and mass

Accounting for the size of MPs at each location, most were smaller than 100 μm (Table S2). In order to compare the size and mass distribution of MPs of different sampling locations, a non-parametric Kruskal-Wallis test (as data were not normally distributed as tested by a Shapiro-Wilk normality test) was performed (Table S4 and S5 and Fig. S2). No spatial pattern was seen for the particle size and particle mass distributions of MPs, and mass and size distribution of MPs in many, but not all, locations were similar ($p > 0.05$). This led to the conclusion that preferential accumulation of heavy and large particles had not occurred.

Despite the absence of any trends, there were some locations that showed different size and mass distribution ($p < 0.05$), which probably was due to random deposition patterns. In other words, closeness to potential sources such as the upstream wetland, the combined sewer overflows and stormwater outfalls on the northern shore, and the WWTP discharge at the southeast part of the lake did not affect the MP size and mass at the sampling locations.

3.3. The effect of MP size on MP abundance and distribution pattern

The occurrence of buoyant and non-buoyant MPs in the bed sediments at high concentration but with no obvious pattern of distribution, brough up the question how they spread across the lake. One reason for not seeing a pattern might be turbulence induced by wind and inflows, that causes eddies, which then mix the water (Bentzen et al., 2009). Small particles will follow the eddies as their intrinsic sinking or rising velocities are much smaller than the local water velocity inside the eddy (Shamskhany and Karimpour, 2022). Even dense sub-millimetre particles do not sink along a straight path but move chaotically depending on time and space-dependent flow-patterns (Molazadeh et al., 2023). Another reason could be that MPs in sediments reflect long-term accumulation. The lake is quite shallow, and strong winds can cause sediments to resuspend and redeposit. How and where will depend on parameters such as wind direction and strength. Such reshuffling of the sediments could easily mask an intrinsic pattern caused by closeness to

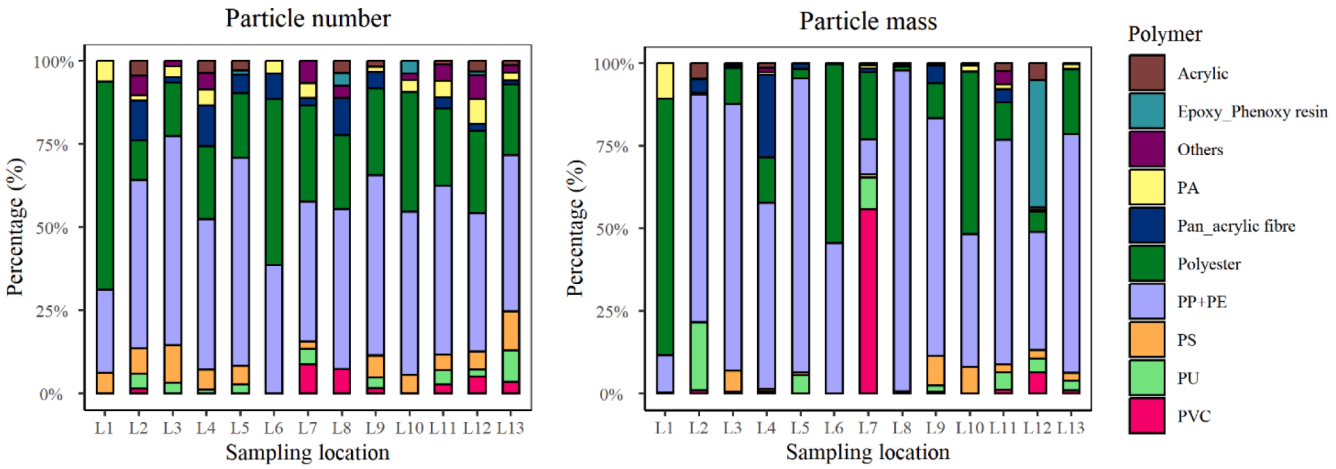

Fig. 6. Polymer composition of the MPs identified by μFTIR at each sampling locations, measured by particle counts (A) and mass (B).

sources. Moreover, from sediment transport theory it is well-known that size can play an important role in transport and sinking of particles (Shamskhani and Karimpour, 2022). For instance, regardless of their high density, small particles like silt (0.004–0.062 mm) and sand (0.06–2 mm) can be transported over long distances before reaching a low-velocity zone and settle (Shamskhani et al., 2021).

The equivalent spherical diameter (D_{eq}), which to some degree also covers the effect of shape, was applied to see if particle size had impacted the occurrence of polymers, both buoyant and non-buoyant ones (excluding tyre wear particles) (Fig. 7A and Table S6). The first question was whether particles which intrinsically should float behaved differently than particles which should intrinsically sink, i.e., buoyant versus non-buoyant MPs. A Wilcox test showed no significant difference ($p > 0.05$) between the size of buoyant and non-buoyant polymers after lumping all the MPs identified from the lake (Fig. 7A). When the test was done per sampling location, again, no significant difference was found, i.e., the size of buoyant and non-buoyant polymers was similar ($p > 0.05$). The only exception was *L*10 ($p < 0.05$).

This implies that it probably was similar processes that brought MPs to the sediment, regardless of their density. It is worth noting that 90 % of the detected particles had a D_{eq} below 250 μm. Such small particles can get entrained by flow regardless of their density, and thus behave in a similar manner (Shamskhani and Karimpour, 2022). For such small sizes, MPs' vertical motion is mainly dominated by turbulent dispersion, and the density has a minimal effect on their dispersal. This was also concluded by the modelling study of Shamskhani and Karimpour (2022), who observed that the motion of fine MPs is mainly governed by the ambient turbulent flow, while large particles' vertical motion may be dominated by gravitational settling or rising. Depending on the energy of flow, particles of different sizes and densities can become entrained and thus deviate from their natural sinking or floating behaviour and consequently be carried by the flow. Shamskhani and Karimpour (2022) for instance, showed that in a stream with a turbulent kinetic energy of 0.06 m^2/s^{-2}, 2 mm PE particles (ρ_p = 940 kg m^{-3}) could get entrained by the flow, hence hampering their rising to the surface.

This means that the vertical motion of MPs can be strongly influenced by mixing and their behaviour in turbulent flow similarly affected. How significant the effect is will depend on the turbulence, the density, and the size of the MP. A thought experiment can illustrate this. If density was the sole plastic property governing the transport and distribution of MPs, all land-based debris composed of sinking polymers

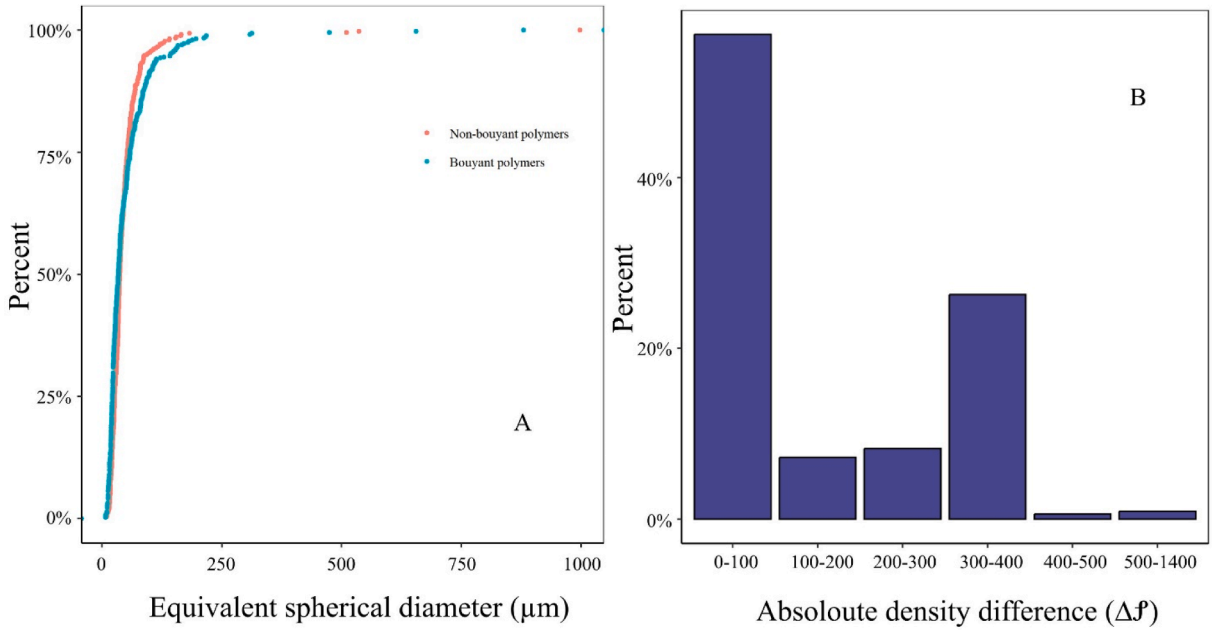

Fig. 7. Equivalent spherical diameter (D_{eq}), for buoyant and non-buoyant MPs identified by μFTIR (A) and their marginal density (B).

like PVC and PET would settle in the close vicinity of an emission source, depending on their intrinsic settling velocity in quiescent water. Moreover, low-density particles such as PE and PP would not be present in sediment and high-density polymers, such as PVC and PET ($\rho > 1.1$ g cm^{-3}), would not be found at the water surface (Liu et al., 2019a). This is obviously not the case as small particles with low marginal density ($|f_p - f_w|$) can be expected to behave like passive scalers and follow flow paths. Eddies caused by turbulence will hence occasionally cause them to encounter the sediment bed where they might get trapped. The marginal density of all MPs identified by μFTIR is shown in Fig. 7B. Most particles (57 %) had a low marginal density, i.e., within ± 10 % of that of the lake water, and 63 % of particles were < 100 μm (Fig. 7A). For fine particles, the smaller the marginal density, the more likely the particle follows the path of the flow, i.e., the streamlines. It must, though be noted that turbulent particle transport is not the only explanatory process which can contribute to explaining the observations. Small MPs have a large exterior surface area to volume ratio and their overall density would hence be more affected by biofouling and agglomeration.

3.5. Water depth and pedologic characteristics

Neither MP content identified by μFTIR nor TWP correlated to the water depth at the sampling locations. It must though be kept in mind that the water depth varied little, namely only from 0.5 to 1.5 m (Table S7). Gholizadeh and Cera (2022) also studied MPs in sediments at low water depth without finding a correlation to water depth. For a deeper lake, Cera et al. (2022) on the other hand found that deeper stations were more contaminated.

A rather weak positive correlation was found between the abundance of MPs measured as counts and the organic matter content of the sediments (Table S7) ($r^2 = 0.59$) and silt content ($r^2 = 0.47$), and there was only a rather weak or no correlation between MP concentration measured as mass and sediment properties (Fig. S3). This held true both for MPs identified by μFTIR and for TWP. Similarly, Hengstmann et al. (2018), Renzi et al. (2018) and Vermaire et al. (2017) did not observe a correlation between MP abundance and organic matter of the sediments they studied. In disagreement herewith, several other studies found that there was a positive correlation between sediment organic matter content and MP concentration (Molazadeh et al., 2022; Liu et al., 2021b; Corcoran et al., 2020). In terms of the effect of sediment grain size on MP occurrence, Alamor et al. (2016) and Laju et al. (2022) did not observe a clear trend between sediment grain size and MP deposition in coastal shallow sediments whereas Falahudin et al. (2020) and Liu et al., (2021a), Liu et al., (2021b) found that MP correlated positively with the silt content of marine and river sediments, respectively.

Conclusions on whether MP abundance varies with sediment characteristics are hence vastly diverging, indicating that other factors and environmental conditions might play a significant role on how MPs distribute in the sediments of a water body. According to our findings, the distribution of MPs in the lake sediments could be treated as random, as no parameter could predict its accumulation. The reason can be site-specific hydrodynamics of this shallow lake, in which sediment and MPs contained herein occasionally are resuspended due to waves and inflow, redistributed, and redeposited, leading to a chaotic and random distribution pattern.

4. Conclusion

High concentrations of MPs, identified by μFTIR and Py-GC/MS, were detected in the sediments of a Danish urban lake. The average level of MPs other than TWP exceeded that of sewage sludge, suggesting that the lake sediments had served as a long-term sink of plastic. The spatial variability in MP mass estimated by μFTIR imaging was up to 6 orders of magnitude, while TWP measured by Py-GC/MS varied up to 5 orders of magnitude. There was no spatial pattern in the MP distribution, indicating that a fine sampling grid is needed to accurately reflect MP abundance and distribution in such lake. PP was the most abundant polymer found in the sediments, followed by TWP, emphasising the importance of considering TWP when assessing MP contamination. The study also showed that buoyant and non-buoyant MPs shared similar distribution and were of similar size, suggesting that the same process governed their transport to the sediments.

Declaration of Competing Interest

The authors declare that they have no known competing financial interests or personal relationships that could have appeared to influence the work reported in this paper.

Data availability

Data will be made available on request.

Acknowledgements

This work was carried out within the Limnoplast project. This work was supported by European Union's Horizon 2020 research and innovation programme [860720].

Appendix A. Supplementary data

Supplementary data to this article can be found online at https://doi.org/10.1016/j.envint.2023.108282.

References

Abidli, S., Toumi, H., Lahbib, Y., Trigui El Menif, N., 2017. The first evaluation of microplastics in sediments from the complex lagoon-channel of Bizerte (northern Tunisia). Water, Air, Soil Pollution. 228, 1–10. https://doi.org/10.1007/s11270-017-3439-9.

ASTM, 2000. Standard test methods for moisture, ash, and organic matter of peat and other organic soils. Method D 2974-00. American Society for Testing and Materials, West Conshohocken, PA 2000. American Society for Testing and Materials.

Ballent, A., Corcoran, P.L., Madden, O., Helm, P.A., Longstaffe, F.J., 2016. Sources and sinks of microplastics in Canadian Lake Ontario nearshore, tributary and beach sediments. Mar. Pollut. Bull. 110, 383–395. https://doi.org/10.1016/j.marpolbul.2016.06.037.

Bentzen, T.R., Larsen, T., Rasmussen, M.R., 2009. Predictions of Resuspension of Highway Detention Pond Deposits in Interrain Event Periods due to Wind-Induced Currents and Waves. J. Environ. Eng. 135, 12. https://doi.org/10.1061/(ASCE)EE.1943-7870.0000108.

Besseling, E., Hasselerharm, P.R., Foekema, E.M., Koelmans, A.A., 2019. Quantifying ecological risks of aquatic micro- and nanoplastic. Crit. Rev. Environ. Sci. Technol. 49, 32–80. https://doi.org/10.1080/10643389.2018.1531688.

Bharath, K., M., Srinivasalu, S., Natesan, U., Ayyamperumal, R., Kalam, S.N., Anbalagan, S., Sujatha, K., Alagarasan, C.,, 2021. Microplastics as an emerging threat to the freshwater ecosystems of Veeranam lake in south India: A multidimensional approach. Chemosphere. 264. Part 2, 0045–6535. https://doi.org/10.1016/j.chemosphere.2020.128502.

Cera, A., Pierdomenico, M., Sodo, A., Scalici, M., 2022. Spatial distribution of microplastics in volcanic lake water and sediments: Relationships with depth and sediment grain size. Sci. Total Environ. 829, 0048–9697. https://doi.org/10.1016/j.scitotenv.2022.154659.

Chand, R., Kohansal, K., Toor, S., Pedersen, T.H., Vollertsen, J., 2022. Microplastics degradation through hydrothermal liquefaction of wastewater treatment sludge. Journal of Clean Production. 335, 130383 https://doi.org/10.1016/j.jclepro.2022.130383.

Cole, M., Lindeque, P., Halsband, C., Galloway, T.S., 2011. Microplastics as contaminants in the marine environment: a review. Mar. Pollut. Bull. 62, 2588–2597. https://doi.org/10.1016/j.marpolbul.2011.09.025.

Cole, M., Lindeque, P., Fileman, E., Halsband, C., Galloway, T.S., 2015. The Impact of Polystyrene Microplastics on Feeding, Function and Fecundity in the Marine Copepod Calanus helgolandicus. Environ. Sci. Tech. 49 (2), 1130–1137. https://doi.org/10.1021/es504525u.

Corcoran, P.L., 2020. Degradation of Microplastics in the Environment. Handbook of Microplastics in the Environment. https://doi.org/10.1007/978-3-030-10618-8_10-1.

Corcoran, P.L., Belontz, S.L., Ryan, K., Walzak, M.J., 2020. Factors controlling the distribution of microplastic particles in benthic sediment of the Thames River. Canada. Environmental Science & Technology. 54 (2), 818–825. https://doi.org/10.1021/acs.est.9b04896.

Dean, B.Y., Corcoran, P.L., Helm, P.A., 2018. Factors influencing microplastic abundances in nearshore, tributary and beach sediments along the Ontario shoreline

of Lake Erie. J. Great Lakes Res. 44, 1002–1009. https://doi.org/10.1016/j.jglr.2018.07.014.
Ding, L., Mao, R.F., Guo, X., Yang, X., Zhang, Q., Yang, C., 2019. Microplastics in surface waters and sediments of the Wei River, in the northwest of China. Sci. Total Environ. 667, 427–434. https://doi.org/10.1016/j.scitotenv.2019.02.332.
Dong, X., Liu, X., Hou, Q., Wang, Z., 2023. From natural environment to animal tissues: A review of microplastics(nanoplastics) translocation and hazards studies. Sci. Total Environ. 10, 158686 https://doi.org/10.1016/j.scitotenv.2022.158686.
Eriksen, M., Mason, S., Wilson, S., Box, C., Zellers, A., Edwards, W., Farley, H., Amato, S., 2013. Microplastic pollution in the surface waters of the laurentian great lakes. Mar. Pollut. Bull. 77, 177–182. https://doi.org/10.1016/j.marpolbul.2013.10.007.
Falahudin, D., Cordova, M.R., Sun, X., Yogaswara, D., Wulandari, I., Hindarti, D., Arifin, Z., 2020. The first occurrence, spatial distribution and characteristics of microplastic particles in sediments from Banten Bay. Indonesia. Science of the Total Environment. 705, 135304 https://doi.org/10.1016/j.scitotenv.2019.135304.
Gholizadeh, M., Cera, A., 2022. Microplastic contamination in the sediments of Qarasu estuary in Gorgan Bay, south-east of Caspian Sea. Iran. Science of the Total Environment. 838, 0048–9697. https://doi.org/10.1016/j.scitotenv.2022.155913.
Gopinath, K.P., Nagarajan, V.M., Krishnan, A., Malolan, R., 2020a. A critical review on the influence of energy, environmental and economic factors on various processes used to handle and recycle plastic wastes: development of a comprehensive index. J. Clean. Prod. 274, 123031 https://doi.org/10.1016/j.jclepro.2020.123031.
Gopinath, K., Seshachalam, S., Neelavannan, K., Anburaj, V., Rachel, M., Ravi, S., Bharath, M., Achyuthan, H., 2020b. Quantification of microplastic in Red Hills Lake of Chennai city, Tamil Nadu. India. Environmental Science and Pollution Research. 27, 33297–33306. https://doi.org/10.1007/s11356-020-09622-2.
Goßmann, I., Halbach, M., Scholz-Böttcher, B.M., 2021. Car and truck tire wear particles in complex environmental samples – A quantitative comparison with “traditional” microplastic polymer mass loads. Sci. Total Environ. 773, 0048–9697. https://doi.org/10.1016/j.scitotenv.2021.145667.
Gündoğdu, S., Eroldoğan, O.T., Evliyaoğlu, E., Turchini, G.M., Wu, X.G., 2021. Fish out, plastic in: global pattern of plastics in commercial fishmeal. Aquaculture. 534, 736316. https://doi.org/10.1016/j.aquaculture.2020.736316.
Hengstmann, E., Tamminga, M., Bruch, C.M., Fischer, E.K., 2018. Microplastic in beach sediments of the Isle of Rügen (Baltic Sea) - Implementing a novel glass elutriation column. Mar. Pollut. Bull. 126, 263–274. https://doi.org/10.1016/j.marpolbul.2017.11.010.
Hengstmann, E., Weil, E., Wallbott, P., C., Tamminga, M., Fischer, E.K.,, 2021. Microplastics in lakeshore and lakebed sediments – External influences and temporal and spatial variabilities of concentrations. Environ. Res. 197, 0013–9351. https://doi.org/10.1016/j.envres.2021.111141.
Islam, T., Li, Y., Rob, M.M., Cheng, H., 2022. Microplastic pollution in Bangladesh: research and management needs. Environ. Pollut. 308, 119697 https://doi.org/10.1016/j.envpol.2022.119697.
Kelly, A., Lannuzel, D., Rodemann, T., Meiners, K.M., Auman, H.J., 2020. Microplastic contamination in east Antarctic sea ice. Mar. Pollut. Bull. 154, 111130 https://doi.org/10.1016/j.marpolbul.2020.111130.
Kirstein, I.V., Hensel, F., Gomiero, A., Iordachescu, L., Vianello, A., Wittgren, H.B., Vollertsen, J., 2021. Drinking plastics? – Quantification and qualification of microplastics in drinking water distribution systems by μFTIR and Py-GCMS. Water Res. 188, 0043–1354. https://doi.org/10.1016/j.watres.2020.116519.
Knight, L.J., Parker-Jurd, F.N.F., Al-Sid-Cheikh, M., Thompson, R.C., 2020. Tyre wear particles: an abundant yet widely unreported microplastic? Environ Science and Pollution Research. 27, 18345–18354. https://doi.org/10.1007/s11356-020-08187-4.
Laju, R.L., Jayanthi, M., Immaculate Jeyasanta, K., Patterson, J., Asir, G.G., N., Narmatha Sathish, M., Patterson Edward, J.K., 2022. Spatial and vertical distribution of microplastics and their ecological risk in an Indian freshwater lake ecosystem. Sci. Total Environ. 820, 0048–9697. https://doi.org/10.1016/j.scitotenv.2022.153337.
Lechner, A., Ramler, D., 2015. The discharge of certain amounts of industrial microplastic from a production plant into the River Danube is permitted by the Austrian legislation. Environ. Pollut. 200, 159–160. https://doi.org/10.1016/j.envpol.2015.02.019.
Lenaker, P.L., Baldwin, A.K., Corsi, S.R., Mason, S.A., Reneau, P.C., Scott, J.W., 2019. Vertical distribution of microplastics in the water column and surficial sediment from the milwaukee river basin to Lake Michigan. Environ. Sci. Tech. 53, 12227–12237. https://doi.org/10.1021/acs.est.9b03850.
Li, L., Geng, S., Wu, C., Song, K., Sun, F., Visvanathan, C., Xie, F., Wang, Q., 2019. Microplastics contamination in different trophic state lakes along the middle and lower reaches of Yangtze River Basin. Environ. Pollut. 254, Part A, 0269–7491. https://doi.org/10.1016/j.envpol.2019.07.119.
Liu, F., Olesen, K.B., Borregaard, A.R., Vollertsen, J., 2019. Microplastics in urban and highway stormwater retention ponds. Science of the Total Environment. 671, 992–1000. https://doi.org/10. 1016/j.scitotenv.2019.03.416.
Liu, F., da Silva, V.H., Chen, Y., Lorenz, C., Simon, M., Vollertsen, J., Strand., J., 2023. R&D project regarding development of methods for sampling and analysis of microplastics in Danish waters. Report to the Danish EPA, pp. 73.
Liu, F., Vianello, A., Vollertsen, J., 2019b. Retention of microplastics in sediments of urban and highway stormwater retention ponds. Environ. Pollut. 255, 113335 https://doi.org/10.1016/j.envpol.2019.113335.
Liu, F., Lorenz, C., Vollertsen, J., 2021a. Havstrategi – Analyse af mikroplast-partikler i sedimenter (Microplastic particles in sediments from Danish waters 2018–2021). Last downloaded September 9th, 2023 from Report to the Danish EPA 64. https://www.emodnet-ingestion.eu/submissions/submissions_details.php?menu=39&tpd=1185&step_more=11_10_13_14&step=0821.
Liu, H., Sun, K., Liu, X., Yao, R., Cao, W., Zhang, L., Wang, X., 2022. Spatial and temporal distributions of microplastics and their macroscopic relationship with algal blooms in Chaohu Lake. China. Journal of Contaminant Hydrology. 248, 0169–7722. https://doi.org/10.1016/j.jconhyd.2022.104028.
Liu, Y., Zhang, J., Tang, Y., He, Y., Li, Y., You, J., Breider, F., Tao, S., Liu, W., 2021b. Effects of anthropogenic discharge and hydraulic deposition on the distribution and accumulation of microplastics in surface sediments of a typical seagoing river: the Haihe River. Journal of Hazardous Material. 404, 124180 https://doi.org/10.1016/j.jhazmat.2020.124180.
Lobelle, D., Cunliffe, M., 2011. Early microbial biofilm formation on marine plastic debris. Mar. Pollut. Bull. 62, 197–200. https://doi.org/10.1016/j.marpolbul.2010.10.013.
Lusher, A.L., O’Donnell, C., Officer, R., O’Connor, I., 2016. Microplastic interactions with North Atlantic mesopelagic fish. ICES J. Mar. Sci. 73, 1214–1225. https://doi.org/10.1093/icesjms/fsv241.
Malla-Pradhan, R., Suwunwong, T., Phoungthong, K., Joshi, T.P., Pradhan, B.L., 2022. Microplastic pollution in urban Lake Phewa, Nepal: the first report on abundance and composition in surface water of lake in different seasons. Environ. Sci. Pollut. Res. 29 (26), 39928–39936. https://doi.org/10.1007/s11356-021-18301-9.
Matamoros, V., Arias, C.A., Nguyen, L.X., Salvadó, V., Brix, H., 2012. Occurrence and behavior of emerging contaminants in surface water and a restored wetland. Chemosphere 88, 1083–1089. https://doi.org/10.1016/j.chemosphere.2012.04.048.
Mercy, F.T., Alam, A.R., Akbor, M.A., 2023. Abundance and characteristics of microplastics in major urban lakes of Dhaka. Bangladesh. Heliyon. 9, 4. https://doi.org/10.1016/j.heliyon.2023.e14587.
Merga, L.B., Redondo-Hasselerharm, P.E., Van den Brink, P.J., Koelmans, A.A., 2020. Distribution of microplastic and small macroplastic particles across four fish species and sediment in an African lake. Sci. Total Environ. 741, 0048–9697. https://doi.org/10.1016/j.scitotenv.2020.140527.
Miller, J.V., Marskrey, J.R., Chan, K., Unice, M., K.,, 2022. Pyrolysis-Gas Chromatography-Mass Spectrometry (Py-GC-MS)Quantification of Tire and Road Wear Particles (TRWP) inEnvironmental Matrices: Assessing the Importance ofMicrostructure in Instrument Calibration Protocols. Anal. Lett. 55, 1004–1016. https://doi.org/10.1080/00032719.2021.1979994.
Molazadeh, M., Liu, F., Simon-Sánchez, L., Vollersten, J., 2023. Buoyant microplastics in freshwater sediments – How do they get there? Sci. Total Environ. 860, 0048–9697. https://doi.org/10.1016/j.scitotenv.2022.160489.
Monclús, l., Smith, M.E., Ciesielski, T.M., Wagner, M., Jaspers, V.L.B., 2022. Microplastic Ingestion Induces Size-Specific Effects in Japanese Quail. Environ. Sci. Tech. 56 (22), 15902–15911. https://doi.org/10.1021/acs.est.2c03878.
More, S.L., Miller, V., J., Thornton, S.T., Chan, K., Barber, T.R., Unice, K.M., 2023. Refinement of a microfurnace pyrolysis-GC–MS method for quantification of tire and road wear particles (TRWP) in sediment and solid matrices. Sci. Total Environ. 874, 0048–9697. https://doi.org/10.1016/j.scitotenv.2023.162305.
Mun, S., Chong, H., Lee, J., Lim, Y., 2022. Characteristics of Real-World Non-Exhaust Particulates from Vehicles. Energies 16, 177. https://doi.org/10.3390/en16010177.
OECD, 2023. https://www.oecd.org/environment/plastic-pollution-is-growing-relentlessly-as-waste-management-and-recycling-fall-short.htm (accessed 18 August 2023).
Olesen, K.B., Stephansen, D.A., van Alst, N., Vollertsen, J., 2019. Microplastics in a stormwater pond. Water (Switzerland). 11, 1466. https://doi.org/10.3390/w11071466.
Panasiuk, O., Hedström, A., Marsalek, J., Ashley, R.M., Viklander, M., 2015. Contamination of stormwater by wastewater: A review of detection methods. J. Environ. Manage. 152, 241–250. https://doi.org/10.1016/j.jenvman.2015.01.050.
Primpke, S., Christiansen, S.K., Cowger, W., Frond, H.D., Deshpande, A., Fischer, M., Holland, E.B., Meynes, M., O’Donnell, B.A., Ossmann, B.E., Pittroff, M., Sarau, G., Scholz-Böttcher, B.M., Wiggin, J.K., 2020a. Critical assessment of analytical methods for the harmonised and cost-efficient analysis of microplastics. Appl. Spectrosc. 74, 1012–1047. https://doi.org/10.1177/0003702820921465.
Primpke, S., Cross, R.K., Mintenig, S.M., Simon, M., Vianello, A., Gerdts, G., Vollertsen, J., 2020b. EXPRESS: toward the systematic identification of microplastics in the environment: evaluation of a new independent software tool (siMPle) for spectroscopic analysis. Appl. Spectrosc. 74, 1127–1138. https://doi.org/10.1177/0003702820917760.
Primpke, S., Fischer, M., Lorenz, C., Gerdts, G., Scholz-Böttcher, B.M., 2020c. Comparison of pyrolysis gas chromatography/mass spectrometry and hyperspectral FTIR imaging spectroscopy for the analysis of microplastics. Anal. Bioanal. Chem. 412, 8283–8298. https://doi.org/10.1007/s00216-020-02979-w.
Qin, Y., , Z, Wang., Li, W., Chang, X., Yang, J, Yang, F., 2020. Microplastics in the sediment of Lake Ulansuhai of Yellow River Basin, China. Water Environment Research. https://doi.org/10.1002/wer.1275.
Rasmussen, L.A., Lykkemark, J., Andersen, T.R., Vollertsen, J., 2023. Permeable pavements: A possible sink for tyre wear particles and other microplastics? Sci. Total Environ. 869, 0048–9697. https://doi.org/10.1016/j.scitotenv.2023.161770.
Reimonn, G., Lu, T., Gandhi, N., Chen, W.T., 2019. Review of microplastic pollution in the environment and emerging recycling solutions. Journal of Renewable Material. 7 (18), 1251–1268. https://doi.org/10.32604/jrm.2019.0805.
Renzi, M., Blašković, A., Fastelli, P., Marcelli, M., Guerranti, C., Cannas, S., Barone, L., Massara, F., 2018. Is the microplastic selective according to the habitat? Records in Amphioxus Sands, Mäerl Bed Habitats and Cymodocea Nodosa Habitats, Marine Pollution Bulletin. 130, 179–183. https://doi.org/10.1016/j.marpolbul.2018.03.019.

Rødland, E.S., Gustafsson, M., Jaramillo-Vogel, D., Järlskog, I., Müller, K., Rauert, C., Rausch, J., Wagner, S., 2023. Analytical challenges and possibilities for the quantification of tire-road wear particles. TrAC Trends Anal. Chem. 165, 0165–9936. https://doi.org/10.1016/j.trac.2023.117121.

Scopetani, C., Chelazzi, D., Cincinelli, A., Esterhuizen-Londt, M., 2019. Assessment of microplastic pollution: occurrence and characterisation in Vesijärvi lake and Pikku Vesijärvi pond. Finland. Environmental Monitoring and Assessment. 191, 652. https://doi.org/10.1007/s10661-019-7843-z.

Semcesen, O.P., Wells, G.M., 2021. Biofilm growth on buoyant microplastics leads to changes in settling rates: implications for microplastic retention in the Great Lakes. Mar. Pollut. Bull. 170, 112573 https://doi.org/10.1016/j.marpolbul.2021.112573.

Shamskhany, A., Karimpour, S., 2022. Entrainment and vertical mixing of aquatic microplastics in turbulent flow: The coupled role of particle size and density. Mar. Pollut. Bull. 184, 0025–0326. https://doi.org/10.1016/j.marpolbul.2022.114160.

Shi, M., Li, R., Xu, A., Su, Y., Hu, T., Mao, Y., Qi, S., Xing, X., 2022. Huge quantities of microplastics are "hidden" in the sediment of China's largest urban lake—Tangxun Lake. Environ. Pollut. 307, 0269–7491. https://doi.org/10.1016/j.envpol.2022.119500.

Simon, S., Van Last, N., Vollertsen, J., 2018. Quantification of microplastic mass and removal rates at wastewater treatment plants applying Focal Plane Array (FPA)-based Fourier Transform Infrared (FT-IR) imaging. Water Res. 142, 0043–1354. https://doi.org/10.1016/j.watres.2018.05.019.

Simon-Sánchez, L., Grelaud, M., Lorenz, C., Garcia-Orellana, J., Vianello, A., Liu, F., Vollertsen, J., Ziveri, P., 2022. Can a sediment core reveal the Plastic Age? – Microplastic preservation in a coastal sedimentary record. Environ. Sci. Tech. 56, 16780–16788. https://doi.org/10.1021/acs.est.2c04264.

Søndergaard, M., Jeppesen, E., Jensen, J.P., Lauridsen, T., 2008. Lake restoration in Denmark. Lakes & Reservoirs: Science, Policy and Management for Sustainable Use. 5, 133–212. https://doi.org/10.1046/j.1440-1770.2000.00110.x.

Unice, K.M., Kreider, M.L., Panko, J.M., 2013. Comparison of tire and road wear particle concentrations in sediment for watersheds in France, Japan, and the United States by quantitative pyrolysis GC/MS analysis. Environ. Sci. Tech. 47, 8138–8147. https://doi.org/10.1021/es400871j.

Unice, K.M., Weeber, M.P., Abramson, M.M., Reid, R.C.D., Gils, J.A.G.V., Markus, A.A., Vethaak, A.D., Panko, J.M., 2019. Characterising export of land-based microplastics to the estuary - Part I: Application of integrated geospatial microplastic transport models to assess tire and road wear particles in the Seine watershed. Sci. Total Environ. 646, 1639–1649. https://doi.org/10.1016/j.scitotenv.2018.07.368.

Vermaire, J.C., Pomeroy, C., Herczegh, S.M., Haggart, O., Murphy, M., 2017. Microplastic abundance and distribution in the open water and sediment of the Ottawa River, Canada, and its tributaries. FACETS. 2, 301–314. https://doi.org/10.1139/facets-2016-0070.

Vianello, A., Jensen, R.L., Liu, L., Vollertsen, J., 2019. Simulating human exposure to indoor airborne microplastics using a Breathing Thermal Manikin. Sci. Rep. 9, 8670. https://doi.org/10.1038/s41598-019-45054-w.

Wadell, H. Volume, Shape, and Roundness of Rock Particles., 1932. J. Geol. 40, 443−451.

Wang, F., Lai, Z., Peng, G., Luo, L., Liu, K., Huang, X., Xu, Y., Shen, Q., Li, D., 2021. Microplastic abundance and distribution in a Central Asian desert. Sci. Total Environ. 800, 0048–9697. https://doi.org/10.1016/j.scitotenv.2021.149529.

Wang, C., O'Connor, D., Wang, L., Wu, W.M., Luo, J., Hou, D., 2022. Microplastics in urban runoff: Global occurrence and fate. Water Res. 225, 0043–1354. https://doi.org/10.1016/j.watres.2022.119129.

Yang, S., Zhou, M., Chen, X., Hu, L., Xu, Y., Fu, W., Li., C.,, 2022. A comparative review of microplastics in lake systems from different countries and regions. Chemosphere 286, 131806. https://doi.org/10.1016/j.chemosphere.2021.131806.

Yin, L., Wen, X., Du, C., Jiang, J., Wu, L., Zhang, Y., Hu, Z., Hu, Z., Feng, Z., Zhou, Z., Long, Y., Gu, Q., 2020. Comparison of the abundance of microplastics between rural and urban areas: A case study from East Dongting Lake. Chemosphere 244, 0045–6535. https://doi.org/10.1016/j.chemosphere.2019.125486.

Yonkos, L.T., Friedel, E.A., Perez-Reyes, A.C., Ghosal, S., Arthur, C.D., 2014. Microplastics in Four Estuarine Rivers in the Chesapeake Bay, U.S.A. Environ. Sci. Tech. 48, 24, 14195–14202. https://doi.org/10.1021/es5036317.

Ziajahromi, S., Drapper, D., Hornbuckle, A., Rintoul, L., Leusch, F.D.L., 2020. Microplastic pollution in a stormwater floating treatment wetland: detection of tyre particles in sediment. Sci. Total Environ. 713, 136356 https://doi.org/10.1016/j.scitotenv.2019.136356.

Further reading

Shamskhany, A., Li, Z., Patel, P., Karimpour, S., 2021. Evidence of microplastic size impact on mobility and transport in the marine environment: a review and synthesis of recent research. Front. Mar. Sci. 8, 1869. https://doi.org/10.3389/fmars.2021.760649.

Paper-III

The role of turbulence in the deposition of intrinsically buoyant MPs.

The role of turbulence in the deposition of intrinsically buoyant MPs

Marziye Molazadeh, Guilherme Calabro, Fan Liu, Bruno Tassin, Lorenzo Rovelli, Andreas Lorke, Rachid Dris, Jes Vollertsen

PII: S0048-9697(23)07168-1

DOI: https://doi.org/10.1016/j.scitotenv.2023.168540

Reference: STOTEN 168540

To appear in: *Science of the Total Environment*

Received date: 29 July 2023

Revised date: 22 October 2023

Accepted date: 10 November 2023

Please cite this article as: M. Molazadeh, G. Calabro, F. Liu, et al., The role of turbulence in the deposition of intrinsically buoyant MPs, *Science of the Total Environment* (2023), https://doi.org/10.1016/j.scitotenv.2023.168540

The role of turbulence in the deposition of intrinsically buoyant MPs

Marziye (Shabnam) Molazadeh[1], Guilherme Calabro[2], Fan Liu[1], Bruno Tassin[2] , Lorenzo Rovelli[3], Andreas Lorke[3], Rachid Dris[2], Jes Vollertsen[1]

[1]Aalborg University, Section of Civil and Environmental Engineering, Department of the Built Environment, Thomas Manns Vej 23, 9220 Aalborg Øst, Denmark

[2] LEESU, Ecole des Ponts, Univ Paris Est Creteil, Marne-la-Vallée, France

[3]Institute for Environmental Sciences, RPTU Kaiserslautern Landau, Landau, Germany

Corresponding autour E-mail address: marziyem@build.aau.dk

Abstract

Intrinsically floating microplastics (MP) such as polyethene (PE) or polypropylene (PP) are among the most common MPs found in aquatic sediments. There must hence be mechanisms that cause lighter-than-water MPs to deposit despite them being buoyant. How these MPs end up in the sediment bed is only partly understood. This study explores how turbulence in the water can affect the vertical movement of buoyant MP and bring them in contact with the bed. The deposition of PE (995 kg m^{-3}) in slow-flowing water (average flow velocities of 1.85 and 4.17 cm s^{-1}) was measured by tracking them and analyzing their motion in an open, rectangular, glass-sided flume. Flow characteristics in terms of turbulent kinetic energy and shear velocity was measured by particle image velocimetry. Experiments were conducted at a water depth of 27 cm and at various hydraulic conditions created by adjusting inflow speeds and using different bed materials: medium gravel, fine gravel, medium sand, cohesive sediment, and glass. The results showed that the vertical velocity of the MPs in the turbulent flow regimes varied over 4 orders of magnitude from their predicted rising velocity in quiescent water (laminar flow). Turbulence mixing resulted in distribution throughout the water column with a substantial quantity consistently subject to downward vertical transport, which in turn increased the chance of the PE particles encountering the bed and potentially getting immobilized. This work

provides a plausible explanation and further experimental validation for the concept of mixing induced transfer of MPs from the water surface to the sediments of shallow waters.

Keywords: Buoyant MPs, Vertical transport, Turbulent flow, PTV

1. Introduction

Plastic pollution in the aquatic environment causes major problems, ranging from macroscopic impacts such as the entanglement of marine wildlife by macroplastics (> 5 mm), to the ingestion of tiny plastic fragments called microplastics (MPs) (< 5 mm) by organisms. Plastic pollution is linked to its widespread use and inadequate practices in waste management, as well as the physical properties of plastics such as durability and floating ability. These properties result in their easy transport in water bodies (Moore, 2008).

With growing concern about the adverse environmental impacts of plastics, this topic has seen increasing interest from the public, from legislators, and researchers. There has been a particular focus on MPs due to their potential harm to organisms. These particles are released into the environment either as primary MPs (i.e., as plastic particles intentionally produced to sizes below 5 mm) (Cole et al., 2011) or from the fragmentation of larger plastic items under impact of light, heat, mechanical forces, and other factors (secondary MPs) (Andrady, 2011).

Studies of MPs in various water bodies have shown that they cover a wide spectrum of properties in terms of polymer, size, shape, density, etc. which all affect their mobility and eventual fate (Khatmullina and Chubarenko, 2019). MPs in a flowing water body, for example a river (Lu et al., 2023) or the currents of a lake (Yan et al., 2022) or ocean (Liu et al., 2023), can be transported longitudinal over long distances . At the same time, they are transported vertically due to gravitational forces and the eddies of turbulent flow (Molazadeh et al., 2023). The vertical transport ultimately leads to the MPs arriving at the bottom of the water body, where they can become part of the sediment bed (Simon-Sanchez et al., 2022).

One of the physical characteristics commonly associated with the mobility and fate of MPs is their density. The density of MPs varies widely, with some having densities as low as 0.8 g cm^{-3} and others as high as 2 g cm^{-3} (Koelmans et al., 2022). Positively buoyant MPs are lighter than the ambient fluid; hence based on the density alone, they are supposed to be present at the surface of a water body and not close to or in its bed. Nevertheless, lower-than-water-density polymers such as PP and PE are among

the most common MPs found in freshwater sediments (Molazadeh et al., 2023; Olesen et al., 2019; Liu et al., 2019; Bharath et al., 2020).

MP density, and consequently their sinking behavior, have been widely reported to change in the environment due to various mechanisms, such as material ageing, biofouling, aggregation with other organic/inorganic particles, vertical mixing, etc. (Long et al., 2015; Semcesen and Wells, 2021; Molazadeh et al., 2023). However, a recent paper by Jalón-Rojas et al. (2022) contradicts the general assumption that the attachment of biofilm to a plastic particle will result in faster descent. The authors showed that the irregular attachment of biofilm decreased the sinking velocity of sheets due to triggering motion instabilities, despite an increase in density. These and other findings (Besseling et al., 2017; Li et al., 2019) indicate that processes other than simple sinking or rising can affect the vertical transport of MPs, and that they should be given more attention.

Another process which can affect the vertical transport of MPs is turbulence-induced mixing driven by factors such as surface wind, temperature gradients, river flow, and waves, as they cause motion in addition to gravity and buoyancy, which then affects the fate of particles (Shamskhani and Karimpoor, 2022). However, so far, physical drivers of MP transport within turbulent aquatic environments have only sporadically been investigated. The gravitational velocity of MPs in quiescent water has been examined by several researchers (Ballent et al., 2013; Reisser et al., 2015; Kowalski et al., 2016; Khatmullina and Isachenko, 2017; Kaiser et al., 2019; Waldschläger and Schüttrumpf, 2019). However, water bodies like rivers and the upper layers of lakes, fjords, and seas are not quiescent (laminar flow conditions) but turbulent, and experimental studies of the vertical velocity of MPs under such conditions are scarce. Studies addressing turbulent conditions have been limited to modelling exercises (Dily and Hoffman, 2020; Shamskhany and Karimpour, 2022). For example, in the study by Shamskhany and Karimpour (2022), the authors modelled the effect of MP size and density on their mixing behavior in response to different turbulence intensities, and they found that the motion of small MPs is highly influenced by the ambient turbulent flow. Additionally, field measurements (Kukulka et al., 2012; Kooi et al., 2016) as well as regional large-eddy simulations of oceans (Liang et al., 2012; Yang et al., 2014; Brunner et al., 2015; Taylor, 2018) have shown the presence of vertical concentration profiles within the ocean mixed layer. These profiles are largely caused by wind and wave breaking at the ocean surface (Chamecki et al., 2019), leading to buoyant particles being distributed in the ocean mixed layer instead of accumulating at its surface.

Moreover, whether turbulence can transfer buoyant MPs from the water surface to the sediments has not yet been experimentally investigated. In a study by Molazadeh et al. (2023) the authors concluded that mixing was likely to have caused the transfer of PP and PE polymers to the bed sediments of a small water body. They substantiated this by computational fluid dynamics modelling. However, to prove this concept, in-depth laboratory experiments are needed. Studying this fundamental mechanism can help to answer the question of why much plastic seems to be missing in the global plastic mass budget. The lack of balance between plastic production and observed plastic in the oceans (Isobe and Iwasaki, 2022) suggests the possibility of buoyant polymers existing in the water column and entering the sediments rather than staying at the water surface. Furthermore, understanding the role of turbulence in MP transport is a prerequisite to predict the pathways and final endpoints of MPs in water bodies, which in turn will allow better estimates on local concentrations and consequently environmental impacts.

The objective of this study was to better understand the turbulent transport of buoyant MPs. It was done by tracking the movement of marginally buoyant MPs (PE particles) under turbulent flow conditions to see how the ambient flow regime and conditions affect their movement. The probability that a particle can encounter the bed at different flow turbulent kinetic energies and bed types was also assessed. For this, Particle Tracking Velocimetry (PTV) and Particle Image Velocimetry (PIV) were applied to separately monitor the trajectory and velocities of individual PE particles and measure turbulence characteristics. Different sets of experiments with different flow conditions and bed types were conducted.

2. Material and methods

2.1 Experimental setup and experimental conditions

The experiments were conducted in a 2 m long, 0.3 m wide, and 0.3 m deep, rectangular, glass-sided, flume in the hydraulics laboratory of the National Research Institute for Agriculture, Food and the Environment (INRAE) at Antony, France (Fig. 1). For all experiments, the flume was filled to a height of h = 27 cm with tap water with a measured density of 1001 kg m^{-3}. Five test beds were examined, ranging from a glass bed (no sediment in the flume) to a gravel bed (Table 1). The size distribution of each bed sediment can be seen in Fig. S1. Before each experiment, sediments were washed until the residual water was clear. It was necessary to remove dirt from the medium gravel, fine gravel, and medium sand beds as it otherwise could have interfered with the flow analysis. The cohesive sediments consisted of clay and silt. The sediment size distribution for this bed type was found by laser diffraction.

The median grain diameters (d50) of the beds are given in Table 1. Each bed was established at the bottom of the flume with a thickness of 0.05 m. The test section was located 1.2 m downstream of the water inlet (Fig. 1). The water temperature was around 20°C throughout the experiments.

Water entered the flume through 2 customized pipes, placed 1.2 m upstream of the measuring location (Fig. 1A). The pipes were parallel, horizontal, and had holes pointing in the direction of the flow (Fig. 1B). At its lowest and highest level, the pump generated a flow resulting in an average velocity in the flume of 1.85 and 4.17 cm s^{-1}, corresponding to Reynolds numbers of 3674 and 8282, respectively. The flow conditions created when the pump was set at its highest and lowest level are subscripted with respectively 1 and 2 in Table 1. In addition, to create a less turbulent flow condition at the lowest flow rate, the inflow pipes (Fig. 1B) were turned in the opposite direction of the flow, that is, the holes pointed towards the upstream flume wall. By hitting the wall and being reflected back into the flume, some of the energy of the flow was dissipated, creating less turbulence. This flow condition is subscripted with 3 in Table 1.

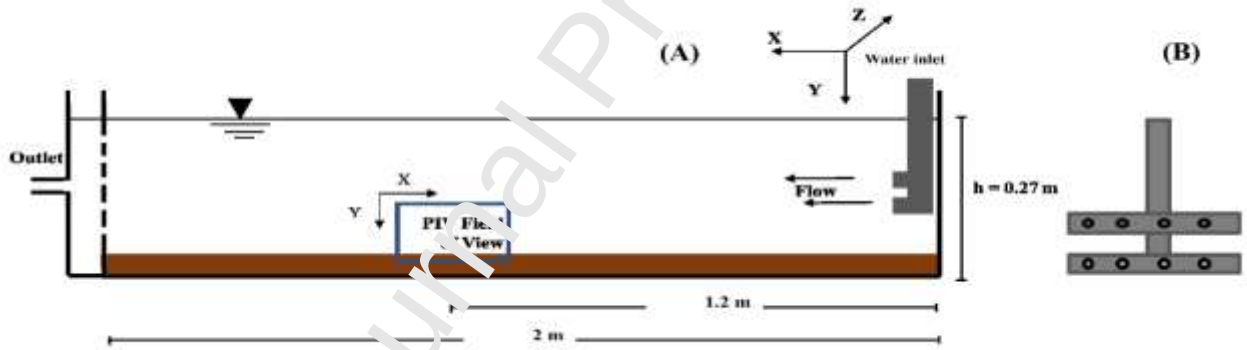

Fig. 1. Schematic of the experimental set-up (A) front view of the customized water inlet pipe (B)

2.2 Measuring particle trajectories

Instantaneous velocities for each test were measured by two-dimensional particle image velocimetry (PIV). The flow was seeded with small tracer particles and illuminated with a pulsed laser light sheet. A camera recorded images of the illuminated area during each light pulse. The displacement of the particle between the light pulses was used to determine the velocity vectors. A high-speed camera (Dantec Dynamics FlowSense 4M (CCD) digital camera) with a resolution of 2048×2048 pixels and an Nd: YAG double-pulse laser (Litron Lasers Nano -S200 15 PIV, wavelength: 532 nm), fitted with a powell lens line optics to generate a planar light sheet, was used for the PIV measurements.

The measurements were conducted in the vertical centerline of the flume at a distance of 15 cm from the side walls, and the field of view (FOV) was irradiated by the laser. The thickness of the laser sheet was approximately 1 mm, and it entered the flow through the free surface allowing simultaneous measurements of the streamwise (u) and wall-normal velocity components (v).

The seeding particles to trace the flow, and thus measure flow characteristics according to their instantaneous motion, were 20 µm Polyamide particles (PSP) with a specific gravity of 1,030 kg m^{-3}. A calibration target was used to provide a reference scale for the physical dimensions in the captured images and the corresponding distances in the real-world flow field. The camera recorded double-frame images for 90 s at a rate of 7.4 Hz within the FOV of approximately 8×6 cm. The FOV varied between 5.6 and 6.4 cm for different experiments, and was calculated from calibration images that captured the water from ~1 cm above the bed. The time interval between each frame, i.e., between laser pulses, was 22 ms. The image pairs were processed using the open-source software PIVlab (Thielicke and Stamhuis, 2014). An FFT deformation algorithm (direct Fourier transform correlation with multiple passes and deforming windows) was used within the PIVlab software to derive the velocity field. The data were analyzed by this algorithm in 3 passes with 128, 64, and 32-pixel interrogation areas (Thielicke and Stamhuis, 2014).

To track the path of MPs and measure their velocity, 40 – 47 µm spherical and fluorescent PE particles (UVPMS-BR, Cospheric) with a density of 995 kg m^{-3} were injected into the flume, and their trajectories tracked. The laser sheet for illuminating the fluorescent particles was approximately 2 cm deep. The particles emitted light in a red color when excited by the laser, clearly distinguishing them from other particles in the flow. A long-pass optical filter was mounted on the camera lens to capture only the emitted (fluorescent) red light from the MP particles.

At the start of each experiment, the FOV was checked to see how many particles were left from previous experiments. Depending on the leftover particle concentration, approx. 8.5 mg of fluorescent particles was dispersed in a small amount of water and added to the flume. This step involved some trial-and-error checking of the FOV to see if there were enough particles to be tracked, as some particles got stuck in the tubing's and other parts of the flume, thus leading to some loss of particles.

A series of images was recorded at 14.8 Hz for 30 s. Because the images were taken rapidly, individual MPs could be tracked and followed over the time of measurement while passing the FOV. Each measurement was repeated 6 times, for a total of 3 minutes per experiment. The sequences of captured images were processed to identify and track individual particles over time using algorithms developed

by Standford University to track the trajectories of particles moving in fluids (Particle Tracking, Standford). The image processing toolbox of MATLAB (The MathWorks Inc., 2020a) was used to pre-process images, for instance, to increase image intensities or to draw the bed topography.

2.3 Particle transport

Turbulence data were computed based on the fluctuating velocity obtained from a classical Reynolds decomposition; that is, the instantaneous horizontal and vertical velocity components were decomposed into a mean value and a fluctuation term (Eq. 1; Reynolds, 1895). Data from the PIV measurements provided the streamwise, *u*, and wall-normal, *v*, instantaneous flow velocity fields.

$$u' = u - \bar{u} \text{ and } v' = v - \bar{v} \quad (1)$$

where *u* and *v* are the instantaneous velocity components, $\bar{u}$ and $\bar{v}$ the time-averaged components, and the primes indicate their fluctuation terms. The turbulent kinetic energy (TKE, Eq. 2) was used to quantify the intensity of the turbulent flow. The lateral velocity component is not measured by 2D PIV, and 2D PIV hence provides velocity information in a plane only, meaning in the streamwise-vertical plane, neglecting the lateral velocity component. The estimated TKE could hence not fully account for the energy associated with the lateral turbulence.

$$\text{TKE} = \frac{1}{2}(\overline{u'^2} + \overline{v'^2}) \quad (2)$$

To investigate entrainment of hypothetical particle sizes and densities not physically tested in the flume experiments, the dimensionless Rouse parameter was introduced (Eq. 3).

$$\text{P} = \frac{\text{W}_\text{s}}{\beta \text{K} \text{u}^*} \quad (3)$$

where W_s is the particle terminal settling/rising velocity [m s^{-1}], k is the von Karman constant [-] set to 0.4, β [-] is a parameter that adjusts the assumption of parabolic eddy diffusivity for the Rouse profile (assumed to be 1) (Leeuw et al., 2020), and u* is the spatially averaged shear velocity [m s^{-1}] of the flow calculated from Eq. 4.

$$\text{u}^* = \sqrt{\overline{u'v'}} \quad (4)$$

To calculate the Rouse parameter, the particle terminal velocity (W_s) must be derived. For small spherical particles, like the 40 – 47 µm PE particles of the present study, W_s can be determined by Stokes law (Eq. 5) as it is valid for spherical particles < 100 µm.

$$W_s = \frac{gd^2(\rho_p - \rho_w)}{18\mu} \quad (5)$$

where g is the gravitational acceleration [m s^{-2}], d the particle diameter [m], ρ_p the particle density [kg m^{-3}], ρ_w the density of the ambient water [kg m^{-3}], and μ is the kinematic viscosity [m^2 s^{-1}] of the flow at 20°C.

For larger particles, the Dietrich formula (Dietrich, 1982) was used to calculate the particle settling or rise velocity, as it is valid for particles up to 4.9 mm. Only spherical particles were considered, and the Dietrich formula could be simplified to Eq. 6 (Isachenko, 2020).

$$W_s = \sqrt[3]{W_* \frac{(\rho_p - \rho_w)}{(\rho_w)^2} g\mu} \quad (6)$$

where

$$W_* = 10^R$$

$$R = -3.76715 + 1.92944 \log_{10} D_* - 0.09815(\log_{10} D_*)^2 - 0.00575(log_{10} D_*)^3 + 0.00056 (log_{10} D_*)^4$$

$$D_* = \frac{|\rho_p - \rho_w| g d^3 \rho_w}{\mu^2}$$

Results and discussion

3.1. Measured flow characteristics

The measured flow characteristics, including turbulent kinetic energy (TKE) and shear velocity (u*), did not increase with bed roughness (Table 1). There were several reasons for this. One was that the flume was too short (2 m) to ensure a fully developed velocity profile, that is, the upstream and downstream discharge points affected the flow pattern and hence the measurements. The bed form with its undulations could in principle induce a similar effect within the studied 6 cm from it. However, the effect was seen for all bed forms, also the glass bed, and the first reason hence probably the dominant one. This means that the experiments did not reflect idealized hydraulic conditions, which on the other hand was not the purpose of the experiments. The purpose was to study non-ideal conditions which are not uncommon in the real world. Table 1 summarizes the flow turbulence characteristics measured during each experiment. The flow characteristics could not be measured for the cohesive sediment bed

experiments due to the presence of suspended solids in the flow, which made it impossible to solely detect tracer particles.

Table 1. Investigated flow conditions and bed types, TKE (turbulent kinetic energy), u* (shear velocity) and d50 (median grain diameter of the sediment bed) of each experiment.

Test bed / Flow condition	TKE (J/kg)	u* (cm/s)	d50 (mm)	Bed types
Medium gravel 1	6.9×10^{-4}	0.7	8.3284	
Medium gravel 2	3.8×10^{-4}	0.5	8.3284	
Medium gravel 3	2.6×10^{-4}	0.48	8.3284	
Fine gravel 1	6.6×10^{-4}	1.05	3.2288	
Fine gravel 2	8.0×10^{-4}	0.95	3.2288	
Fine gravel 3	2.6×10^{-4}	0.47	3.2288	
Medium sand 1	5.0×10^{-4}	0.8	0.2641	
Medium sand 2	3.0×10^{-4}	0.65	0.2641	
Medium sand 3	6.3×10^{-4}	0.49	0.2641	
Cohesive sediment 1	N.A.	N.A.	0.0336	
Cohesive sediment 2	N.A.	N.A.	0.0336	
Cohesive sediment 3	N.A.	N.A.	0.0336	
Glass 1	1.2×10^{-3}	1.26	-	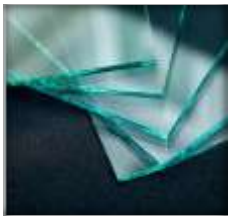
Glass 2	6.1×10^{-4}	0.62	-	
Glass 3	8.7×10^{-4}	0.86	-	

3.2. Settling and rising velocity of PE particles

The nature of particle motion is determined by the balance between the forces acting upon the particle. In a motionless water column, a freely moving particle's terminal velocity (falling or rising) is defined under the assumption that gravity, buoyancy, and fluid drag are acting on the particle, and these forces are properly in balance. Stokes formulated the first theoretical model relating the terminal velocity of a particle in a liquid to the gravitation and drag forces acting on said particle. Stokes' law provides a convenient measure for calculating particles' settling or rising velocity; however, it applies only to small spherical particles existing in laminar flow, i.e., low Reynolds numbers (Stokes, 1851).

Fig. 2 shows the measured time-averaged velocities of the PE particles for the fine gravel bed at different flow conditions (the full set of experiments is shown in supplementary information, Fig. S2). $\bar{v}$ and $\bar{u}$ denote respectively the average vertical and horizontal velocity of each tracked PE particle (blue stars in Fig. 2A). The measured vertical velocity of particles deviated substantially from the Stokes velocity. The Stokes terminal velocity for the tested MPs (40 – 47 µm) was between -0.000434 and -0.000599 cm s^{-1}, meaning the particles had positive buoyancy in quiescent water and would have risen towards the water surface at 0.000434 – 0.000599 cm s^{-1}. However, in the experiments the tracked PE particles showed both positive and negative vertical velocity (Fig. 2 A, B, and Fig. S2.), meaning some particles moved towards the bed and some towards the water surface. Moreover, the numerical particle velocity was magnitudes above what would be expected for quiescent water as predicted by Stokes law.

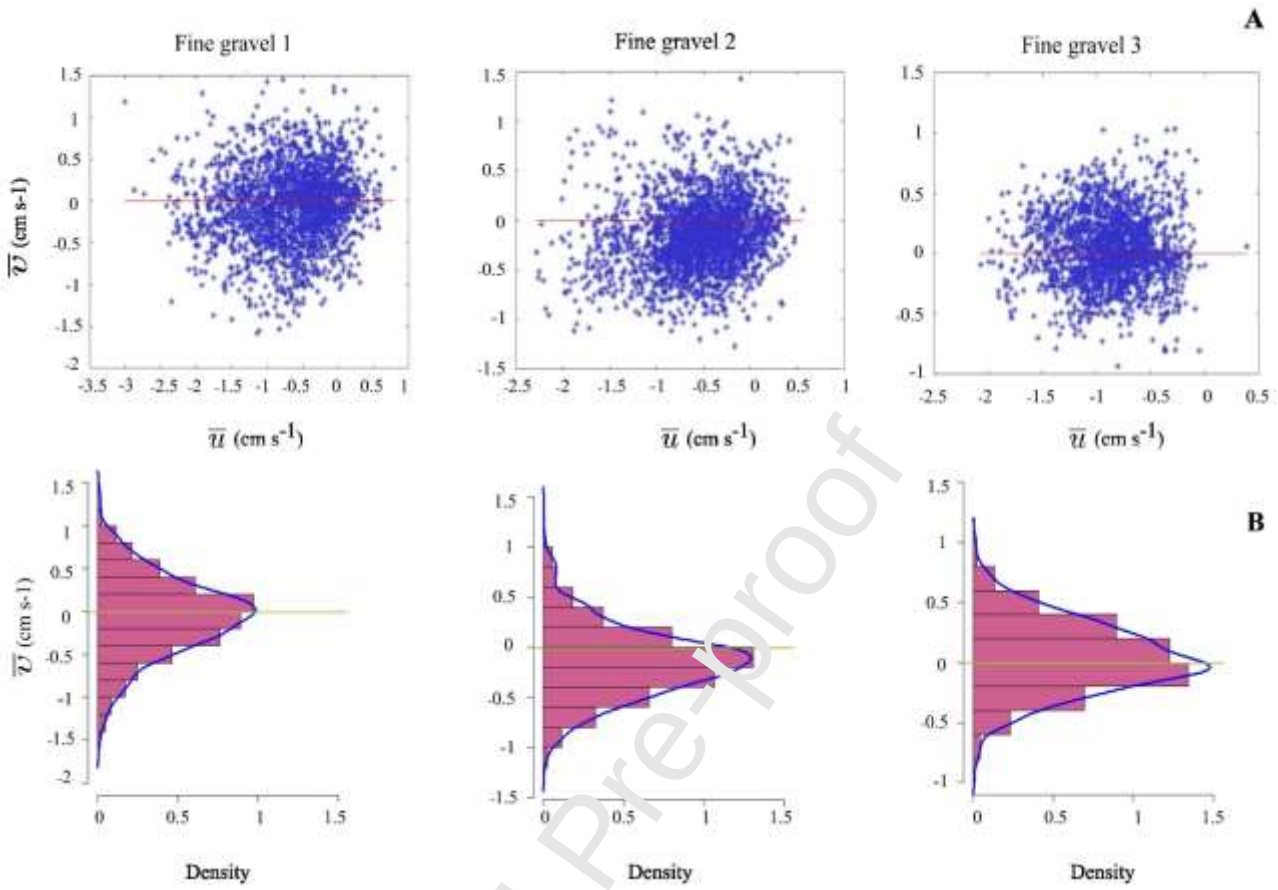

Fig. 2. The mean (tracked average) velocity obtained during 30 s of measurements for PE particles (A). The red line depicts the Stokes rising velocity of a 47 µm PE particle, which was the upper size of the particles tested in this study. I.e., the velocity which would be expected had the flow been completely quiescent. B: Histogram of the mean (tracked average) vertical particle velocity with the estimated density distribution (blue curve). The green line shows the Stokes velocity of a 47 µm PE particle.

A dimensionless parameter (Z) was defined as the relative ratio of the effective value $\bar{v}$ (average vertical velocity of all tracked PE particles in an experiment) measured in each flow regime to that expected in quiescent water (Stokes velocity) for 47 µm particles, i.e., the upper size of the particles added to the flow. Thus, values of Z > 1 indicate ‘‘enhanced’’ average rising rates (particles moving toward the surface), and Z < 1 diminished average rising rates or enhanced downward movement (particles moving towards the bed).

For all bed types and flow intensities, the average particle velocity deviated substantially from the predicted Stokes velocity (Table S1 and Fig. S3). No clear enhancement or diminishment pattern was observed for the different tested conditions. Medium sand 3 (TKE = 0.000625 J/kg) had the highest

average enhancement of downward movement (Z < 1), namely 255. I.e., the numerical value of the average particle velocity deviated 255 times from the intrinsic Stokes rising velocity. For this test condition, the particle with the most extreme downward movement had a velocity of 1.19 cm s^{-1}, that is, 1987 times higher than expected Stokes velocity and in the opposite direction of it. For the fine gravel bed 2 (TKE = 0.0008 J kg^{-1}), particles were on average moving toward the surface 250 times faster than predicted by Stokes law.

This finding implies that even though the average velocity was either upwards or downwards, there was in each cohort of particles always individual velocities in the downwards (or upwards) direction with Z >> 1 or Z << 1 (Table S1 and Fig S3). In other words, even in flow regimes where the net transport was upwards, many single particles were conveyed towards the bed. Such phenomenon was also reported by Kukulka et al. (2012) who observed that wind-driven turbulent mixing within the surface boundary layer in the ocean transferred and redistributed buoyant MPs lower in the water column and hence reduced the surface concentration. Rapid conveyance of particles towards the bed (downward movement) and towards the surface (upward movement) was hence driven by flow eddies. Such movement can sweep particles along and give them an increased momentum. When a flow eddy interacts with the bed, the inertia of a particle it carries can cause it to leave the diverted flow eddy and get into physical contact with the bed, where it may become immobilized. On the other hand, such flow eddies might also cause ejection of particles as they get swept off the bed. Whether a particle sticks to the bed would depend on both particle and bed characteristics. In a coarse bed, for example, a particle might get carried into the bed and get immobilized in its pores (Phillips et al., 2019). In a finer bed, the particle might adhere to the bed due to cohesive forces (Arnon et al., 2010).

The effect of different turbulence conditions on the vertical velocity distribution of PE particles is shown in Fig. S4. For each of the three conditions, the variability of particle velocities around the median velocity was quite similar, indicating that the bed type did not significantly affect the pattern of particle movement (Fig. S4). Neither did the bed type affect the median of the movement. There was, however, a clear decrease in the variation of particle velocity with decreasing turbulence. At high turbulence rates, more eddies with higher energy occurred, imposing larger random flow fluctuations. This then resulted in higher extreme values of upward and downward particle velocity.

3.3. Generic prediction of particle transport mode and fate

Turbulent motions in the flow can induce mixing of suspended particles, here MPs, if the turbulence intensity is notably larger than the rising or settling velocity of the particle. Somewhat counterintuitive, this means that particles of a density lower than that of water will not necessarily be found predominantly at the water surface, and particles of a density higher than that of water will not necessarily be found predominantly at the bed. Whether a lighter than water particle will mainly be at the water surface, or a heavier than water particle mainly at the bed, depends on both the properties of the MP and the vertical mixing.

Crucial MP properties cover size, shape, and density, while the properties of the flow include the turbulent shear velocity. The Rouse parameter (P) was used to quantify where in the flow a particle will be most likely to occur. P is a dimensionless parameter used to describe the relative significance of inertial vertical movements of particles due to gravity and buoyancy compared to turbulent-induced particle entrainment (Rouse, 1937). It represents the ratio between the rising/settling ability of a particle versus its vertical motion due to turbulent mixing and integrates the effects of particle size and density with the intensity of a turbulent shear flow (Eq. 3). The application of the Rouse parameter for buoyant and non-buoyant plastic particles has been confirmed by Cowger et al. (2021) and Born et al. (2023). When the shear velocity is low, the particle distribution in the water column is expected to be mainly governed by the rising or settling ability of the particles, whereas turbulent mixing plays a minor role. When the shear velocity is high, the distribution is expected to be mainly governed by turbulent mixing, i.e., the particles tend to be evenly distributed in the flow irrespective of their size and density.

Cowger et al. (2021) stated that $P < -2.5$ characterizes surface load particles (travelling only at the surface); $-2.5 < P < -0.8$ characterizes rising suspended load particles (partially distributed throughout the water column with higher concentrations at the surface); $0.8 > P > -0.8$ characterizes wash load particles (equally distributed throughout the water column); $2.5 > P > 0.8$ characterizes settling suspended load particles (partially distributed throughout the water column with higher concentrations at the bed); $7.5 > P > 2.5$ characterizes bed load particles (moving primarily along the bed by rolling, skipping, and saltating along the bottom-most portion of the flow field); and $P > 7.5$ characterizes immobile particles (in contact with the bed and not moving). In the present work, three flow conditions were assessed experimentally for spherical PE particles of 40 – 47 µm. Applying the Rouse parameter, these results were extrapolated to cover particles of 10 – 1000 µm and densities of 880 – 1550 kg m^{-3} at the highest and lowest shear velocity measured.

The effect of increasing turbulence intensity on the particle's transport is shown in Fig. 3. For illustration purposes, the upper size range of the PE particles of the current study (47 µm) is indicated by a star. With increasing turbulence intensity, a wider range of particles can be transported as wash load. This means that larger particles with higher densities can be kept in suspension due to the mixing caused by eddies, and hereby overcome the gravitational force acting on them. Particles with a density close to that of water would occur as wash load in a wider size range, regardless of turbulence intensity. For example, a 250 µm PE particle (995 kg m^{-3}) and 250 µm PS particle 1040 kg m^{-3} would behave quite similarly at all tested turbulence levels. Regardless of their densities, these would all occur as wash load for the tested shear velocities, meaning that all such particles would be distributed over the full water depth. Non-spherical particles would be even less affected by their density as the settling velocity of a non-spherical particle is lower than that of a spherical particle of the same mass (Wang et al., 2021).

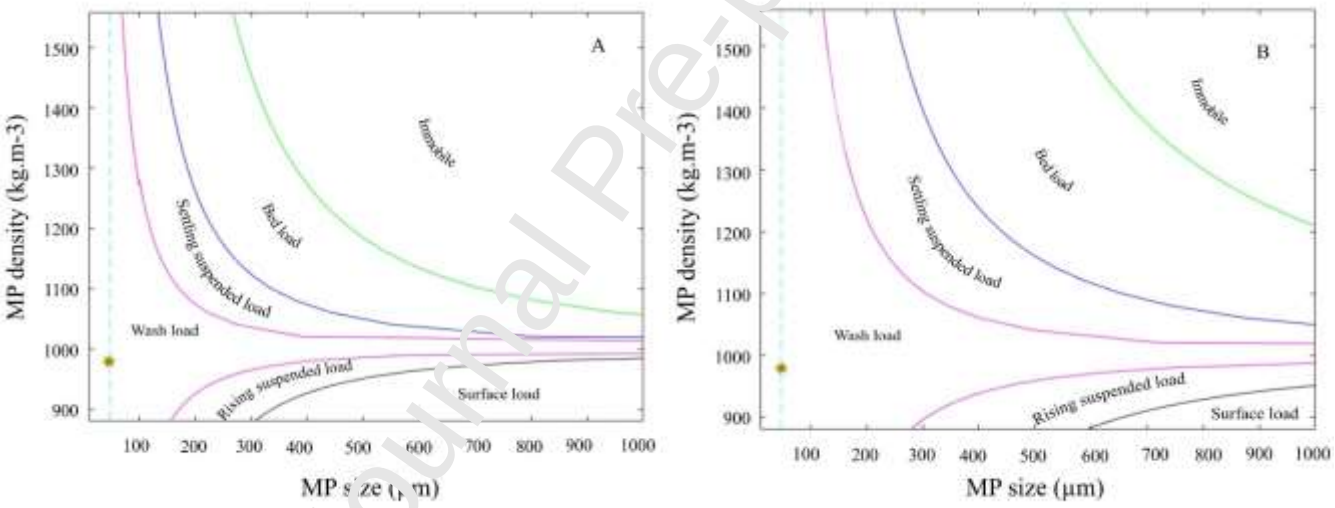

Fig. 3 Rouse domains for lowest (A) and highest measured shear velocity (B). The star shows the location of a 47 µm PE particle in the Rouse domain (the upper size of PE particles used). The vertical turquoise line shows particles with different densities and 47 µm diameter.

While the impact of density on the motion of small particles is not significant, it does become significant for larger particles. Considering for example PVC particles of 1150 kg m^{-3} and 500 µm size under the highest turbulence intensity condition (Fig. 3B): While a portion of these particles would stay in the water column due to turbulent mixing, a larger fraction would be close to the bed and moving as settling suspended load. At the lowest turbulence intensity, these particles would be at the bed and transported as bed load (Fig. 3A). For similar reasons, for example 500 µm PE particles (940 kg m^{-3})

would at the highest turbulence intensity move as rising suspended load while they would float at the water surface (surface load) at the lowest turbulence intensity. Turbulence would, in other words, be insufficient to pull them down (Fig. 3).

This is in accordance with the findings of DiBenedetto et al. (2023) who investigated MP segregation by rising of buoyant MPs under strong winds (wind-driven turbulence) in the ocean surface mixed layer. The authors stated that physical characteristics of the MPs will also control their vertical distribution. DiBenedetto et al. (2023) showed that MPs with high rising velocity were more abundant at the ocean surface, and turbulent mixing was unable to entrain them far below the surface. MPs with lower rising velocity were, on the other hand, well mixed in the free surface boundary layer at the same turbulence condition. Similarly, the findings of Kooi et al. (2016) showed that not all types of MP behaved the same while in the ocean. Less buoyant MPs tended for example to be mixed deeper than more buoyant ones. They also suggested that vertical distribution of buoyant MPs not only depends on environmental conditions, but also on their size and shape.

3.4. PE particles trajectories

The spatial movement of the PE particles were tracked to gain insights into particle movement patterns and entrainment behavior (fluid-particle interactions) in response to factors such as changes in fluid velocity and turbulence. Fig. 4 shows the trajectories which reached the lowest ~6 cm of the flume for the gravel bed at different flow conditions. The particle trajectory patterns were similar for repetitions of the experiment under identical flow and bed type conditions. For reasons of clarity, only 1 repetition (30 s of measurement) is hence shown (further instances of repetitions and other bed types are shown in Fig. S5).

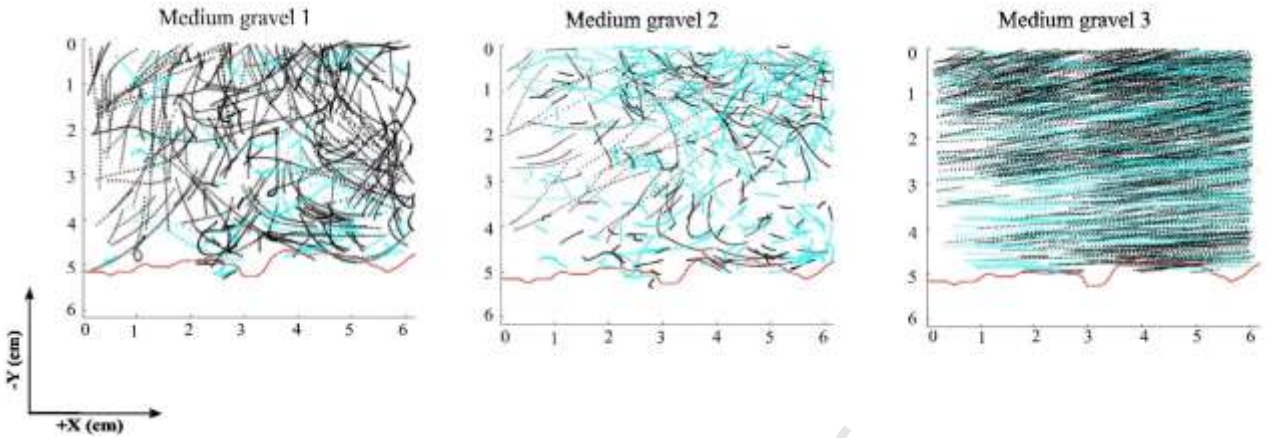

Fig. 4. Selected particle trajectories from one of the six repetitions (30 s) for the medium gravel bed. The first, second, and third illustration show trajectories for flow condition 1, 2, and 3, respectively. Particle trajectories in black move towards the bed and trajectories in turquois move towards the surface. The flow direction is from right to left. The red lines show the bed topographies.

For each flow condition, the pattern of particle trajectories was similar regardless of the bed type. At flow condition 1, i.e., where the pump was at its highest flow rate, particle motion was quite chaotic, and particles followed seemingly random trajectories. Most particles could not be followed all the 6 cm which the laser sheet covered in the y-x directions, as they moved out of the plane (i.e., in the z-direction). At flow condition 2, the particle trajectories were still erratic. At flow condition 3, particles followed smooth semi-parallel trajectories. Moreover, particles could be tracked over longer distance before disappearing and their trajectories ended, indicating that particles were moving longer in the x-y plane (laser sheet) in the observation period.

3.5. Interaction between particles and bed

While the turbulence caused particles to move vertically at velocities higher than their intrinsic settling/rising velocity, this did not tell whether they physically touched the bed and hence experienced a finite probability of becoming immobilized at the bed. The rate at which the particles arrived at the beds hence remained unknown. To assess this, and since the first prerequisite for a particle to encounter the bed is that it must move towards it, the abundance of tracked particles moving towards the bed in the 3 min of measurement time was calculated.

The highest and lowest number of particles moving downward were seen for medium sand 3 and fine gravel 2 with 66% and 30%, respectively. The abundance of sinking and rising PE particles at different test beds and flow conditions is displayed in Fig. S6 of the supplementary information. For all flow

conditions and bed types, there hence was a significant number of particles moving towards the bed within the field of view, albeit no clear trend could be found with the shear velocity (u*) and the bed type. To get closer to assessing the rate of particle/bed encounters, a near-bed zone was defined as a region 2 mm from the bed (bed zone). The median percentage of particles in the field of view reaching the bed zone within the 3 minutes was 4.2%, with highest and lowest values of 0.8% and 8.8% for the glass bed 3 and medium gravel 2, respectively. I.e., even though the Rouse parameter indicated that the MPs were conveyed as wash-load, they still had a quite significant probability of getting into contact with the bed. Trajectories of particles coming in close contact with the bed are exemplified in Fig. 5. The full set is shown in Supplementary Information Fig. S7.

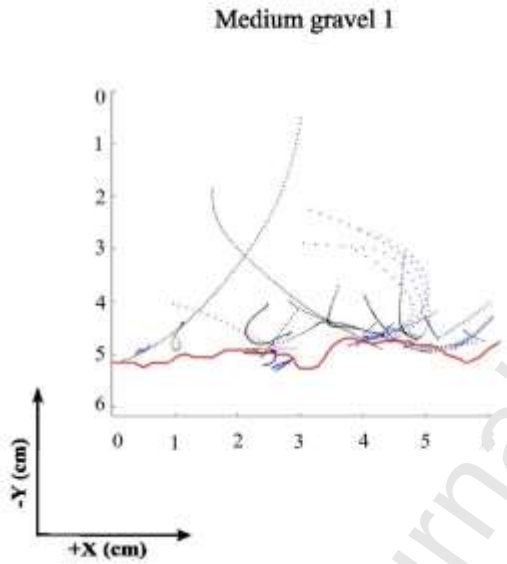

Fig. 5 Examples of PE particles which within a 30 s measuring window had been within 2 mm of the bed. Particles with trajectories shown in black moved towards the bed and those in blue moved away from it (some of these particles might have hit the bed and bounced off it). The red line shows the bed topography.

Assuming an infinitely long flume, and that particles are not resupplied, this would lead to around 99% of all beads in the flow getting into close contact with the bed within a day. Although the particles tracked in the bed zone had the highest probability of hitting the bed and thus potentially getting trapped by the bed, the experiments were not designed to quantify how many of the close encounters resulted in physical contact with the bed. Nevertheless, the experiments illustrate how turbulent particle movement can lead to entrapment of microplastics within a rather short time span.

While the experiments were done in the waters of a slow flowing flume, the general conclusion on turbulence-driven MP transport holds true for any water body which exhibits a similar turbulence regime (McWilliams and Sullivan, 2000). Whether the turbulence is induced by the flow of water in a channel or waves of an open water body (Chor et al., 2018), the conclusions of eddies driving the transport of MPs holds true. In a shallow lake, for example, where wind and waves cause turbulence all the way to the lakebed (Reardon et al., 2014), the eddies may transport lighter-than-water MPs to the bed where they may become immobilized. In the open ocean where the upper water layer is completely mixed, turbulent eddies may transport such particles towards the deeper quiescent water layers where flow is laminar (Brunner et al., 2015). Once there, the lighter-than-water MPs would have to shift to a different transport mode to reach the bottom, for example ballasted settling due to biofilm growth and/or particle coagulation (Galgani et al., 2022). While turbulence alone hence cannot explain why MPs reach the deep ocean floor, it is crucial in understanding the processes in the upper water layers. Without this understanding and including it in MP transport models, these would struggle to predict MP transport accurately (Onink et al., 2022). This would lead to poorer predictions of MP pathways and their final destination, which then would lead to poorer assessment of the impacts these MPs can have on the environment.

4. Conclusion

The vertical transport velocities of 40 – 47 µm PE particles (ρ = 995 kg m^{-3}) in a flume (1.85 – 4.17 cm s^{-1}) were orders of magnitude above the rising velocity as calculated by Stokes law (0.43 – 0.6 µm s^{-1}). Within the investigated 6 cm of the bed, both the upwards and downwards velocity of individual MPs reached as much as 2.4 cm s^{-1}. There was no clear preference for these lighter-than-water particles to either rise or sink. Zooming in on the 2 mm closest to the bed showed that some particles came into close encounters with, or even hit, the bed. Together this illustrated that the eddies generated in the flume overcame the rising tendency of the MPs and brought them to the bottom part of the flume where they could be captured by the bed.

Applying the results to well-established particle transport theory presented an approach to predict MP distribution in a turbulent water body. The results however also showed that these yield average distributions only. Even though a MP on average is predicted to stay suspended in the water, turbulence causes eddies, which sometimes can convey such an MP close to the bed where it might become immobilized. The study clearly showed that the fate of MPs in turbulent waters is linked to turbulent transport, which hence must be considered when predicting the transport and fate of MPs in aquatic

environments and for developing strategies to mitigate their impact on the ecosystem. To predict the pathways of MPs in aquatic environments and their final destinations, it is essential to comprehend the influence of turbulence. This understanding will in turn lead to improved predictions of local concentrations and, consequently, provide a better understanding of their environmental impacts.

Acknowledgements

This work was carried out within the Limnoplast project. This project has received funding from the European Union's Horizon 2020 research and innovation programme under grant agreement No 860720. The authors wish to thank Bruno J. Lemaire and Cedric Chaumont from INRAE to provide the hydraulic lab.

References

Andrady, A.L., 2011. Microplastics in the marine environment. Mar. Pollut. Bull. 62, 1596–1605. https://doi.org/10.1016/j.marpolbul.2011.05.030.

Arnon, S., Marx, L.P., Searcy, K.E., Packman, A.I., 2010. Effects of overlying velocity, particle size, and biofilm growth on stream-subsurface exchange of particles. Hydrological Processes, 24 (1), 108-114, https://doi.org/10.1002/hyp.7490

Ballent, A., Pando, S., Purser, A., Juliano, M.F., Thomsen, L., 2013. Modelled transport of benthic marine microplastic pollution in the Nazaré Canyon. Biogeosciences 10 (12), 7957. https://doi.org/10.5194/bg-10-7957-2013

Besseling, E., Quik, J.T.K., Sun, M., Koelmans, A.A., 2017. Fate of nano- and microplastic in freshwater systems: A modeling study. Environmental Pollution, 540-548, 220. https://doi.org/10.1016/j.envpol.2016.10.001.

Born, M, P., Brulle, C., Schaefer, D., Hillebrand, G., Schuttrumpf, H., 2023. Determination of Microplastics' Vertical Concentration Transport (Rouse) Profiles in Flumes. Environ. Sci. Technol. 57, 5569−5579. https://doi.org/10.1021/acs.est.2c06885

Brunner, K., Kukulka, T., Proskurowski, G., Law, K.L., 2015. Passive buoyant tracers in the ocean surface boundary layer: 2. Observations and simulations of microplastic marine debris. Journal of Geophysical Research – Oceans, 120 (11): 7559-7573. https://doi.org/10.1002/2015JC010840

Chor, T., Yang, D., Meneveau, C., Chamecki, M., 2018. A Turbulence Velocity Scale for Predicting the Fate of Buoyant Materials in the Oceanic Mixed Layer. Geophysical Research Letters, 45 (21), 11817-11826. https://doi.org/10.1029/2018GL080296

Cole, M., Lindeque, P., Halsband, C., Galloway, T.S., 2011. Microplastics as contaminants in the marine environment: a review. Mar. Pollut. Bull. 62, 2588–2597. https://doi.org/10.1016/j.marpolbul.2011.09.025.

Cowger, W., Gray, A. B., Guilinger, J. J., Fong, B., Waldschlager, K., 2021. Concentration Depth Profiles of Microplastic Particles in River Flow and Implications for Surface Sampling. Environ. Sci. Technol., 55, 6032−6041. https://doi.org/10.1021/acs.est.1c01768

Daily, J and Hoffman, M, J., 2020. Modelling the three-dimensional transport and distribution of multiple microplastic polymer types in Lake Erie. Marine Pollution Bulletin, 154, 111024, 0025-326X, https://doi.org/10.1016/j.marpolbul.2020.111024.

De Leeuw, J., Lamb, M. P., Parker, G., Moodie, A. J., Haught, D., Venditti, J. G., Nittrouer, J. A., 2020. Entrainment and Suspension of Sand and Gravel. Earth Surf. Processes Landforms, 8, 485−504. https://doi.org/10.5194/esurf-8-485-2020

DiBenedetto, M.H., Donohue, J., Tremblay, K., Edson, E., Law, K.L., 2023. Microplastic segregation by rise velocity at the ocean surface. Environmental Research Letters. 18, 024036. 10.1088/1748-9326/acb505.

Dietrich, W.E. (1982). Settling velocity of natural particles. Water Resour. Res., 18 (6), 1615-1626, https://doi.org/10.1029/WR018i006p01615.Galgani, L., Gossmann, I., Scholz-Boettcher, B., Jiang, X.T., Liu, Z.F., Scheidemann, L., Schlundt, C., Engel, A., 2022. Hitchhiking into the Deep: How Microplastic Particles are Exported through the Biological Carbon Pump in the North Atlantic Ocean. Environmental Science & Technology, 56 (22), 15638–15649. https://doi.org/10.1021/acs.est.2c04712

Isachenko, I., 2020. Catching the variety: Obtaining the distribution of terminal velocities of microplastics particles in a stagnant fluid by a stochastic simulation. Marine Pollution Bulletin, 159, 111464. https://doi.org/10.1016/j.marpolbul.2020.111464

Isobe, A., Iwasaki, S., 2022. The fate of missing ocean plastics: Are they just a marine environmental problem? Science of The Total Environment, 825, 153935. https://doi.org/10.1016/j.scitotenv.2022.153935

Jalón-Rojas, I., Romero-Ramirez, A., Fauquembergue, K., Rossignol, L., Cachot, J., Sous, D., Morin, B., 2022. Effects of Biofilms and Particle Physical Properties on the Rising and Settling Velocities of Microplastic Fibers and Sheets. Environ. Sci. Technol. 56, 8114− 8123. https://doi.org/10.1021/acs.est.2c01302

Kaiser, D., Estelmann, A., Kowalski, N., Glockzin, M., Waniek, J.J., 2019. Sinking velocity of sub-millimeter microplastic. Mar. Pollut. Bull. 139, 214–220. https://doi.org/10.1016/j.marpolbul.2018.12.035

Khatmullina, L., Chubarenko, I., 2019. Transport of marine microplastic particles: why is it so difficult to predict? Anthropocene Coasts, 2 (1), 293-305, https://doi.org/10.1139/anc-2018-0024

Khatmullina, L., Isachenko, I., 2017. Settling velocity of microplastic particles of regular shapes. Mar. Pollut. Bull. 114 (2), 871–880. https://doi.org/10.1016/j.marpolbul.2016.11.024

Koelmans, A.A., Redondo-Hasselerharm, P.E., Nor, N.H.M. et al., 2022. Risk assessment of microplastic particles. Nat Rev Mater, 7, 138–152. https://doi.org/10.1038/s41578-021-00411-y.

Kooi, M., Reisser, J., Slat, B., Ferrari, F.F., Schmid, M.S., Cunsolo, S., Brambini, R., Nobel, K., Sirks, L.A., Linders, T.E.W., Schoeneich-Argent, R.I., Koelmans, A.A., 2016. The effect of particle properties on the depth profile of buoyant plastics in the ocean. Scientific Report, 33882. https://doi.org/10.1038/srep33882

Kowalski, N., Reichardt, A.M., Waniek, J.J., 2016. Sinking rates of microplastics and potential implications of their alteration by physical, biological, and chemical factors. Mar. Pollut. Bull., 109 (1), 310–319. https://doi.org/10.1016/j.marpolbul.2016.05.064

Kukulka, T., Proskurowski, G., Morét-Ferguson, S., Meyer. D.W., Law, K.L., 2012. The effect of wind mixing on the vertical distribution of buoyant plastic debris, Geophys. Res. Lett., 39, L07601, https://doi.org/10.1029/2012GL051116

Li, Y., Wang, X., Fu, W., Xia, X., Liu, C., Min, J., Zhang, W., Crittenden, J.C., 2019. Interactions between nano/micro plastics and suspended sediment in water: Implications on aggregation and settling, Water Research, 161, 486-495. https://doi.org/10.1016/j.watres.2019.06.018.

Liu, F., Vianello, A., Vollertsen, J., 2019. Retention of microplastics in sediments of urban and highway stormwater retention ponds. Environ. Pollut., 255, 113335. https://doi.org/10.1016/j.envpol.2019.113335.

Liu, Y., Lorenz, C., Vianello, A., Syberg, K., Nielsen, A.H., Nielsen, T.G., Vollertsen, J., 2023. Exploration of occurrence and sources of microplastics (>10 μm) in Danish marine waters. Science of The Total Environment,.865, 0048-9697. https://doi.org/10.1016/j.scitotenv.2022.161255.

Long, M., Moriceau, B., Gallinari, M., Lambert, C., Huvet, A., Raffray, J., Soudant, P., 2015. Interactions between microplastics and phytoplankton aggregates: impact on their respective fates. Mar. Chem. 175, 39–46. https://doi.org/10.1016/j.marchem.2015.04.003Lu, X., Wang, X., Liu, X., Singh, V.P., 2023. Dispersal and transport of microplastic particles under different flow conditions in riverine ecosystem. Journal of Hazardous Materials. 442, 0304-3894 https://doi.org/10.1016/j.jhazmat.2022.130033.

Manikanda, B., K., Srinivasalu, S., Natesan, U., Ayyamperumal, R., Kalam S, N., Anbalagan, S., Sujatha, K., Alagarasan, C., 2021. Microplastics as an emerging threat to the freshwater ecosystems of Veeranam lake in south India: A multidimensional approach. Chemosphere, 264, Part 2, 128502, https://doi.org/10.1016/j.chemosphere.2020.128502.

McWilliams, J.C., Sullivan, P.P., 2000. Vertical mixing by Langmuir circulations. Spill Science & Technology Bulletin, 6 (3-4), 225-237, https://doi.org/10.1016/S1353-2561(01)00041-X

Molazadeh, M., Liu, F., Simon-Sánchez, L., Vollersten, J.,2023. Buoyant microplastics in freshwater sediments – How do they get there? Science of The Total Environment, 860, 160489, 0048-9697,https://doi.org/10.1016/j.scitotenv.2022.160489.

Moore, C. J. (2008). Synthetic polymers in the marine environment: A rapidly increasing, long-term threat. Environmental Research, 108(2), 131–139. https://doi.org/10.1016/j.envres.2008.07.025

Olesen, K.B., Stephansen, D.A., van Alst, N., Vollertsen, J., 2019. Microplastics in a stormwater pond. Water (Switzerland), 11 (7), 1466. https://doi.org/10.3390/w11071466.

Onink, V., van Sebille, E., Laufkotter, C, 2022. Empirical Lagrangian parametrization for wind-driven mixing of buoyant particles at the ocean surface. Geoscientific Model Development, 15(5), 1995-2012. https://doi.org/10.5194/gmd-15-1995-2022

Phillips, C.B., Dallmann, J.D., Jerolmack, D.J., Packman, A.I., 2019. Fine-Particle Deposition, Retention, and Resuspension Within a Sand-Bedded Stream Are Determined by Streambed Morphodynamics. Water Resources Research, 55 (12), 10303-10318, https://doi.org/10.1029/2019WR025272

Reardon, K.E., Bombardelli, F.A., Moreno-Casas, P.A., Rueda, F.J., Schladow, S.G., 2014. Wind-driven nearshore sediment resuspension in a deep lake during winter. Water Resources Research, 50 (11), 8826-8844. https://doi.org/10.1002/2014WR015396

Reisser, J.W., Slat, B., Noble, K.D., Plessis, K.D., Epp, M., Proietti, M.C., de Sonneville, J., Becker, T., Pattiaratchi, C., 2015. The vertical distribution of buoyant plastics at sea: an observational study in the North Atlantic Gyre. Biogeosciences, 12, 1249–1256. https://doi.org/10.5194/bg-12-1249-2015

Reynolds, O., 1895. On the Dynamical Theory of Incompressible Viscous Fluids and the Determination of the Criterion. Philosophical Transactions of the Royal Society of London, 186, 123-164. https://doi.org/10.1098/rsta.1895.0004

Rouse, H., 1937. Modern Conceptions of the Mechanics of Fluid Turbulence. Trans. Am. Soc. Civ. Eng., 102, 463−505. https://doi.org/10.1061/TACEAT.0004872

Semcesen, O.P., Wells, G.M., 2021. Biofilm growth on buoyant microplastics leads to changes in settling rates: implications for microplastic retention in the Great Lakes. Mar. Pollut. Bull. 170, 112573. https://doi.org/10.1016/j.marpolbul.2021.112573.

Simon-Sanchez, L., Grelaud, M., Franci, M., Ziveri, P., 2022. Are research methods shaping our understanding of microplastic pollution? A literature review on the seawater and sediment bodies of the Mediterranean Sea. Environmental Pollution, 292, 118275. https://doi.org/10.1016/j.envpol.2021.118275

Shamskhany, A and Karimpour, S., 2022. Entrainment and vertical mixing of aquatic microplastics in turbulent flow: The coupled role of particle size and density. Marine Pollution Bulletin, 184, 114160, 0025-326X, https://doi.org/10.1016/j.marpolbul.2022.114160.

Stokes, G. G., 1851. On the Effect of the Internal Friction of Fluids on the Motion of Pendulum. Pitt. Press, 9.1. https://doi.org/10.1017/CBO9780511702266.002

Thielicke, W., Stamhuis, E., 2014. PIVlab–towards user-friendly, affordable, and accurate digital particle image velocimetry in MATLAB. Journal of Open Research Software, 2,1, https://doi.org/10.5334/jors.bl; https://web.stanford.edu/~nto/software_tracking.shtml/ (accessed 25 July 2023)

Wang, Z., Dou, M., Ren, P.J., Sun, B., Jia, R.P., Zhou, Y.Z., 2021. Settling velocity of irregularly shaped microplastics under steady and dynamic flow conditions. Environmental Science and Pollution Research, 28 (44), 62116- 62132. https://doi.org/10.1007/s11356-021-14654-3

Yan, M., Yang, J., Sun, H., Liu, C., Wang, L., 2022. Occurrence and distribution of microplastics in sediments of a man-made lake receiving reclaimed water. Science of The Total Environment, 83, 0048-9697. https://doi.org/10.1016/j.scitotenv.2021.152430.

Graphical abstract

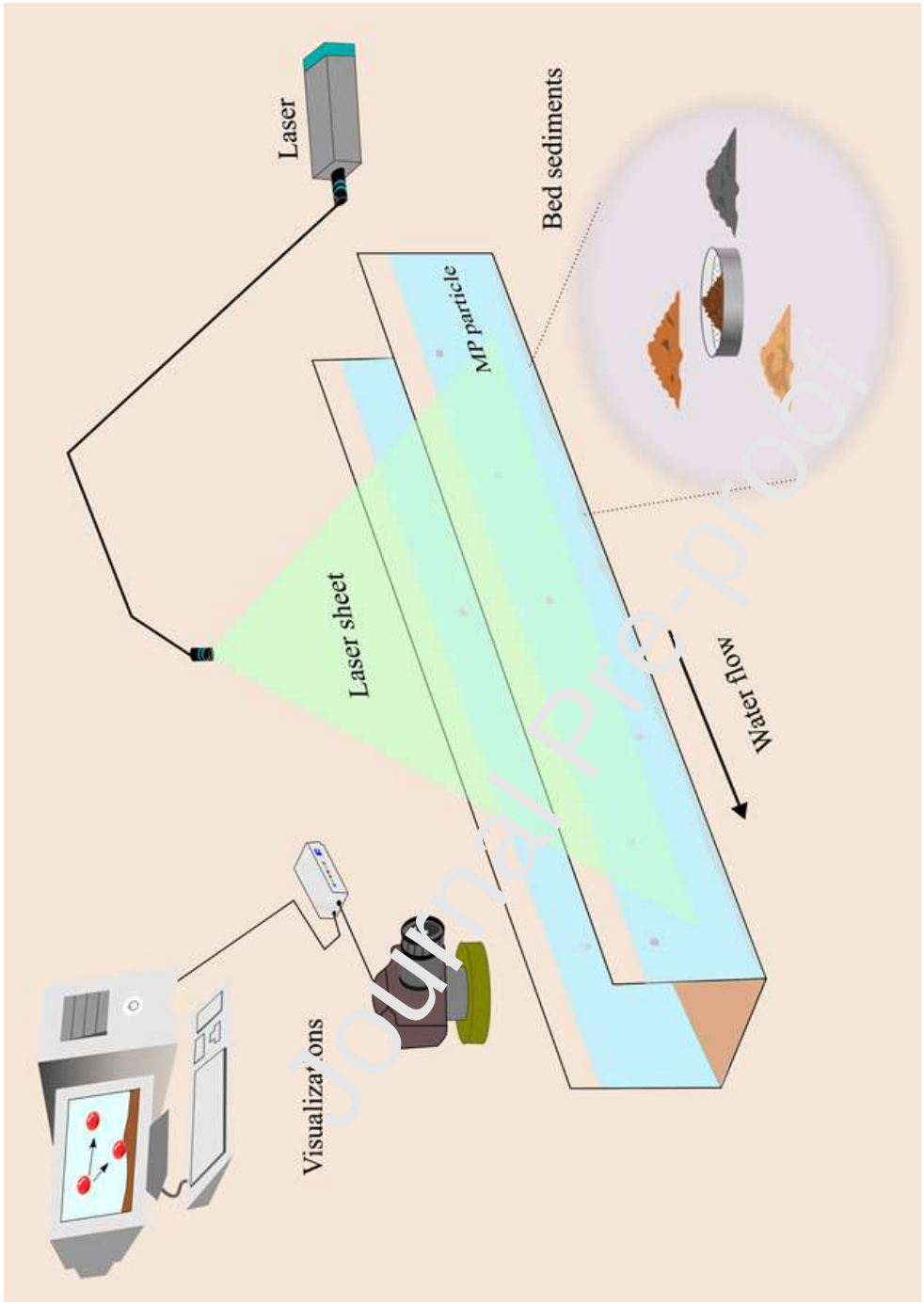

Highlights :

Experimental validation on mixing induced transfer of MPs from water surface to sediments

Substantial quantity of PE particles was subject to downward vertical transport

Vertical velocity of PE in turbulent flows varied over 4 orders of magnitude from predicted rising velocity in still water

Declarations Conflict of interest: The authors declare no competing interests.

CRediT authorship contribution statement

Marziye (Shabnam) Molazadeh carried out the experiments, interpreted the results, and wrote the original draft. Guilherme Calabro helped with carrying out the experiments. Fan Liu, Rachid Dris and Bruno Tassin co-supervised the project. Andreas Lorke and Lorenzo Rovelli providing resources. Jes Vollertsen supervised the project. All authors contributed to the final manuscript.

ISSN (online): 2446-1636
ISBN (online): 978-87-7573-593-8

AALBORG UNIVERSITY PRESS